CONTRIBUTIONS TO THE STUDY OF THE SURFACE ENERGY AND SURFACE TENSION OF SOLIDS

A THESIS

Presented to

The Faculty of the Graduate Division

by

William James Corbett

In Partial Fulfillment

of the Requirements for the Degree

Doctor of Philosophy in the

School of Chemical Engineering

Georgia Institute of Technology

June, 1964

"In presenting the dissertation as a partial fulfillment of the requirements for an advanced degree from the Georgia Institute of Technology, I agree that the Library of the Institution shall make it available for inspection and circulation in accordance with its regulations governing materials of this type. I agree that permission to copy from, or to publish from, this dissertation may be granted by the professor under whose direction it was written, or, in his absence, by the dean of the Graduate Division when such copying or publication is solely for scholarly purposes and does not involve potential financial gain. It is understood that any copying from, or publication of, this dissertation which involves potential financial gain will not be allowed without written permission.

CONTRIBUTIONS TO THE STUDY OF THE SURFACE ENERGY

AND SURFACE TENSION OF SOLIDS

Approved:

[redacted]

Date approved by Chairman: May 28, 1964

ACKNOWLEDGEMENTS

The author is indebted to the many individuals who have contributed to the success of this work. To Dr. Clyde Orr, who introduced the author to the problem, goes sincere appreciation for his aid, counsel, and continued encouragement. Thanks are due Dr. W. T. Ziegler for his critical review and suggestions. By his example of thorough and precise investigative technique, which the author did his best to emulate, Dr. Ziegler contributed more than he realizes. Appreciation is also expressed for the conscientious service of Dr. Robert A. Pierotti as a member of the reading committee.

Special thanks are due Dr. G. C. Benson of the National Research Council, Ottawa, Canada, and Mr. John L. Brown of the Georgia Institute of Technology, Engineering Experiment Station. Dr. Benson was most helpful in allowing the author to visit his laboratories, making available details of his calorimeter, corresponding quite freely concerning details of his research and suggestions about this research, and making a special effort to meet with the author to discuss this research. The splendid cooperation and imaginative ability of Mr. Brown in the phase dealing with electron microscopy and electron diffraction are acknowledged as being among the major factors contributing to the success of this research.

Thanks are due Dr. F. Kenneth Hurd for valuable assistance in the design and construction of the calorimeter, as well as for many stimulating discussions. An attempt to acknowledge all the individuals who have

contributed through stimulating discussions and constructive suggestions, over the almost seven years that the author has been involved in this research, can only result in serious omissions. However, with apologies for these omissions, thanks are expressed to Dr. R. A. Young, Dr. J. D. Fleming, Jr., Dr. Robert F. Hochmann, Mr. John H. Burson, and Mr. Joseph C. Mullins. Mr. Mullins is also due acknowledgement for the least-squares analysis of the thermopile calibration data. The author also appreciates the benefit he derived from the experience of Mr. Warren P. Hendrix concerning the measurement of the surface area of solids.

Appreciation is expressed for the support of the National Institutes of Health and the Engineering Experiment Station of the Georgia Institute of Technology through research grants, employment, and facilities.

Finally, for some of the most important assistance of all, the author is greatly indebted to his entire family for their patient support and encouragement during this undertaking.

TABLE OF CONTENTS

LIST OF TABLES

LIST OF FIGURES

LIST OF FIGURES (Continued)

SUMMARY

A portion of the energy of every solid resides in its body and part of its energy is associated with its surface. The larger the specific surface area, the larger, of course, is the fraction of the total energy that resides in the surface. Surface energy is of importance to catalysis, adsorption, solid state reaction, lubrication, fracture, and a number of other phenomena. In spite of its importance there have been very few attempts to measure the surface energy of solids. This is due principally to the difficulties involved with such measurements. What few attempts there have been have often suffered from an incomplete understanding of the basic concepts of surface energy and surface tension as applied to solids.

The specific surface Gibbs free energy of a solid is defined as the work required to create a unit area of equilibrium surface reversibly and isothermally. In this concept a solid is no different from a liquid. However, unlike liquids, the specific surface Gibbs free energy of a solid cannot be measured directly, and some indirect manifestation of the quantity must be analyzed instead. The most acceptable measurement is the enthalpy associated with the surface, which differs from the surface energy only by a negligible pressure-volume quantity. From a knowledge of the surface energy and measurements of the excess heat capacity of the solid due to the presence of its surface, it is possible to arrive at a measure of the specific surface Gibbs free energy.

The initial objective of this research was to measure the surface energy of a number of ionic solids by differential, heat-of-solution calorimetry. In this technique the heats of solution of extremely fine and very coarse crystals are obtained. The excess heat of solution of the fine crystals is a measure of the enthalpy resulting from their greater surface area. A sensitive adiabatic, heat-of-solution calorimeter was constructed for making such determinations and a procedure was adopted for preparing finely divided samples of sodium and potassium chloride. The preparation technique was one that had been used by various investigators over the past decade to produce finely divided samples of these materials. It involved maintaining a melt of the alkali halide in a shallow platinum crucible, passing a stream of dry nitrogen gas over the crucible, and collecting the submicron size crystals thus produced in an electrostatic precipitator.

Using this volatilization technique, a number of samples of the two alkali halides were produced having specific surface areas ranging from about 5 to 50 m^2/gm. It was found, in agreement with the observation of other investigators, that these samples had to be protected from exposure to even very low concentrations of water vapor in order to maintain their high specific surface areas. Reagent-grade salts as purchased commercially constituted the coarse materials.

Mean values for the heat of solution of coarse samples (i.e. less than 0.1 m^2/gm) of sodium and potassium chloride were determined from several tests with each material. Values were then obtained for the heat of solution of a number of samples of sodium and potassium chloride having large specific surface areas. Plots, constructed from the

difference between these values and the mean values for the coarse material as a function of specific surface area, exhibited, instead of a linear variation of the difference in heats of solution with specific surface area as expected, a pronounced curvature with non-zero intercepts at zero specific surface area. Also these data did not agree with similar measurements for the same compounds as obtained by other investigators. The results indicated that an effect in addition to the surface energy was being observed.

Investigation of the structure and morphology of the finely divided materials produced by the volatilization technique was next undertaken. Reports were uncovered that were not only in conflict with the generally accepted findings as to the shape of the volatilized particulates, but one account even described the particulates as amorphous in structure. These accounts of research in fields entirely unrelated to surface energetics indicated that the shape of the particulates were actually spherical rather than cubic as long as they were protected from exposure to water vapor. Utilizing thermal precipitation and electron microscopy, the spherical shape was confirmed. However, it was not confirmed that such particulates are amorphous despite attempts to reproduce the exact conditions from which the previous results were obtained. In this investigation the volatilized material was found to be crystalline. The mechanics of the volatilization process was unraveled through experiments using various generators for producing the volatilized samples of sodium and potassium chloride and experiments involving the temperature control of the surroundings. The process of fine particle production by volatilization was deduced to be one of vapor condensation

immediately over the melt forming droplets of molten material followed by droplet cooling to solid particles by radiative heat transfer. The spherical shape of the volatilized particles was a condition imposed by rapid cooling. Control of the cooling rate resulted in a change in the particle shape from spherical to cubic.

Investigations of the surface structure of the resulting particles by platinum-carbon replication and gold decoration in conjunction with electron microscopy showed the surfaces to be smooth at least to the order of 12 angstroms with a total absence of any structural features. Adsorption and desorption of gaseous nitrogen on samples of finely divided sodium and potassium chloride at the boiling temperature of liquid nitrogen revealed no unusual surface conditions.

A thermodynamic analysis based on the observed and deduced structural features of the spherical particles appears to describe the observed deviations of the heats of solution of the finely divided material. The significant features of the analysis include the presence of crystallite boundaries, the external area of the particles, and the strain associated with spherical shape of the particles. Using this analysis and the experimentally determined differences in the heats of solution, estimates of the surface tension were obtained for sodium and potassium chloride. Unlike the case for ideal, one-component liquids, the surface tension of a solid (the work required to extend the surface by stretching) is not necessarily equal to the specific surface Gibbs free energy. Values of 1.5×10^4 and 4.5×10^4 dynes/cm were obtained for the surface tension of sodium and potassium chloride, respectively. These values are higher than previously thought. There are no other

experimental determinations of the surface tension of the alkali halides against which to check, however.

The unusually high energies determined for the spherical particles of volatilized sodium and potassium chloride explains the abnormal sensitivity of the volatilized material to the presence of water vapor. The high energy content found for coarse samples of volatilized sodium chloride is in agreement with that found by other investigators for large spheres of sodium chloride prepared in an entirely different manner. It is pointed out that the results of these latter investigators do not represent the surface energy of sodium chloride as they mistakenly assumed. It is concluded that the volatilization process as it has been used in the past is unsuitable for producing samples for the measurement of equilibrium surface properties. It is pointed out that previous experimental values for the surface energy of sodium and potassium chloride, determined with samples prepared by volatilization, are quite probably high due to the presence of non-equilibrium particles in the samples.

CHAPTER I

INTRODUCTION

Despite the fact that much of man's contact with his environment is through the medium of surfaces, less is known today about the nature and properties of solid surfaces than about the nucleus of the atom. This situation has developed, of course, because understanding the nature of the atom and atomic processes has many military and commercial ramifications, whereas surfaces have been utilized since the dawn of civilization even though their nature and properties were not understood. However, if significant future advances are to be made in such fields as catalysis, adsorption, adhesion, lubrication, nucleation, dissolution, solid state reactions, composite materials, powder metallurgy, and comunition, a better understanding of the fundamental nature and properties of solid surfaces must be achieved.

For a solid the surface is important because this is where reactions initiate, vapors and gases are adsorbed, sintering occurs, growth takes place, etc. These processes indicate that the surface is active, for if the surface were inert these interactions would not occur. This activity might be best described in terms of the forces residing in the surface. However, forces are more difficult to measure or describe than energy quantities. Consequently, surface energies rather than surface forces are usually used in characterizing the activity of solid surfaces.

To be able to calculate theoretical values for the surface energy

of the different faces of crystals of various substances and then to verify the theoretical calculations experimentally would be of immense importance to an understanding of crystal structure and the theory of the crystalline lattice. Unfortunately, this problem is far from solved. Even for the simple, widely studied crystals of the alkali halides there are as many theoretical values of surface energy as there are authors who have attempted to calculate them. This shows that a unified theory of the crystalline lattice has not yet been developed and that every investigator makes different assumptions in calculating surface energies. The situation is no better with regard to the experimental determination of surface energies.

Theoretical calculations of surface energy antedate by about a decade serious attempts at experimental determination. The early calculation efforts (1)(2)(3)(4)(5) were based on classical crystal models and were made for the different crystal faces of the alkali halides. At best they resulted in rough approximations. Later calculations (6)(7)(8)(9)(10) were principally concerned with attempts to correct for van der Waals forces and surface distortions. More recently, van Zeggeren and Benson (11) have used quantum mechanical considerations to arrive at theoretical estimates for the surface energies of the alkali halides.

Unlike the case for liquids, the surface energy of solids cannot be measured directly by surface extension except for amorphous materials at elevated temperatures. Experimental techniques for measuring the surface energy of crystalline solids must be based on indirect manifestations of the energy. The three most generally recognized techniques for

accomplishing this involve (1) the energy required for cleavage, (2) the increase in solubility as a function of particle size (specific surface area), and (3) measurements of heat-of-solution as a function of specific surface area. There have been a number of attempts to determine the surface energy of crystalline substances on the assumption that the work expended in fracture of the crystal is equal to the surface energy of the new surfaces formed when the fracture is brittle (12)(13)(14). The results obtained in such experiments are, strictly speaking, unreliable, since a part of the work of breaking is expended in the form of heat in partial deformation of the crystals and in the energy of plastic deformation remaining in the crystals. Also, most experiments of this kind have been conducted in the presence of air which renders the splitting process thermodynamically irreversible.

The method of increased solubility was one of the earliest techniques employed (15) and has been used in a few subsequent investigations (16)(17)(18). In principal, small crystals should show a higher solubility than large ones. However, in practice the problems of accurately determining the particle size with which the solution is in equilibrium and the concentration of the solution are formidable and have not been completely resolved. Also, the quantity obtained from measurements of this type is the value of the interfacial energy between solute and solution rather than the surface energy of the solid.

The most straightforward technique for measuring the surface energy of a solid, from the standpoint of both execution and interpretation of the physical significance of the measurements, is by differential heat-of-solution calorimetry. Basically, the heat-of-solution

technique consists of measuring the heats of solution of a sample of a material having a low specific surface area and a sample of equal mass having a high specific surface area. The energy of the material due to the presence of the surface will then appear as a small difference. In spite of the straightforwardness of this technique, there are many experimental difficulties not the least of which is the precise measurement of the small difference between two large quantities. Lipsett, Johnson and Maass (19) are apparently the first investigators to attemp measurements of the surface energy of a solid in this manner. These investigators obtained sufficiently precise measurements of heats of solution by employing a calorimeter of low heat capacity (approximately 50 cal/^{o}C, including the contents) and measuring the magnitude of the temperature changes to the order of 10^{-4} ^{o}C. Their results, however, are open to question because the surface area of their samples were estimated from particle size measurements. This method of obtaining specific surface area generally yields a value lower than the actual one; this work, however, did provide valuable guidelines. Differential, heat-of-solution measurements were again employed by several investigators following the development of gas adsorption techniques for the more accurate determination of specific surface areas. The results of these investigations, which represent the most reliable determinations of the surface energies of solids to date, are presented in Table I. Independent confirmation of none of these values is available, and, as will be seen in the discussion of the results of this work, at least some of them are certainly open to question.

The lack of agreement in the few cases where more than one

Table 1. Experimental Surface Energies of Solids at or Near 25°C

Substance	Surface Energy ($ergs/cm^2$)	Investigators
Magnesium Oxide	1090	Jura and Garland (20)
Sodium Chloride	276 ± 5	Benson, et al. (21)
Calcium Oxide	1310 ± 200	Brunauer, et al. (23)
Calcium Hydroxide	1180 ± 100	Brunauer, et al. (23)
Amorphous Silica (Siloxane)	259 ± 3	Brunauer, et al. (24)
Amorphous Silica (Silanol)	129 ± 8	Brunauer, et al. (24)
Tobermorite ($Ca_3Si_2O_7 \cdot 2H_2O$)	386 ± 20	Brunauer, et al. (25)
Potassium Chloride	252 ± 2	Balk and Benson (26)

investigation has been performed for a particular substance is further illustrated by the data contained in Table 2, a compilation of reported values of sodium chloride as determined by heat-of-solution measurements.

At the time this research was begun, the value reported for the surface energy of sodium chloride by Benson, et al. appeared to be by far the best if not, indeed, the true one. This seemed to be so because (1) the technique provided a clearly defined quantity, (2) the method used for the determination of specific surface area was well established, and (3) the method for producing the samples of finely divided material appeared to provide equilibrium surfaces suitable for surface energy measurements. Therefore, this research was undertaken with the objective of using a technique similar to that of Benson, et al.

Table 2. Experimental Values for the Surface Energy of Sodium Chloride at or Near 25°C

Surface Energy (ergs/cm^2)	Method of Measuring Surface Area	Investigators
386	particle size	Lipsett, et al. (19)
395	particle size	Boyd and Harkins (27)
130	gas adsorption	Wertz (28)
366	particle size	Hutchinson and Manchester (29)
276	gas adsorption	Benson, et al. (22)

in an effort to provide an independent check on whether or not theirs was the true value for the surface energy of sodium chloride and to provide measurements of the surface energies of a number of other ionic salts (i.e., KCl, $CaCl_2$, $(NH_4)_2SO_4$, and AgI). Measurements of the surface energy of these solids would be of value not only for the basic physical property information but also for comparison with calculated values as a means for advancing the theoretician's efforts to arrive at a satisfactory model for solid surfaces.

As the research progressed toward the original objective, however, the basic question arose as to whether or not the technique used by Benson and co-workers was satisfactory for producing large specific surface area salts for studies of equilibrium surface properties. The reasons for this are explained in detail in subsequent chapters. Therefore, the emphasis of the research was shifted to an examination of the nature

and properties of the surface of solids produced by the vaporization process.

CHAPTER II

THEORETICAL BACKGROUND

A purely mechanistic explanation of surface energy would require complete knowledge of the nature of surfaces on an atomic scale and the force fields between surface atoms and molecules. Since sufficiently precise information of this type is presently unavailable, the problem is best attacked thermodynamically. Thermodynamics offers a powerful quantitative tool for the study of solid surfaces because a specific geometric model of the surface need not be postulated.

In applying thermodynamics to surfaces, it is convenient to associate definite amounts of energy, entropy, and other extensive quantities with a specified surface area. The method of Gibbs (30) is recognized as being the most advantageous for accomplishing this. In a rigorous treatment, Gibbs shows that a certain quantity of energy (or any other extensive quantity: entropy, number of moles, etc.) can be associated with the presence of a physical surface of discontinuity separating two homogeneous phases. If, for example, the two homogeneous phases or masses separated by a surface of discontinuity are taken as a system the amount of energy E associated with the entire system can be unambiguously divided into contributions from phase 1, phase 2, and the surface. This is accomplished by assigning to phase 1 an energy, E_1, equal to the volume of the mass on side 1 of the dividing surface times the energy density in the bulk phase 1; assigning to phase 2 an energy, E_2, similarly defined; and designating the quantity of energy associated

with the presence of the surface of discontinuity, E_s, by

$$E = E_1 + E_2 + E_s \qquad [2.1]$$

An identical division can be made for any other extensive quantity, such as entropy, S, number of molecules, N_i, of the $i^{\underline{th}}$ component, and so forth. The symbol E_s denotes the excess of energy due to the surface of discontinuity of the total system over the energy that it would have, if, on either side of the dividing surface, the energy density was the same up to the surface as it is at an infinite distance from the surface. Since, however, this excess quantity of energy is associated with the presence of the surface of discontinuity and its magnitude is a function of the extent of the surface, it can be referred to as surface energy. Analogous definitions of other extensive quantities such as entropy can also be established.

That the values of the various extensive properties are changed in the neighborhood of a surface of discontinuity can be readily recognized. Imagine that a certain quantity of material is transferred from the internal portions of phases 1 and 2 of the previously defined system to the surface of discontinuity. Such a transfer, for example, can be accomplished when the shape of a body is changed without changing its volume. If in this transfer all the properties of both phases are completely unchanged, neglecting the minor action of gravitational forces, no expediture of work would be required. This is, of course, a contradiction with experiment for it is necessary to expend work in forming a surface of separation. Therefore, Gibbs' assumption that the

properties of the material in the immediate neighborhood of a surface of discontinuity vary from those of interior portions appears quite valid. It is also most logical to suppose that this change in properties is a function of the distance from the surface of discontinuity. Gibbs, however, preferred to simplify the statement of the problem by assuming that the properties of the substance in the immediate neighborhood of the surface of separation do not depend on the distance from this surface. Between the two bulk phases a new phase is supposed to form which differs from the bulk phases in that its thickness is extremely small in comparison with its extension in two dimensions and, in the limit, is equal to one molecule diameter. This assumption allows the application of the general propositions of heterogeneous equilibrium to the surface phase.

Unfortunately, the literature contains many cases of continued carelessness in the application of thermodynamics to surface systems. This has arisen from a general lack of rigor in discussing surface energetics. For example, the same quantity, usually represented by σ or γ, has been variously called surface tension, surface free energy, specific surface free energy, and surface energy. Since these quantities do not have identical meanings and a particular quantity does not necessarily have the same definition for different systems, all quantities and symbols will be defined unambiguously here.

Consider a system of a pure, crystalline, one-component solid with a finite surface area, A_1, in equilibrium with its vapor at constant temperature and pressure. Let some of the material from the bulk of the solid be brought to the surface reversibly and isothermally

(i.e., by some ideal subdivision process). The surface area of the solid is now increased to some new value, A_2. The limitations will be imposed that the solid, before and after undergoing this increase in surface area, must be bounded by plane surfaces, and that these surfaces possess the same crystallographic indices. The reasons for these limitations will be presented later. The change in internal energy of a system, E, as is well-known, can be expressed as a function of the entropy, S, the volume, V, the number of moles, m, of material forming the system, and the work done on the system, i.e., by

$$\Delta E = T\Delta S - p\Delta V + \mu\Delta m + \sigma\Delta A \qquad [2.2]$$

where ΔE, ΔS, etc., represent the difference in the initial and final states of the system, μ is the chemical potential of the solid phase, and the term $\sigma\Delta A$ represents the amount of work required to increase the surface area from A_1 to A_2*. The term σ is numerically equal to the work of formation of a unit area of equilibrium surface by any reversible process and for the system considered here, as will be shown, can be denoted as the specific surface Gibbs free energy.

It has been implicitly assumed that the chemical potential of the material has not been changed by the process of subdivision. The conditions for which this would not be true would be the case where the internal stress, or state of strain of the solid, or the number of lattice

---

* It should be emphasized that $\sigma\Delta A$ represents, for a solid, the amount of work required to increase the surface area by the amount ΔA only by the creation of new surface and not by the extension or stretching of an existing surface. While there is no difference in these two cases for a liquid, there is for a solid due to the relative immobility of the atoms or molecules.

defects was altered by the subdivision process. The state of a pure, one-component, crystalline solid in an interior region free of line and plane defects is characterized (31) by its temperature, T; volume, V; number of atoms, N; and state of strain, U_{ik}, or, alternately, by temperature, T; number of point lattice defects, N_h; number of atoms, N; and stress, g_{ik}. In terms of the Helmholtz free energy, F, or the Gibbs free energy, G, of the region, the chemical potential of the solid can be defined as

$$\mu = \left(\frac{\partial F}{\partial N} \right)_{T,\ N_h,\ V,\ U_{ik}} = \left(\frac{\partial G}{\partial N} \right)_{T,\ N_h,\ g_{ik}} . \qquad [2.3]$$

Therefore, if the internal stress, or state of strain, remains constant during the subdivision process and the number of lattice defects is constant, the chemical potentials of the initial and final states will be equal.

Since, further, there has been no net change in the number of moles of material for the system, at equilibrium Equation [2.2] reduces to

$$\Delta E = T\Delta S + \sigma\Delta A - p\Delta V . \qquad [2.4]$$

Dividing equation [2.4] by the increment of increase in the surface area and introducing new symbols for the quantities obtained, gives

$$\frac{\Delta E}{\Delta A} = E_s ; \frac{\Delta S}{\Delta A} = S_s ; \frac{\Delta V}{\Delta A} = V_s \qquad [2.5]$$

from which

$$E_s = TS_s + \sigma - pV_s . \qquad [2.6]$$

With the use of the foregoing relationships and the definition of enthalpy, an expression for the specific surface enthalpy, H_s, can be written,

$$H_s = E_s + pV_s \quad . \qquad [2.7]$$

Combining the definition of the Gibbs free energy, G, with Equation [2.6] gives

$$G_s = E_s + pV_s - TS_s = \sigma \qquad [2.8]$$

showing that σ becomes equal to the excess in Gibbs free energy of the system associated with the solid as a result of the presence of a unit area of new surface, and that σ, therefore, can be unambiguously denoted as the specific surface Gibbs free energy*.

The pressure-volume work included in the term σ represents the work of the pressure of the surroundings acting through any volume change associated with the creation of a unit area of equilibrium surface. It is quite possible, and theoretical analyses appear to indicate (32), that there is some slight contraction of the surface layer due to the unsymmetrical atomic force field at the surface which produces a volume change proportional to the amount of new surface created. This volume change, however, should be quite negligible when compared with the total volume until the size of the crystals resulting from the

---

* Gibbs (30) chose to call this term, generally, surface tension. When dealing with fluid surfaces or interfaces this name is quite satisfactory, since, it can be shown that there is a surface density of tensile stress numerically equal to σ. For solids, however, this is not necessarily true (32) and the use of the word tension carries a misleading connotation.

sub-division approaches dimensions the order of 10^{-7} cm. As a result this volume change is often neglected and σ defined as the specific surface Helmholtz free energy.

The symbol E_s represents the difference in energy of the system before and after increasing the surface area of the solid divided by the magnitude of the area increase. It is thus the excess energy associated with the solid as a result of the presence of a unit area of the new surface. Therefore, this quantity can be designated as the specific surface energy. The excess entropy, S_s, associated with a unit area of the new surface arises from the heat per unit area, q_s, that must be supplied to the system to maintain isothermal conditions, i.e.,

$$S_s = \frac{q_s}{T} \quad . \qquad [2.9]$$

If this heat were not supplied the temperature of the surface layer would drop in the course of its formation.

Giauque (33) has shown that the entropy of a small crystal approaches zero as the temperature approaches zero provided the infinately large crystal does likewise. Thus, the specific surface entropy is

$$S_s = \int_0^T \frac{C_s \, dT}{T} \qquad [2.10]$$

where C_s is the difference in the specific surface heat capacity of the solid before and after subdivision. It should be emphasized that this quantity is not equal to the heat capacity of the material in the

surface layer, as is sometimes asserted, but is rather the excess heat capacity of the system after increasing the surface area.

To ensure the validity of the foregoing relationships two specific limitations were imposed upon the subdivision process; that the solid be bounded by plane surfaces before and after the increase in surface area, and that the surfaces have the same crystallographic indices. The reason for the latter limitation is that the value of σ, the specific surface Gibbs free energy, is not independent of crystal orientation, but is strongly dependent upon the type of crystallographic plane forming the surface. The arrangement of the atoms at a surface is a function of the crystallographic plane, and it would be expected that the energy of the atoms in the surface would depend strongly upon their packing and bonding to neighbor atoms. Normally the most closely packed planes are expected to have the lowest values of σ. The limitation of plane surfaces is necessary since, for curved surfaces, the value of σ is slightly dependent upon the location of the reference surface. A change in the location of a curved surface changes the surface area to which the work of creating the surface is referred. The value of σ for a plane surface, however, is rigorously independent of the location of the reference surface, since the areas of the physical surface and the reference surface will be equal.

Values can be obtained from appropriate calorimetric and surface area measurements for the specific surface enthalpy, the specific surface entropy, and the specific surface Gibbs free energy of solids if the limitations imposed upon the preceding relationships are met experimentally. The necessary calormetric measurements involve the

difference in the heat of solution of a finely divided (hence, high surface area) sample and a sample of low (essentially zero) surface area and the difference in the heat capacity of the two samples from $0^{o}K$ to the temperature at which the heat of solutions measurements are made. In this procedure, the difference in the heats of solution is a measure of the excess enthalpy of the high surface area material due to the presence of the surface. Since the pressure-volume work associated with the creation of an equilibrium surface is assumed to be quite small, the specific surface enthalpy, H_s, so obtained is often taken as being equal to the specific surface energy, E_s, to a very close approximation.

CHAPTER III

HEAT OF SOLUTION OF FINELY DIVIDED SODIUM CHLORIDE AND POTASSIUM CHLORIDE

Procedure and Apparatus

The procedure and apparatus for measuring the heat of solution of finely divided material as a function of specific surface area were essentially the same as used by Benson and co-workers for sodium chloride (21)(22). While, in principle, a measure of the specific surface enthalpy can be obtained from heat of solution measurements on a sample of material having essentially zero specific surface area (<0.1 m^2/gm) and a sample having a high specific surface area (≈ 10 m^2/gm), a better method is to measure the heats of solution of several samples having a range of specific surface area. These data can then be plotted as the heat of solution versus the specific surface area. The slope of the resulting line should be the value of the specific surface energy. This method tends to reduce random errors and provides a test of whether or not the quantity being measured is only a property of the surface. If a straight line is not obtained then the quantity being measured is other than a direct function of the surface area as the specific surface energy is supposed to be.

In this research, the heat of solution of a number of samples of both sodium chloride and potassium chloride having specific surface areas ranging from less than 0.1 m^2/gm to approximately 50 m^2/gm were determined. The calorimeter constructed for these heat-of-solution

measurements was a rotating, adiabatic-shield type similar to one described by Benson and co-workers (34)(35). A detailed description of the calorimeter, and its operation is presented in the APPENDIX. Basically, the calorimeter consisted of a stainless steel vessel of approximately 200 cc. capacity, hung from nylon threads inside a set of heater shields the temperature of which could be monitored and varied to maintain adiabatic conditions. The vessel and shields were suspended in an evacuated container which was surrounded by a thermostated water bath. The entire assembly of vacuum can, shields, and vessel could be rotated through 90°, from 45° above the horizontal to 45° below. The temperature of the calorimeter vessel was obtained with a 12-junction, copper-constantan thermopile in conjunction with a Leeds and Northrup Co., Philadelphia, Pa., type K-3 potentiometer, and a Leeds and Northrup stabilized, indicating, dc-amplifier. This combination could detect changes in temperature of at least 5×10^{-4} $^{\circ}C$. The heat capacity of the calorimeter vessel and its contents ranged from approximately 100 cal/$^{\circ}C$ to 200 cal/$^{\circ}C$ depending upon the quantity of water used for solution.

The sample of salt for a heat of solution measurement was sealed in a glass bulb and the glass bulb was placed in a guillotine arrangement inside the calorimeter vessel. Sufficient water was added to the vessel to produce a final solute concentration of 0.5000 molal. Distilled, deionized water was used in all solution experiments but no attempt was made to remove dissolved gases. The calorimeter vessel and contents were first bought to an equilibrium temperature near $25^{\circ}C$. During the equilibration period the calorimeter assembly was rotated to

provide agitation. After an equilibrium temperature was attained, the bulb containing the salt sample was broken and the temperature lowering of the vessel and contents was determined with the 12-junction, copper-constantan thermopile. During the solution period the temperature of the adiabatic shields was adjusted to maintain them at the temperature of the vessel. After an equilibrium temperature was re-attained, the heat capacity of the calorimeter vessel and contents was determined by electrical calibration. To do this, an electric current from lead-acid storage batteries was passed through a heater wrapped around the calorimeter vessel and connected in series with a standard resistor. The contents of the vessel were stirred by intermittent rotation of the calorimeter assembly during the solution and electrical calibration periods.

The total temperature change of the vessel and its contents was usually the order of two to three tenths of a degree centigrade during the solution process, and a similar difference range was covered during the electrical calibration. The electrical calibration was performed at least twice with the results usually agreeing to 0.5 per cent or better.

Preparation of Samples

Samples of coarse salt were obtained by using reagent grade material as received. These were given a final drying before use by holding them in the sample bulb under vacuum at 100° C for at least 12 hours. Attemts to determine their specific surface area by the Brunauer, Emmett, and Teller (B.E.T.) technique of low-temperature, nitrogen adsorption (36) indicated that the area was negligibly small (i.e., less

than 0.1 m^2/gm).

The finely divided salt was prepared by a technique similar to that of Craig and McIntosh (37) and Young and Morrison (38). The apparatus employed is shown schematically in Figure 1.

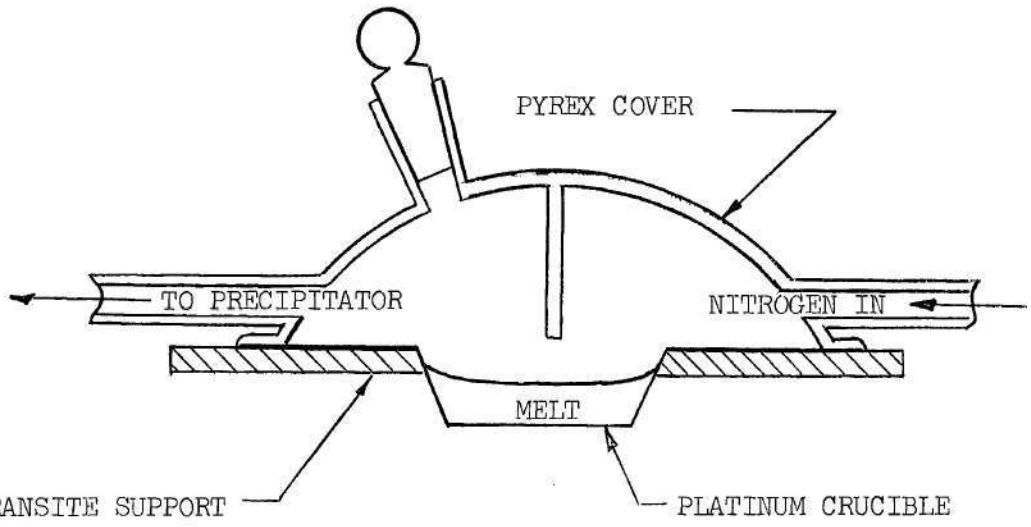

Figure 1. First Generator Design.

The crucible was cold-drawn from a circular piece of platinum 2 inches in diameter and left with a rim 3/4 inch wide around the top. It has an approximate volume of 10 cc. In use the crucible's rim was sealed between the Transite support and the ground surface of the Pyrex cover by springs that passed over the cover and attached to the support. The salt was heated in the crucible by means of a blast burner using a gas-oxygen flame. After the salt became molten, a stream of dry nitrogen was passed through the Pyrex crucible cover. The nitrogen stream after flowing under the baffle passed into the electrostatic precipitator where the smoke of finely divided salt was precipitated. The

electrostatic precipitator consisted of a glass column 122 cm. long and 5.3 cm. in inner diameter. A nichrome wire located in the center of the tube served as one electrode and a layer of metal foil around the outside of the tube as the other. A high-potential source was used to produce differences of up to 7,500 volts dc between the wire and the foil.* The lower end of the precipitator was connected to a glass flask by means of thin-walled rubber tubing and the electrode section was fitted with a ring-shaped brush for periodically sweeping the precipitated salt particles into the flask.

It was possible to produce several tenths of a gram per hour of material having a high specific surface area with this apparatus. The surface area and yield were controlled by the flow rate of dry nitrogen. As the flow rate of gas was increased the rate of heat transfer from the surface of the molten salt was increased significantly and the heat input to the crucible had to be raised in order to keep the surface of the salt molten. Attempts were made to determine the melt temperature by the immersion of thermocouples. However, the temperature indications varied markedly with the depth of immersion, and at best only estimates of the melt temperatures were obtained. These estimates ranged from approximately 950° C for the lowest flow rate (1 l/min.) to approximately 1100° C for the highest (35 l/min.). Samples of both sodium chloride and potassium chloride having specific surface areas ranging from 4 m^2/gm to 48 m^2/gm were prepared by this technique.

---

* Although the source was capable of producing higher potentials, 7,500 volts was used since van Zeggeren et al. have shown (39) that precipitator voltages in excess of 8 kv lead to samples containing excess sodium.

It was discovered early in the preparation program that exposure of the samples having high specific surface areas to the ambient atmosphere for even the briefest interval resulted in a loss of specific surface area. This phenomena had been observed by other investigators (40) and attributed to sintering in the presence of water vapor by a process of solution and recrystallization involving certain parts of the surface. Therefore, the samples were subsequently completely protected from exposure to moisture. After the electrostatic precipitator was swept down, the thin-walled rubber tubing connecting the collector flask to the precipitator was tightly clamped under a positive pressure of dry nitrogen before the flask was removed from the precipitator. The sample flask was immediately transferred to a glove box. The glove box was equipped with an air lock, and the moisture content of its air was maintained at a negligible level with molecular sieve of the Linde Air Products Company, New York, N. Y.

Samples of the finely divided salt weighting approximately one gram were loaded into special thin-walled glass bulbs inside the glove box. These bulbs were fitted with female, 10/30, ground glass joints. The sample bulbs were sealed for transfer and weighing by means of stopcocks fitted with a female, 10/30, ground glass joint on one side and a similar male joint on the other. The stopcock and sample bulb assembly had been previously weighed so that the sample weight was obtained by difference. All weighings were performed with a Mettler, type B6 analytical balance of the Mettler Instrument Corporation, Hightown, N. J. whose accuracy was $\pm$ 0.02 mg. After weighing, the sample bulb and stopcock were attached by means of the female joint to an apparatus for

determining the specific surface area.

The specific surface area of each of the samples was determined by the B.E.T. method of low-temperature, nitrogen adsorption (36). The samples were prepared for the surface area measurements by evacuation to a pressure of at least 1×10^{-4} torr at a sample temperature of 100° C for at least 12 hours. The volumetric adsorption apparatus employed was similar to the one frequently described in the literature (41). The complete adsorption isotherm was obtained for several samples and the findings of MacIven and Emmett (42) concerning the location of the linear portion of the isotherm (i.e., the portion of the B.E.T. plot that includes the relative pressure at which a statistical monolayer is obtained) were confirmed. That is, the linear portions of the adsorption isotherms for both sodium chloride and potassium chloride were found to occur below a relative pressure of about 0.1 instead of in the usual range of relative pressures from about 0.05 to 0.35. Therefore, the slope of the adsorption isotherm below a relative pressure of 0.1 was used in calculating specific surface areas. High purity grade nitrogen of the Linde Air Products Company, New York, N. Y., was used in the adsorption measurements and high purity helium of the Air Reduction Company, Murray Hill, N. J. was used for calibrational purposes. The cross-sectional area of the adsorbed nitrogen molecule was taken as 15.8 Å^2 (43).

After the specific surface area had been determined, the nitrogen gas was pumped off the sample under conditions similar to the initial evacuation. Following this, helium at a pressure of 5 mm Hg was admitted to the sample and the bulb was then sealed by fusing the glass

tube with a gas-oxygen torch and removed from the ground glass joint. The helium served to improve the thermal conductivity and aided in attaining thermal equilibrium. A bulb sealed and ready for use in the calorimeter along with a sample bulb-stopcock assembly are shown in Figure 2.

Results

A number of corrections to the calorimeter data were necessary. These corrections were associated with the energy of the falling guillotine knife, evolution of air from the solution, evaporation or condensation of water to or from the empty vessel space, fracture of the glass sample bulb, and energy associated with the tipping of the calorimeter assembly. The correction for the heat associated with evaporation or condensation of water into the free space as the calorimeter vessel is heated or cooled is easily obtained from latent heat and vapor pressure data. The evolution of nitrogen and oxygen from water at 25° C into the free space created upon breaking the bulb gives a heat effect which can be estimated (34) by

$$q_d = \frac{0.082\ (V_f - V_i)}{1 + (63.9\ V_f/m_w)} + \frac{0.025\ (V_f - V_i)}{1 + (32.3\ V_f/m_w)} \qquad [3.1]$$

where q_d is the heat of evolution in calories, V_i and V_f are the initial and final free volumes of the calorimeter vessel in cubic centimeters, m_w is the weight of water in grams, and the constants depend on the heats of solution and Henry's law coefficients of the gases. The energy of the falling knife of the guillotine was estimated to be only a few hundreths of a calorie and was negligible compared to uncertainties

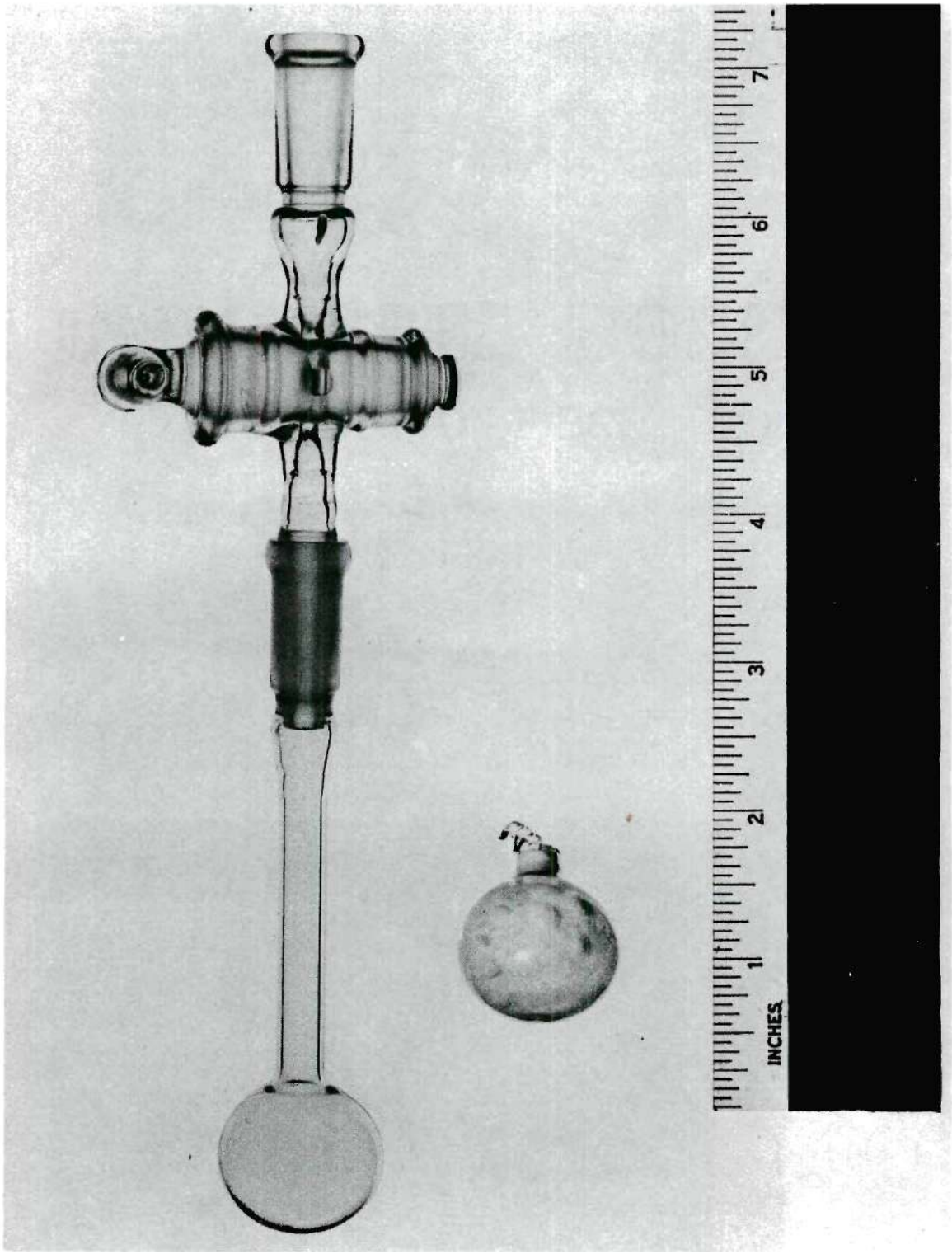

Figure 2. A Sample Bulb-Stopcock Assembly for Transferring and Weighing Samples, and a Sealed Bulb and Sample.

in other correction. The energy of the breaking of the glass bulb is difficult to estimate. Other investigators have measured the heat effect associated with the breaking of glass bulbs and in general have reported that the heat effect is positive (44)(45)(46) or negligibly small (47)(48)(49). Benson and Benson (34) evaluated the heat effects associated with the breaking of bulbs of the size used in this work. They obtained two empirical fits of their data. One involved the sum of an evaporation term and a single term of the evolution type

$$q_t = q_e - \frac{0.10 \quad (V_f - V_i)}{1 + (30\ V_f/m_f)} \qquad [3.2]$$

where q_t is the total heat effect associated with breaking the bulb, and q_e the heat of vaporization of the water into the increased free volume. In every case they observed a temperature decrease and the total heat effect ranged from -0.2 to -0.6 calorie. The mean deviation of their results from this equation was $\pm$ 0.05 cal. Their results could also be expressed by

$$q_t = q_e + q_d - 0.06 \qquad [3.3]$$

where q_d is the evolution effect given by Equation [3.1]. However, the last term of this equation seemed to imply a negative heat associated with the fracture of the glass and they chose to use the semiempirical relationship presented as Equation [3.2]. Since the conditions for this research were the same as were those for which Equation [3.2] was obtained it was chosen for correcting the data of this work.

An attempt was made to determine the amount of energy introduced

by the rotation (tipping) of the calorimeter to stir the contents. A dozen measurements were made of the temperature rise for the calorimeter vessel and contents as a result of 100 tips from 45° above the horizontal to 45° below and return. These tests were made with various amounts of contents in the vessel, since the energy associated with the tipping should be a function of the degree of fullness. In general, these tests revealed no change in the temperature that could be attributed to an energy of tipping. Benson and Benson (34) determined an energy input due to tipping for their calorimeter of about 3×10^{-3} calories per tip. However, their calorimeter rotated through 180° (from 90° above the horizontal to 90° below) and their calorimeter's rotation rate was faster than was employed in this work (12 tips per minute). Therefore, the energy associated with tipping the subject calorimeter was undoubtedly less than the figure reported by Benson and Benson. The number of tips was held constant at ten for all solution and electrical calibration tests, and, even at 3×10^{-3} calories per tip, the error due to this energy input would be less than the uncertainties associated with the breaking of the sample bulb and the dropping of the guillotine knife.

As noted in the APPENDIX, after correction for the heat of evaporation no variation in the heat capacity of the calorimeter vessel and its contents with temperature could be detected over the temperature range utilized. Therefore, no correction was made for the fact that the electrical calibration may not have been performed over the same temperature interval as the solution measurements. However, the average temperature at which the heat capacity determinations were made rarely

differed from the average temperature at which the solution measurement had been made by more than a few tenths of a degree centigrade.

As pointed out by Richard (50), using the heat capacity of the products of a solution experiment leads to a heat-of-solution value for the initial temperature of the experiment. Supplementary specific heat data for the salt, water, and the resulting solution must then be used to correct the heats of solution to 25° C. The defined calorie (4.1840 absolute joules) has been used in stating all results.

A sample computation of a heat of solution is presented in the APPENDIX.

Heats of solution were determined for six samples of sodium chloride and four samples of potassium chloride having essentially zero specific surface area. These data are presented in Table 3. These data

Table 3. Heats of Solution of Low Specific Surface Area Sodium and Potassium Chloride at 25°C.[a]

Sodium Chloride ΔH_s (cal/mole)	Potassium Chloride ΔH_s (cal/mole)
973	4122
985	4104
974	4142
986	4116
976	4121 (mean)
988	
980 (mean)	

a. Expressed as calories per mole of solute dissolving in 2000 grams of water.

give a mean value of 980 cal/mole for heat of solution of sodium chloride and 4121 cal/mole for the heat of solution of potassium chloride. The average deviation for the results on sodium chloride is 6 cal/mole with a maximum deviation of 8 cal/mole. The average deviation for the results on potassium chloride is 11 cal/mole with a maximum deviation of 20 cal/mole.

Heats of solution were determined for nine samples of sodium chloride having specific surface areas ranging from 9 m^2/gm to 49 m^2/gm, and five samples of potassium chloride having specific surface areas ranging from 4 m^2/gm to 20 m^2/gm. These data are presented in Table 4. Figures 3 and 4 show the difference between the heat of solution of each sample and the mean value of the heat of solution found for the samples of sodium chloride and potassium chloride having essentially zero specific surface area. The data of Benson et al. (22)(26) for finely divided samples of these same compounds are also presented for comparison.

The uncertainty in the values presented in Figures 3 and 4 and represented by the vertical lines emanating from the data points were estimated from the deviations associated with the measurements of the heat of solution of samples of coarse salt. That is, since the data points represent the difference in a measured heat of solution from the mean of another set of measurements the uncertainty associated with these values was taken to be least twice the maximum deviation found for the mean value. That this is a reasonable estimate of the maximum uncertainty associated with the values is supported by the fact that the two data points for sodium chloride at about 15 m^2/gm, which almost coincide, fall within these limits and that a smooth curve could

Table 4. Heats of Solution of High Specific Surface Area Sodium and Potassium Chloride at 25°C.[a]

Specific Surface Area (m^2/gm)	ΔH_s (cal/mole)
Sodium Chloride	
9.6	846
14.5	814
14.9	824
24.5	813
30.6	802
43.1	744
46.4	701
47.2	688
49.3	644
Potassium Chloride	
4.2	4011
12.2	3886
14.3	3854
18.5	3601
20.2	3331

a. Expressed as calories per mole of solute dissolving in 2000 grams of water.

be drawn through the data for both sodium chloride and potassium chloride within these limits.

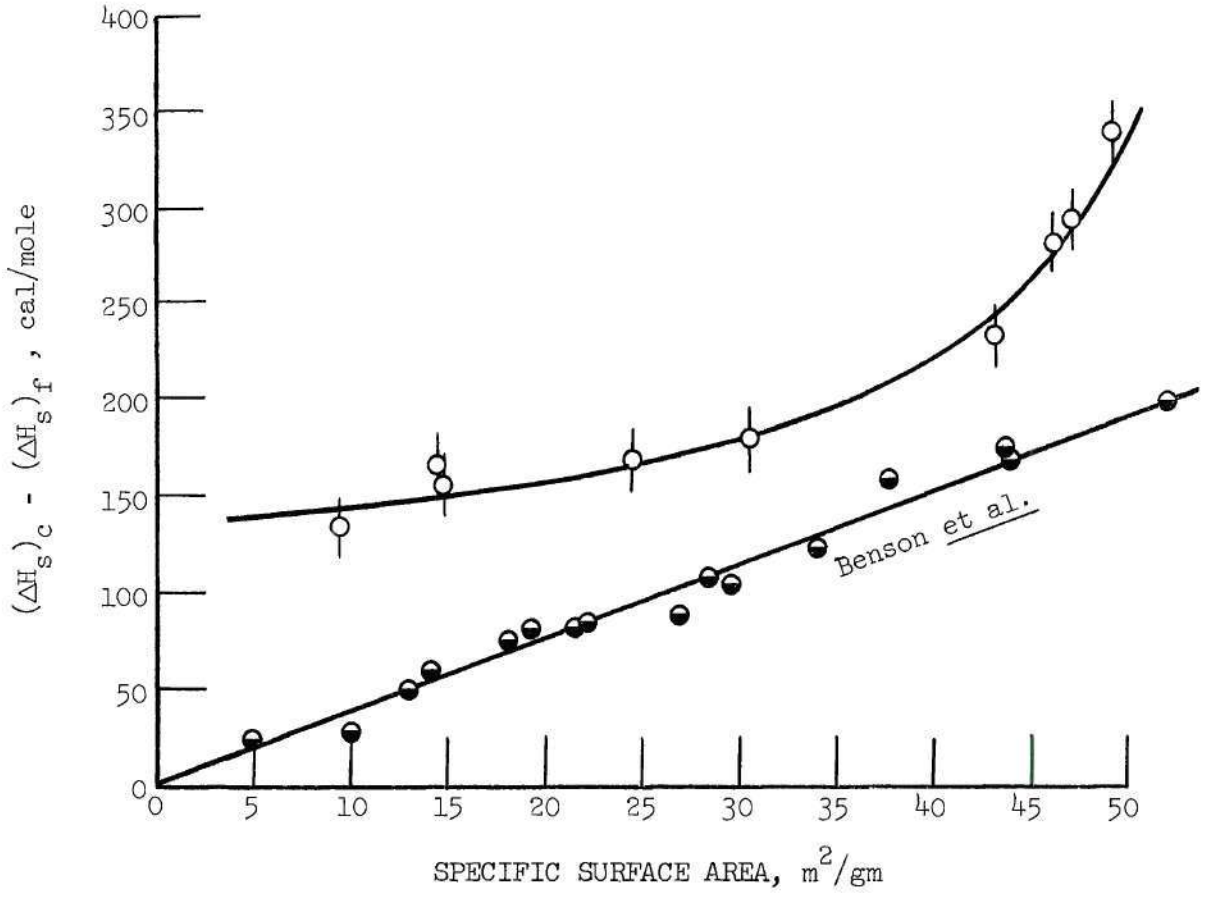

Figure 3. The Variation of the Enthalpy of Solution of Fine Sodium Chloride from that of Bulk Material, $(\Delta H_s)_c - (\Delta H_s)_f$, as a Function of Specific Surface Area.

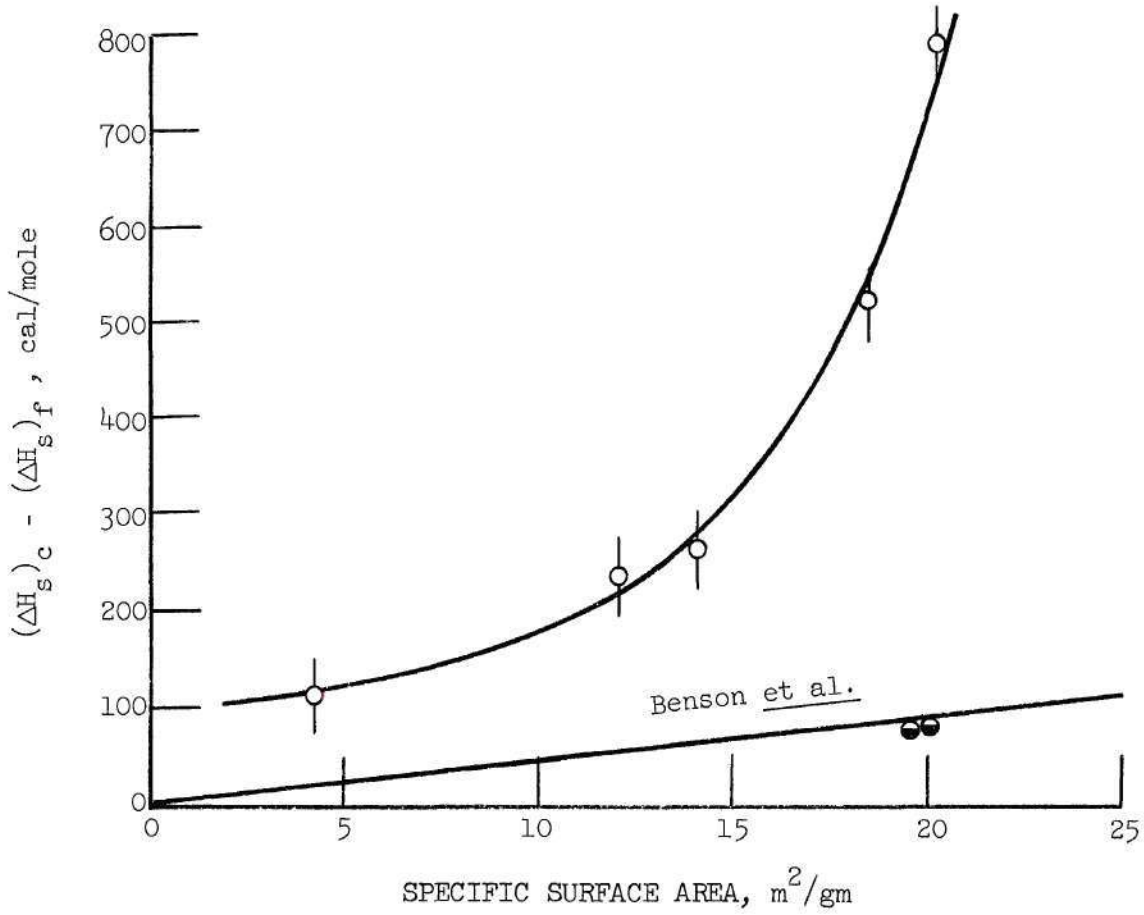

Figure 4. The Variation of the Enthalpy of Solution of Fine Potassium Chloride from that of Bulk Material, $(\Delta H_s)_c - (\Delta H_s)_f$, as a Function of Specific Surface Area.

Despite the relatively high deviation associated with it, a value of 980 cal/mole for the heat of solution of sodium chloride compares well with the values of 984.0 reported by Benson and Benson (34) and the value of 978.5 interpolated from the data of Lipsett, Johnson, and Maass (19). Both of the values fall within the range established by the average deviation of the result from this work. However, the mean value of 4121 cal/mole found for the heat of solution of coarse potassium chloride does not agree as well with the value of 4169 cal/mole interpolated from the table of thermo-chemical data for aqueous potassium chloride solutions at 25°C compiled by the National Bureau of Standards (51). Unfortunately, due to the heterogeneity of the data used in the N.B.S. compilation, nothing is known concerning the confidence that can be placed on this value. The presence of sodium impurities could, of course, result in the lower value obtained in this work.

One other heat of solution measurement was obtained. A sample of finely divided sodium chloride having an initial specific surface area of approximately 22 m^2/gm was exposed to water vapor until the specific surface area was reduced to approximately 0.4 m^2/gm. The heat of solution of this sample was then measured and found to be 975 cal/mole.

It is readily apparent from an examination of the curves in Figures 3 and 4 that the heats of solution of finely divided sodium chloride and potassium chloride do not agree with the data of Benson et al. Neither do these data represent a linear relationship with specific surface area as should be the case if the excess energy due to increased surface area were the only effect being measured. In an effort

to resolve these anomolies, an investigation of the physical characteristics of the finely divided material produced by the volatilization process was undertaken.

CHAPTER IV

MORPHOLOGY AND STRUCTURE OF FINELY DIVIDED SALT PREPARED BY VOLATILIZATION

Particle Morphology Studies

Previous to this phase of the investigation, the salts prepared by volatilization were not examined by electron microscopy. This was not considered necessary since other investigators had reported that electron micrographs of finely divided sodium chloride and potassium chloride prepared in this manner showed the particles to be cubic or at least cubes with rounded corners (38)(40)(52). However, in view of the anomalous results obtained it was decided that such an investigation should be conducted.

Samples of finely divided sodium chloride were taken from the gas stream in the salt generator just ahead of the electrostatic precipitator. These samples were collected by thermal precipitation using a thermal precipitator, Model 100B, of the American Instrument Company, Silver Spring, Maryland. The samples were precipitated directly onto electron microscope grids. Recognizing the previously observed sensitivity to water vapor, the grids were removed from the precipitator in a dry box and placed in a covered Petri dish. The samples were transported to the electron microscope in this dish. The dish was then uncovered, the grid placed in a grid holder, and the grid holder was loaded into an electron microscope, model EM-200, of Phillips Electronic Instruments, Mt. Vernon, N. Y. The operations involving exposure to

air were performed as rapidly as possible. However, the elapsed time varied from one to several minutes.

A mixture of particle shapes was found as shown in the typical electron micrograph presented as Figure 5. The predominant particle shape was cubic, particularly for the smaller particles, with a few large spheres present.

In the search for an explanation of the presence of the larger spherical particles in the samples of volatilized salt, significant reports from two other groups of investigators, Lodge and Tufts (53) and Kerker et al. (54), were encountered. While both groups were working in an area quite unrelated to this study and the technique of generation of Lodge and Tufts was totally different, both neverthless had observed that spherical particles of sodium chloride could be produced and that this shape could not be maintained except under the most anhydrous conditions. Therefore, the technique of transferring to the electron microscope was modified to insure that all exposure to water vapor was eliminated. This was accomplished initially by covering the grids, in a Petri dish, with purified α-pinene. The grids remained moist with α-pinene during loading into the grid holder and into the electron microscope. Once in the electron microscope the α-pinene evaporated into the vacuum of the microscope column.

Later, a technique was developed that consisted of sealing a flexible plastic bag to the column of the electron microscope around the specimen entrance port. This bag had arm holes and could be flushed completely with dry nitrogen. The electron microscope grids upon which the samples had been deposited were then loaded into small

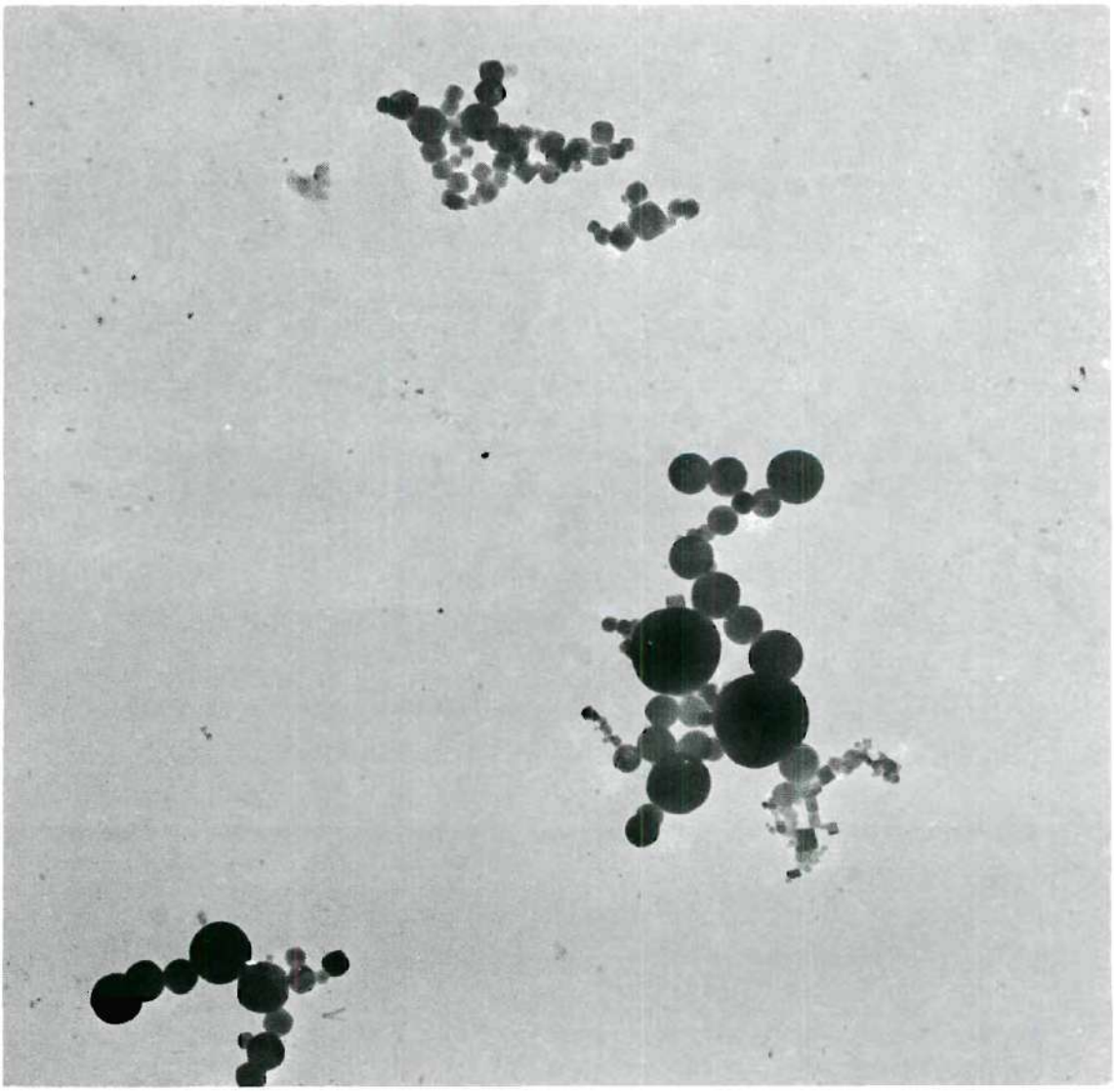

Figure 5. Typical Micrograph of Volatilized Sodium Chloride Paricles That Have Undergone a Brief Exposure to Normal Room Humidity. (Approximately 35,000X).

air-tight, plastic capsules in the dry-box, transported to the location of the electron microscope, loaded, mounted in the grid holder, and loaded into the electron microscope. All the latter steps were conducted within the plastic bag which was under a positive pressure of dry nitrogen.

The sodium chloride samples were found to be composed almost entirely of spherical particles as shown in Figure 6 when they were protected in one of these two ways. After examination, the electron microscope grids were exposed to room atmosphere, and, upon re-examination, the particles were found to reveal the cubic shape. This phenomena is in agreement with the findings of Kerker et al. and is illustrated in Figure 7 by the electron micrographs of the same particles before and after exposure to water vapor. Three additional generator designs were then constructed for the purpose of determining what effect, if any, this had on the shape of the particles produced. What will be called the second generator was produced by removing the baffle in the Pyrex crucible cover of the original design, extending the tube bringing dry nitrogen into the cover until it was directly over the pool of molten salt, and directing this tube downward at the salt. The end of this tube was formed, in addition, into a slit with a total cross-sectional area considerably less than the tube itself. This design is illustrated in Figure 8. The particles produced with it were also spherical. However, at the higher flow rates (approximately 30 l/min.) many of the particles were less spherical and more ligamentized, or dumbell shaped, as shown in Figure 9.

The third generator to be used is illustrated in Figure 10. This

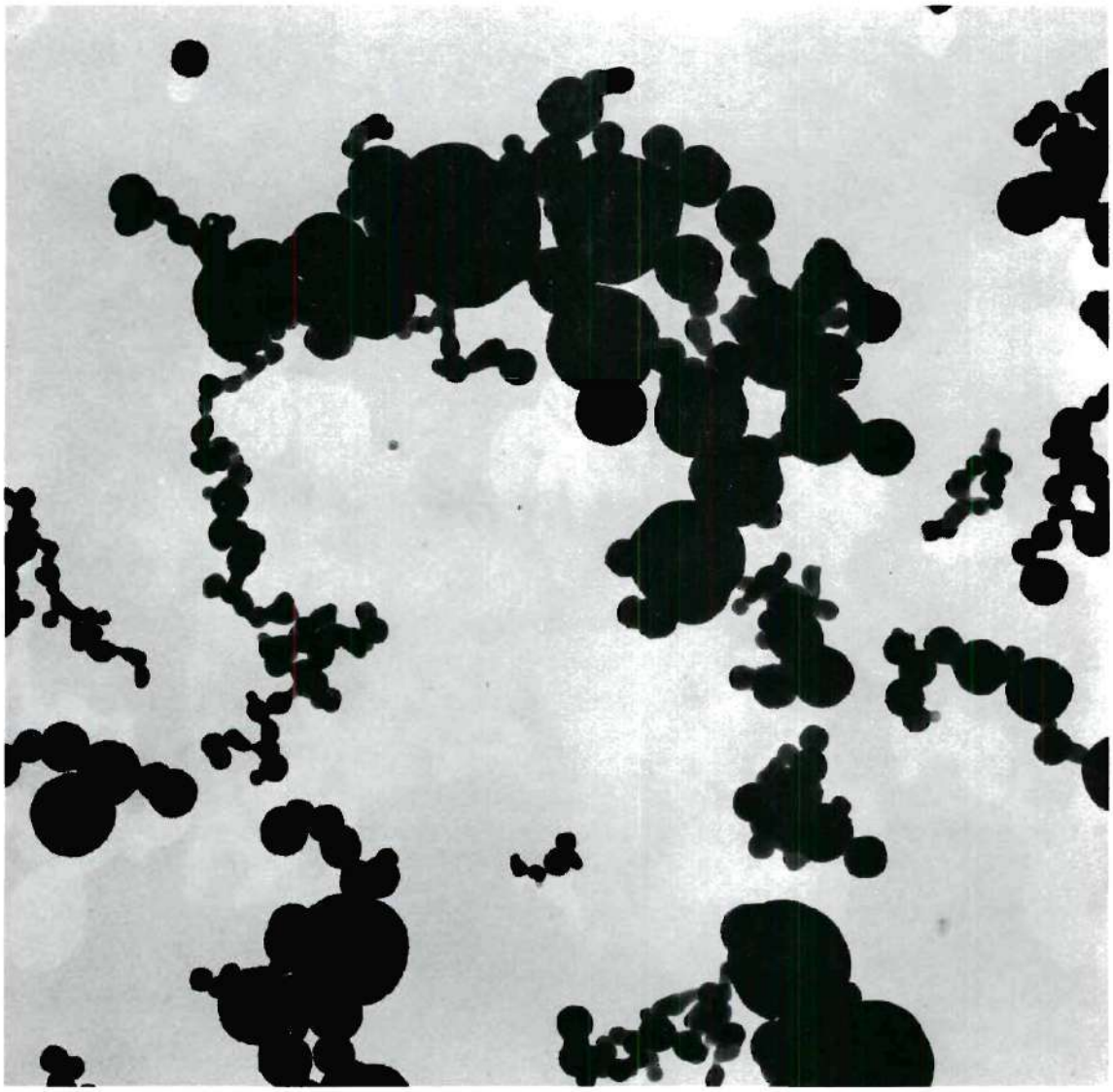

Figure 6. Typical Micrograph of Volatilized Sodium Chloride Particles That Have Not Been Exposed to Water Vapor (Approximately 35,000X).

BEFORE

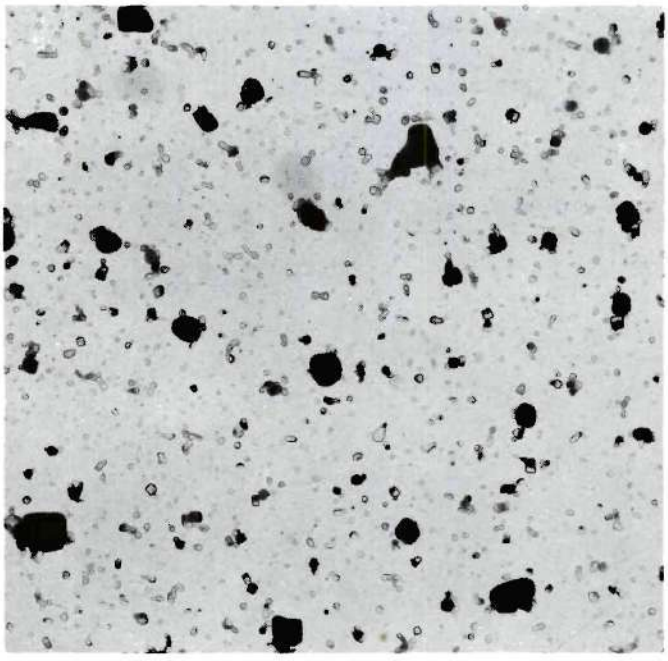

AFTER

Figure 7. Micrograph of a Sample of Volatilized Sodium Chloride Before and After Exposure to Water Vapor (Approximately 7,500X).

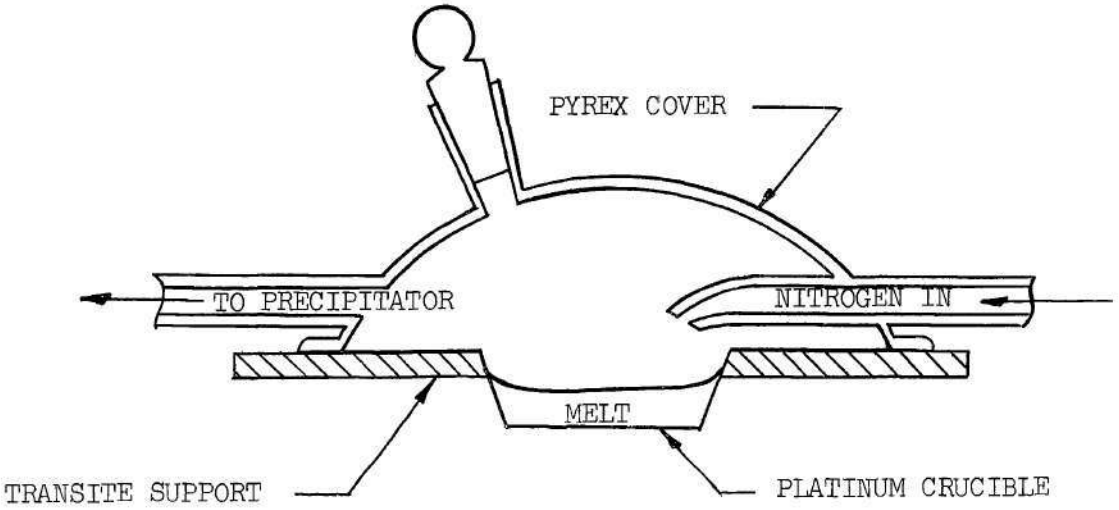

Figure 8. Second Generator Design

generator was constructed from a Pyrex pipe cross and a fused silica crucible. The sodium chloride was heated by means of a thin ribbon of platinum foil immersed in the melt which served as the resistance for a 3 kva output transformer. A stream of dry nitrogen gas entered one arm of the cross and was discharged through the small diameter tube leading from the top. The lower end of this tube was located a few millimeters above the surface of the melt. As the gas stream entered the lower end of this tube it experienced a large increase in velocity, sweeping the sodium chloride smoke along with it out of the chamber. The gas was then directed immediately to the electrostatic precipitator. The particles produced by this generator were also found to be spherical as long as anhydrous conditions were maintained.

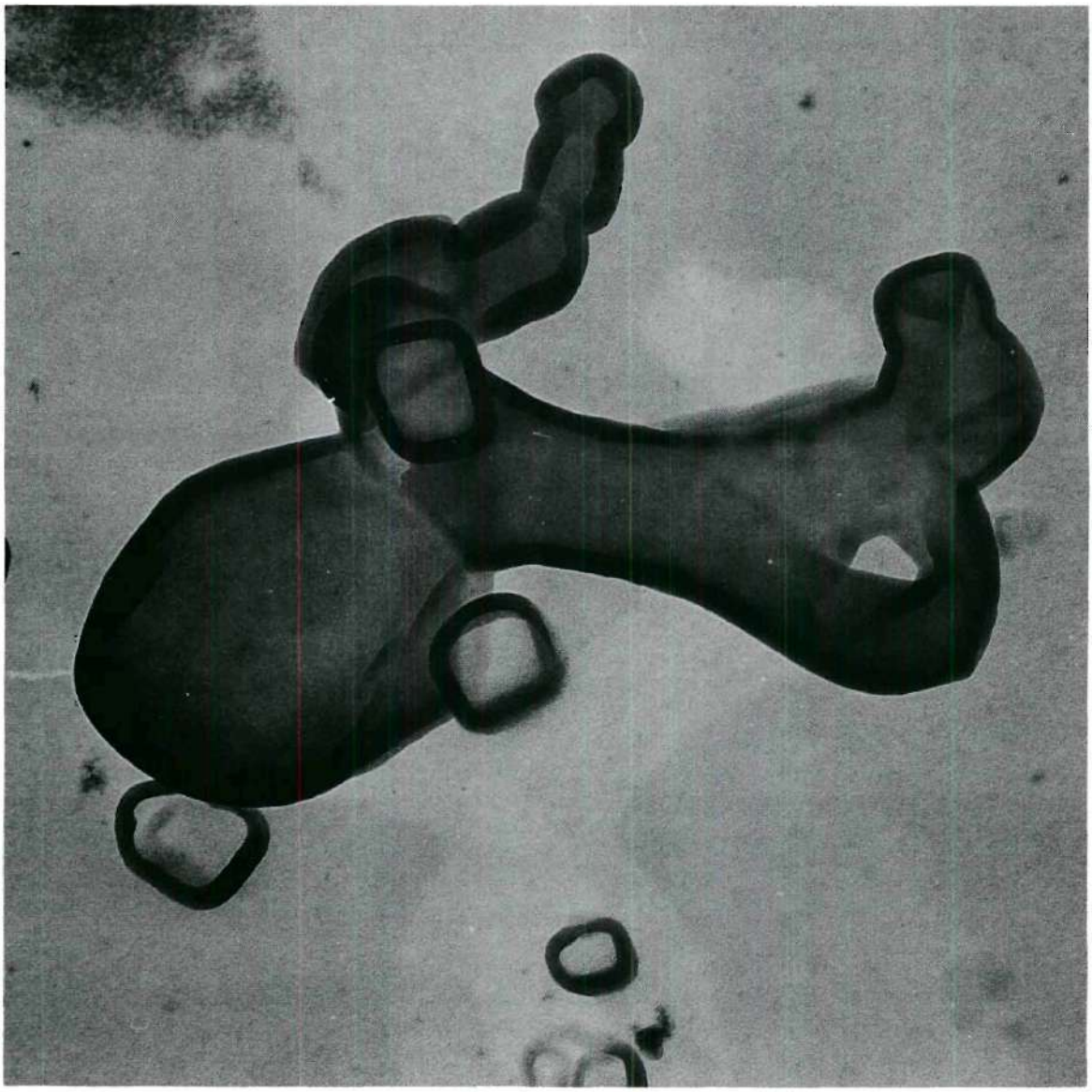

Figure 9. Micrograph of Platinum-Carbon Replica of Sodium Chloride Particles Illustrating Ligament Shaped Particle Resulting From Severe Agitation of Melt Surface During Volatilization (Approximately 100,000X).

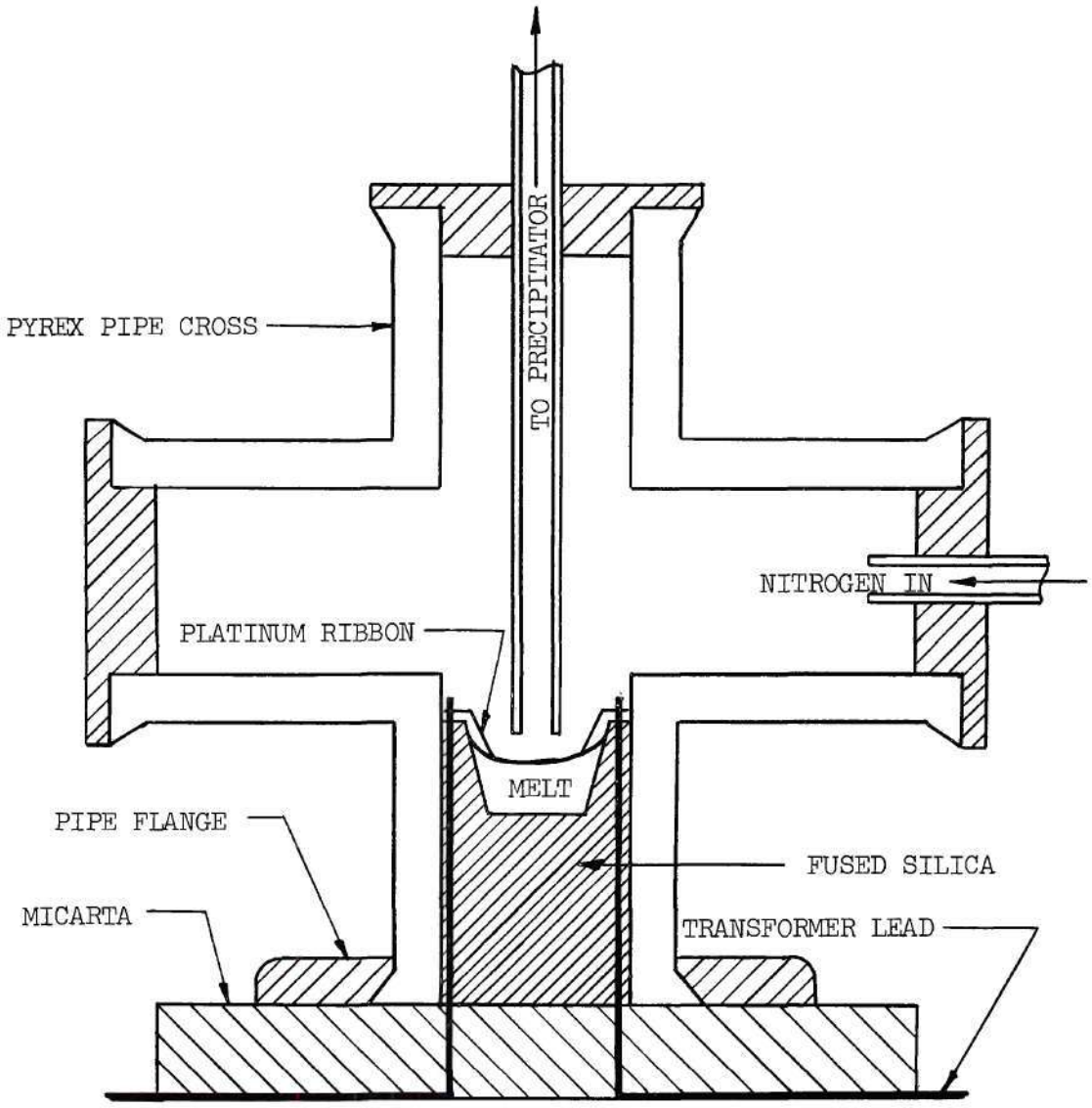

Figure 10. Third Generator Design.

The fourth generator was essentially the same as that used by Kerker et al. In this design a nitrogen gas stream entered one end of a quartz tube that extended through two muffle furnaces. It passed over a platinum boat containing the molten salt in the first furnace and was discharged from the second to the electrostatic precipitator. The muffle furnaces were operated at temperatures ranging from 900°C to 1100°C. The particles produced with this generator were also found to be spherical although their size covered a much wider range than found by Kerker and co-workers.

At this point the original generator design using the baffled, crucible cover was re-assembled. Now instead of passing the gas stream containing the sodium chloride smoke directly to the electrostatic precipitator, the stream was passed immediately into the quartz tube extending through the two muffle furnaces (the length of each furnace was approximately 13 inches) and then to the electrostatic precipitator. If these furnaces were operated at 600°C to 900°C the collected particles were observed to be almost cubic even though the most rigorous anhydrous conditions had been maintained. The use of a single furnace operated in the same temperature range produced a mixture of particle shapes -- spheres, cubes, and polyhedrons. Passing the sodium chloride smoke down the furnace tube without the furnaces being heated resulted in the production of spherical particles almost entirely.

From these observations of the change in crystal habit with the temperature of the downstream environment, it was concluded that the final particle shape was a result of the particles cooling rate. Measurements were made of the gas temperatures entering the

electrostatic precipitator both with and without the use of the muffle furnaces. While the gas temperature when the muffle furnaces were in operation was approximately twice that obtained without the furnaces, the gas temperature did not exceed 100°C even at the lowest flow rates. Since, the gas stream temperature was not raised sufficiently to effect a significant decrease in the particles cooling rate, if the heat transfer mechanism were principally conductive, it was concluded that the heat transfer mechanism was principally radiative.

Crystallinity Studies

It was reported by Kerker et al. (54) that X-ray and electron diffraction examinations showed the spherical particles obtained in their work to be amorphorus. However, after the electron microscope grids were exposed to room moisture so that the spheres recrystallized into cubes, normal diffraction patterns of sodium chloride were obtained (55).

Samples of the sodium chloride produced with the original generator were packed into glass capillary tubes under anhydrous conditions. These tubes were sealed and X-ray diffraction patterns were obtained using a basic Phillips instrument fitted with a Debye-Scherrer powder camera (Phillips Electronic Instruments, Mt. Vernon, N. Y.). Three different samples with specific surface area of approximately 10, 25, and 50 m^2/gm were examined. In every case strong, sharp, diffraction patterns, typical of sodium chloride were obtained.

Many samples of the finely divided sodium chloride deposited on electron microscope grids by thermal precipitation were examined by

transmission electron diffraction using the Phillips EM-200 electron microscope. Spot patterns were obtained for individual spherical particles as shown in Figure 11 and ring patterns were obtained from areas containing many spherical particles as shown in Figure 12. These ring patterns were identical in appearance to those obtained for cubic sodium chloride particles of approximately the same particle size.

The samples of cubic particles were obtained by atomization of a very dilute solution of sodium chloride. A few tenths of one per cent by weight sodium chloride in water was atomized using a No. 180 nebulizer of the DeVilbiss Company, Toledo, Ohio. The aerosol stream was passed over a saturated lithium chloride solution at $0^{\circ}C$ in a large flask to reduce its humidity. The aerosol stream then passed into another large flask from which the sodium chloride particles were deposited on electron microscope grids by thermal precipitation. The particles generated by this technique were of the same order of size as those produced by the volatilization process i.e., a few tenths to a few hundreths of a micron in diameter.

In one particular case, electron reflection diffraction patterns were obtained from a sample of cubic particles, and, immediately following, similar patterns were obtained for a sample of spherical particles having an average radius of about 0.05 micron. An EMU-2 electron microscope manufactured by the Radio Corporation of America, New York, was employed for these determinations. An instrument constant was later obtained for the microscope using finely divided magnesium oxide. With this constant and measurements from the patterns of the two sodium chloride samples, values were obtained for the lattice constants of the

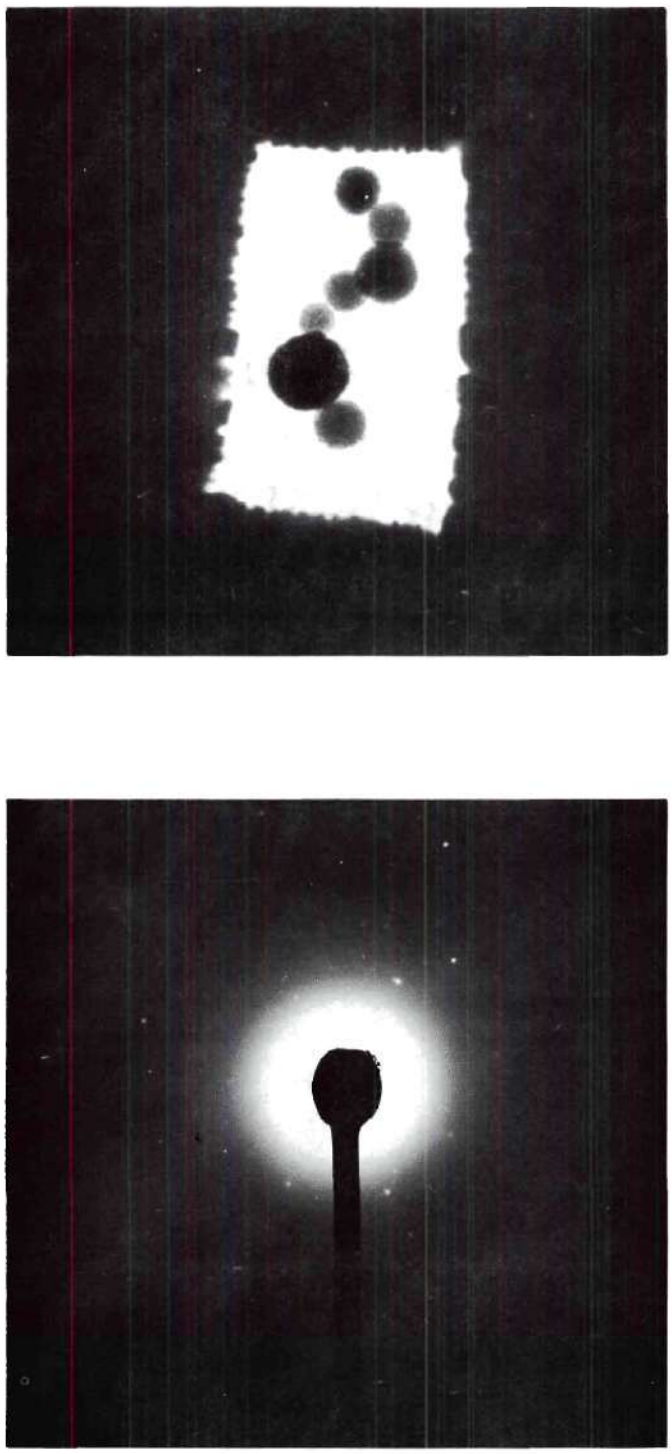

Figure 11. Transmission Electron Diffraction Pattern of Volatilized Sodium Chloride Particles Shown in Accompanying View.

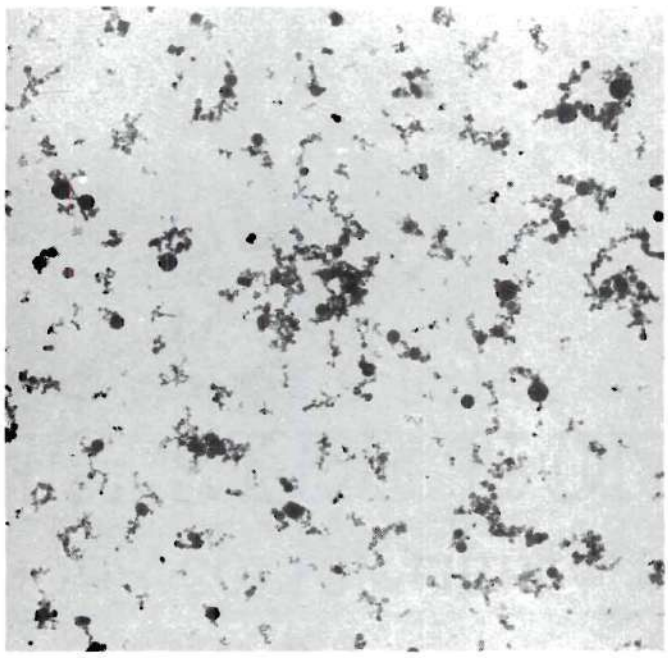

Figure 12. Transmission Electron Diffraction Pattern of Volatilized Sodium Chloride Particles Shown in Accompanying View.

sodium chloride. The lattice constant was found to be 5.602 Å with an average deviation of 0.008 Å, for the sample having cubic particles, and it was 5.582 Å with an average deviation of 0.010 Å for the spherical particles. The deviations associated with these values show that they are relatively imprecise for measurements of this type. However, they do indicate a reduction in the lattice constant of the material when in the spherical form. The deviation of the lattice constant for the cubic particles from the accepted value of 5.640 Å can probably be attributed to the fact that the instrument constant was obtained several days after the measurements on the sodium chloride. However, since the sodium chloride samples were measured one right after the other, any error in the instrument constant should not make a significant error in the relative difference between the constants.

Surface Structure Studies

Surface details cannot be observed directly by electron microscopy except for the very thinnest samples. Therefore, it is usually necessary to replicate the surface with some type of thin film which can be made to assume contours of the surface and to retain these contours when removed. Such a technique was used to study the surface details of the spherical sodium chloride particles in an effort to determine whether or not crystal facets or steps were present.

The conventional technique of evaporating platinum in a vacuum chamber, to reproduce the surface detail and then evaporating carbon to form a continuous film was used initially. The particles to be replicated were sampled by thermal precipitation onto a glass plate.

This plate was then covered with the evaporated films of platinum and carbon, and the film was stripped off the glass and floated onto a water surface. The sodium chloride particles were dissolved from the bottom of the film by the water. A small portion of the replica was finally picked up on an electron microscope grid and allowed to dry.

It was deemed necessary to discontinue the use of α-pinene for the purpose of preventing exposure to water vapor because of the possibility that this might interfere with exact surface replication. Therefore, a simple chamber consisting of two small squares of glass separated by a rubber O-ring was devised. The O-ring was affixed to the upper glass plate with Apiezon wax and a small hook was also attached to the upper side of this plate with the same material. In use the glass slide with the sodium chloride precipitated upon it was placed in the chamber and the chamber selaed with tape, all the manipulation being done in a dry box. The small transporting chamber was then removed from the dry box and placed in the vacuum chamber of the replication unit. Before closing the vacuum chamber, the tape was carefully cut away. The replication device was then evacuated and the upper plate of the small transporting chamber was lifted away by means of a remote manipulator. The valve connecting the vacuum chamber of replication unit to the vacuum manifold had to be opened very slowly, otherwise condensation of the water vapor in the air initially in the chamber occurred due to the rapid expansion. If allowed to happen, this condensation exposed the particles momentarily to a high relative humidity and caused them to recrystallize.

Examination of hundreds of particle replicas from a number of

different samples failed to reveal any definite surface structure. Therefore, a platinum-carbon replicating technique producing better resolution (56) was adopted. This technique -- a simultaneous evaporation of platinum and carbon from rods made with an intimate mixture of the two -- has been used to replicate cleavage steps of the order of 10 Å in height on various crystals. Examination of a few hundred more particles from several samples replicated with this latter technique also failed to reveal any definite surface structure. At least to an order of 10 to 12 Å the surface of the particles appeared to be smoothly rounded without evidence of facets or steps. Some typical electron micrographs of replicas are shown in Figures 13 and 14. Shown in Figure 14 is a particle which, if examined closely, can be seen to possess what appear to be faint facets. This, however, was a rare exception.

A collateral effort to detect the presence of facet intersections or lattice steps on the spherical particles of sodium chloride was made using gold decoration. In this technique, gold was evaporated in a high vacuum onto the particles, a film of carbon was deposited on top of the gold, and the latter film was stripped from the particles and mounted in the usual manner. This should display surface steps on sodium chloride down to atomic heights (57)(58) if such steps existed. The presence of surface edges are revealed by distinct differences in the pattern of the gold nuclei formed on the crystal surface. The gold nuclei along exposed surface edges are more closely spaced and of a smaller size than are nuclei formed on flat parts of the crystal. On two different samples of spherical sodium chloride particles only a heterogeneous distribution of large gold nuclei over the surfaces was found, indicating that

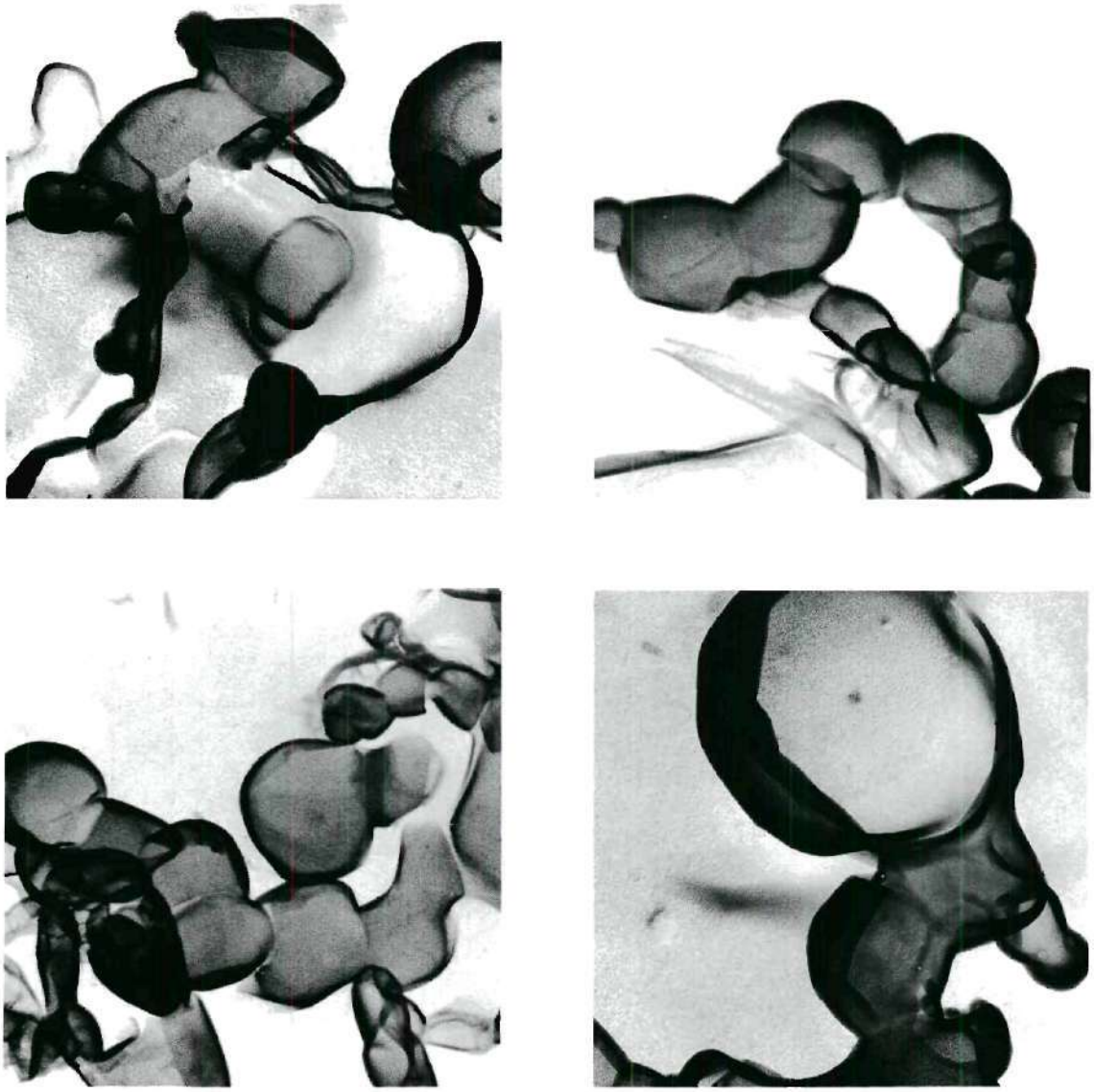

Figure 13. Typical Micrographs of Platinum-Carbon Replicas of Volatilized Sodium Chloride Particles. (Approximately 36,000X).

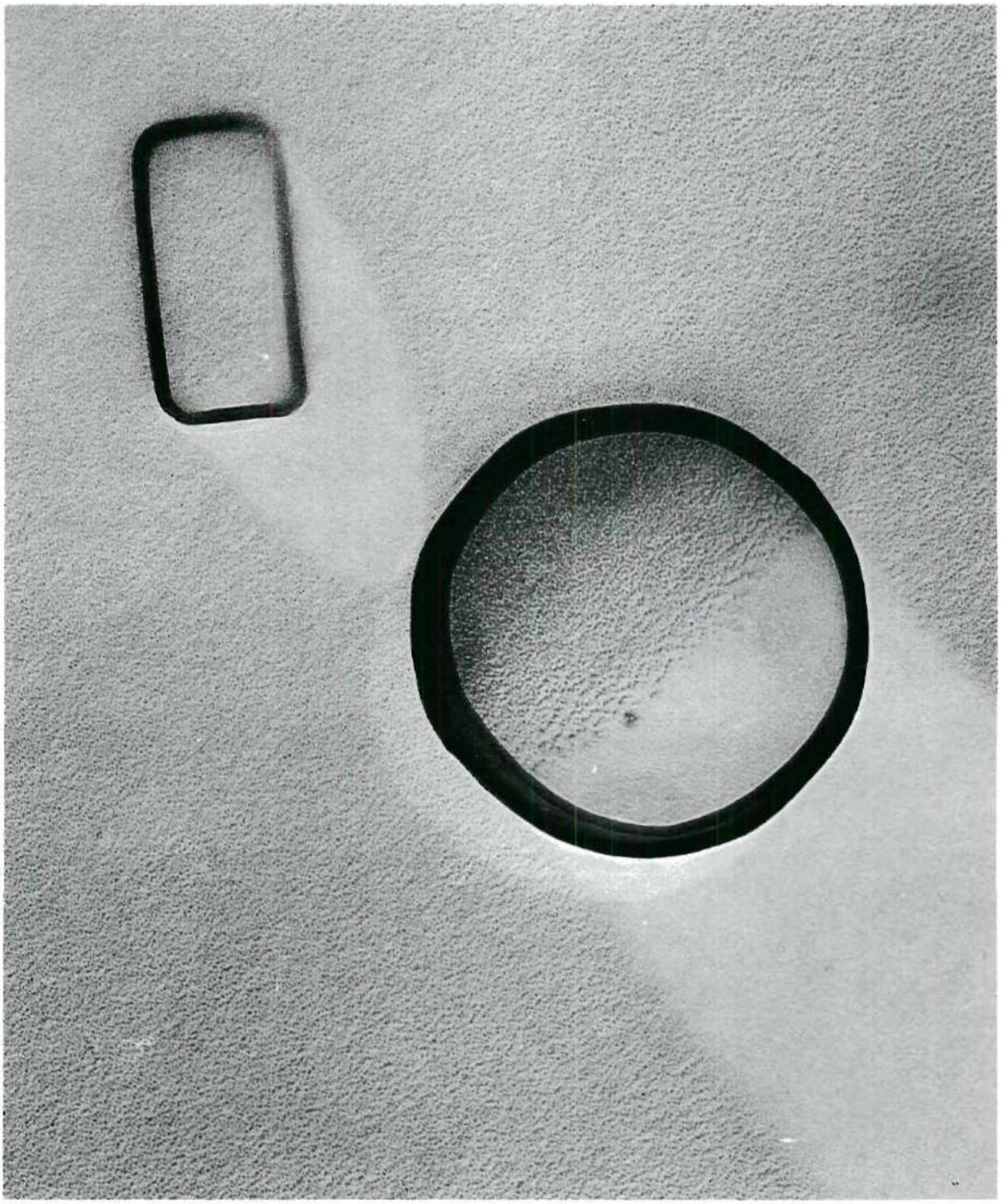

Figure 14. Micrograph of a Platimum-Carbon Replica of Volatilized Sodium Chloride Particles (Approximately 100,000X).

the occurance of steps or edges on these particles was not common at least.

Adsorption and Sintering Measurements

The physical adsorption of gases on the surface of solids can reveal, in addition to the magnitude of the surface area, information concerning the presence of surface irregularities such as cracks, pores, steps and, in theory, the presence of different crystal faces (59). Therefore, complete isotherms were determined for the adsorption of nitrogen gas at liquid nitrogen temperature on samples of both sodium chloride and potassium chloride prepared by volatilization. The specific surface areas of these samples were approximately 30 m^2/gm. The adsorption apparatus was the same one mentioned earlier for the determination of specific surface area.

The isotherms for both sodium chloride and potassium chloride were Type II (60), the sigmoid or S-shaped isotherm with an asymptotic approach to the nitrogen saturation pressure. This contour is typical of crystalline materials that are nonporous such as titanium dioxide. An isotherm for sodium chloride, which was typical also of those for potassium chloride, is shown in Figure 15. Also shown on this plot are the data for desorption of nitrogen gas from the sample. The data points for both adsorption and desorption represent the results of several independent determinations on the same sample.

The absence of hysteresis between the adsorption and desorption isotherms indicates that the particle surfaces were generally uniform and free from cracks, open pores, or crevices (61). No hystersis was

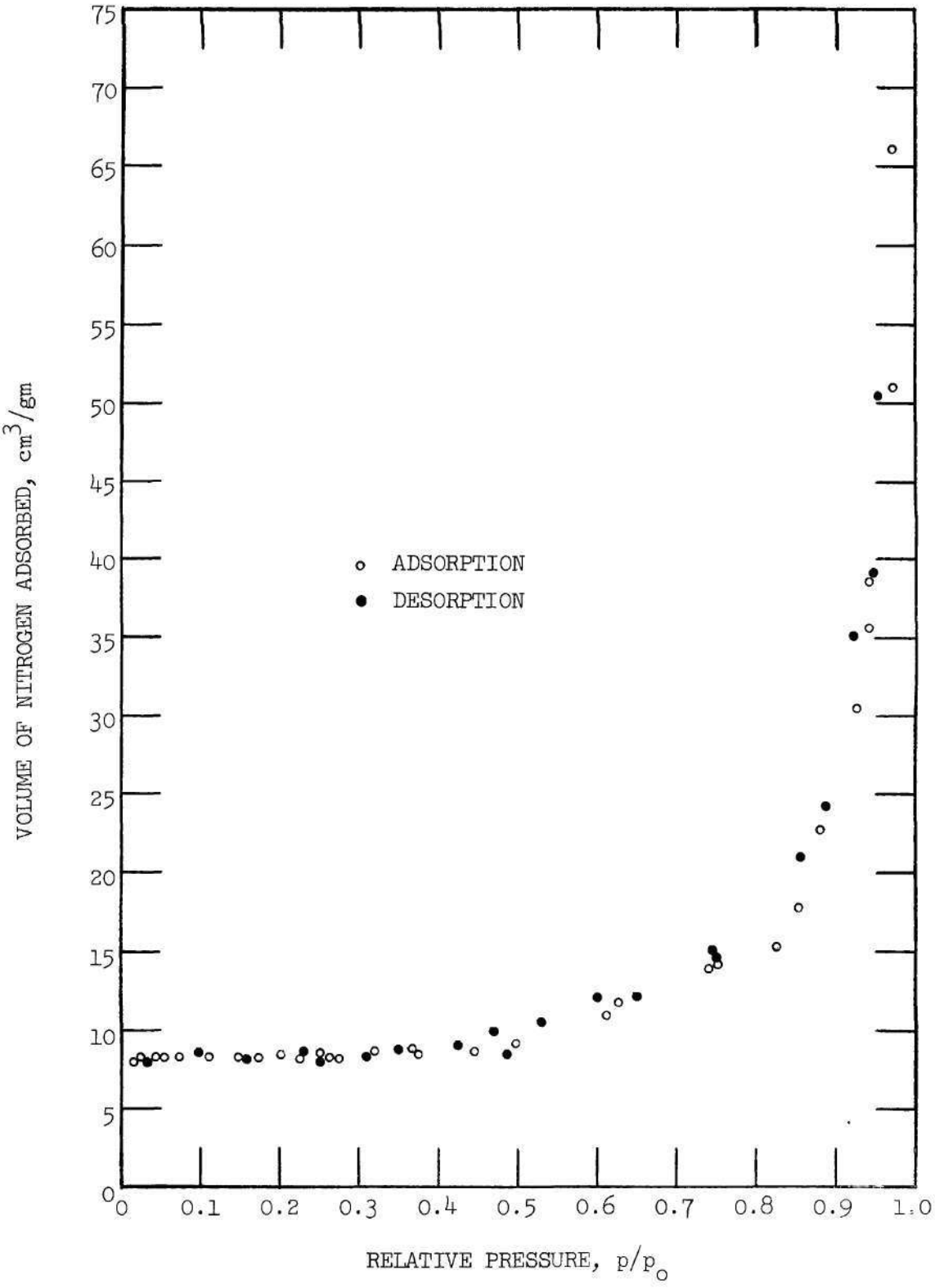

Figure 15. Nitrogen Adsorption-Desorption Isotherm for a Sample of Volatilized Sodium Chloride With a Specific Surface Area of 30.5 m^2/gm.

found between the adsorption and desorption isotherms for potassium chloride either. This absence of hysteresis and the shape of the isotherms are in agreement with the results of Orr (62) and Keenan and Holmes (52) for potassium chloride. The samples used by these investigators were composed of crystals having a normal cubic crystal habit.

Benson and Benson (21) reported that heating samples of finely divided sodium chloride in vacuo for 8 to 10 hours at 200°C would reduce the specific surface area from 40 to 50 m^2/gm to a few tenths of a square meter per gram. Since this temperature is only sufficient to produce surface mobility for sodium chloride (63) the mechanism for surface area reduction appeared to be by sintering. Because of the implication of surface change during heating, a sodium chloride sample previously used for the adsorption isotherm study was sintered in a manner similar to that described and its adsorption isotherm redetermined at various intervals during the sintering process. The sample was sintered in vacuo by heating the sample bulb of the gas adsorption apparatus with a heating mantle controlled at 200°C. The heating was interrupted at various intervals, and both the specific surface area and total adsoprtion isotherms were determined. No change was detected in the form of the adsorption isotherm up to a total sintering time of 120 hours. However, the specific surface area, which did decrease as expected, did not undergo as radical a reduction as had been reported. After 120 hours the specific surface area had only decreased 40 per cent and appeared, as shown in the plot of the data presented as Figure 16, to be approaching asymptotically a total area reduction of only about 43 per cent.

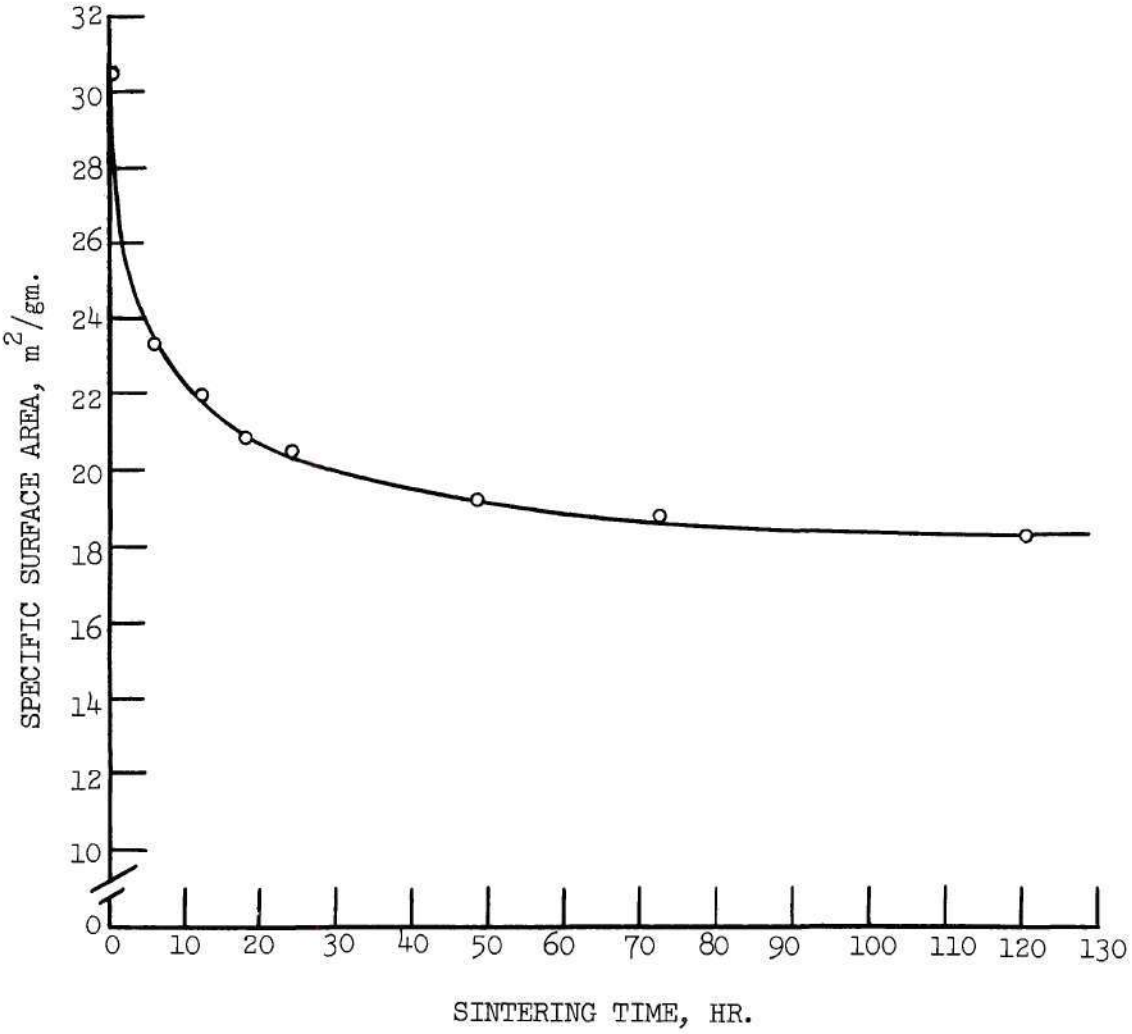

Figure 16. Plot of Specific Surface Area vs. Time for Sample of Volatilized Sodium Chloride Sintered at 200°C in Vacuo.

The reduction in specific surface area thus obtained was in much better agreement with the effects of such sintering that are commonly encountered in catalytic work than the results obtained by Benson and Benson. For example, Maxted and co-workers (64) found that sintering a platinum sample at 400-410°C (the temperature region for which surface diffusion is the principal mechanism) decreased the specific surface area from 11.8 m^2/gm to 8.0 m^2/gm. This is a loss of approximately one-third of the original specific surface area. It was subsequently learned (65) that Benson and co-workers could not reproduce the results previously reported unless the sample was also exposed to water vapor. Sintering by heat alone produced results similar to those found in this work.

CHAPTER V

DISCUSSION OF RESULTS

If the excess energy of a fine sample of material over a sample with a low specific surface area had been attributed to the work necessary to produce the surface, an apparent surface energy of approximately 5×10^2 to 8×10^2 ergs/cm^2 would be obtained for sodium chloride and a value of 1.5×10^3 to 2×10^3 ergs/cm^2 for potassium chloride. Theoretical predictions and previous experimental estimates have indicated that the values should fall in the range 100 to 300 ergs/cm^2 (see CHAPTER I). Therefore, the magnitude of these values would have immediately relegated them to the limbo occupied by similarly unreasonable values obtained for the surface energy of solids* in a number of other studies (13)(37)(66)(67). Fortunately, the technique of plotting values of the heat of solution for samples with various specific surface areas against the value of the specific surface area to obtain the surface energy from the slope was adopted and the fact that this plot did not produce a straight line for the material investigated indicated early in this study that something other than the surface energy was being measured. This was further emphasized by the fact that extrapolation of the curves for sodium chloride and potassium chloride (Figures 3 and 4) to zero specific surface area did not yield values of the heat of solution obtained for the coarse material. The paradox was only compounded when

---

* Careful consideration of the accounts of these determinations reveals that the explanation for them usually lies in the interpretation of what is being measured rather than any experimental discrepancy.

the results were compared with those of Benson et al., whose experimental technique had supposedly been exactly the same as employed in this work.

The most immediate explanations involved the possible occurence of impurities or non-stoichiometry during production of the finely divided material. However, the presence of impurities could not be detected with electron diffraction, and pH measurements of solutions prepared from the finely divided salts did not reveal any stoichiometric deviations. Also, both these explanations became untenable when the sample of the volatilized sodium chloride having an initial specific surface area of approximately 22 m^2/gm was exposed to water vapor until the specific surface area was reduced to approximately 0.4 m^2/gm and the heat of solution was found to be 975 cal/mole. This result indicated that the anomalous heats of solution associated with the finely divided material were a result of the state of subdivision and, as already noted, were due, at least in part, to something other than an increased specific surface area.

Re-examining the literature uncovered a number of cases of anomalous results obtained with finely divided samples of alkali halides prepared by volatilization. The results of Benson and co-workers with sodium and potassium chlorides were anomalous to a degree, since, in both cases values of the surface energy were found that exceeded theoretical ones by 40 to 100 per cent. Morrison et al. (68) found the effect of particle size on heat capacity (surface excess heat capacity) to be 3 or 4 times larger than theoretical. Morrison and co-workers (69)(70)(71) in studies of the chloride in ion diffusion in subsurface layers of volatilized particles of sodium chloride found unusually low

activation energies and other surface anomalies. Craig and McIntosh (37) found an extraordinary sensitivity of volatilized sodium chloride to water vapor and this has been noted to varying degrees in all subsequent investigations with this material. And, of course, Kerker et al. (54) reported a total absence of crystallinity for sodium chloride particles prepared by volatilization. These results, combined with the anomalous results of this investigation, indicated that there was some fundamental difference between the structure of alkali halides prepared by volatilization and the structure normally associated with alkali halide crystals prepared by more conventional means such as crystallization from solution. It was at this point that the detailed investigation of the morphology and structure of the material prepared by volatilization was undertaken.

The observations of previous investigators concerning the volatilization process have not been sufficient to reveal the mechanism of particle formation. From the results with the four generator configurations used in this work it is apparent that, although a high gas velocity across the surface of the molten salt is essential to the production of very fine particles, it is not necessary to have the stream of gas noticably agitate the surface. The size of the particles can be changed significantly by increasing the gas velocity only. When the surface of the melt became significantly agitated larger, ligament-shaped particles began to appear in the collected samples. When no gas was flowing over the surface of the molten salt a dense white smoke could be seen rising from the surface. These observations indicate that molten droplets occur as a result of vapor condensation over the surface

of the melts, and that the rate at which this vapor is swept away controls the size of the resulting particles. There is no question but that the particles exist as molten droplets for a brief time in the gas stream since temperature control downstream at a level below the melting point of the alkali halides can change the resulting particle shape from spherical to polyhedral or cubic. The process of fine particle production by volatization thus is one of vapor condensation over the surface of the melt to form droplets of molten material, and these droplets cooling to solid particles.

The discovery that the particles prepared by this technique were spherical was not particularly revealing in itself. Such particles could still possess high index crystal faces (a mechanically produced crystal sphere may be regarded as a polyhedron on which faces with indices of the very greatest complexity are present), or the surface could be composed of equilibrium {100} faces present as very small steps. The first of these premises seemed unlikely since Kuznetsov (17) has argued that the surface free energy of the higher index faces of sodium chloride, at least through the {111} face, are still only small multiples of the surface free energy of the {100} face (i.e., $\sigma_{\{100\}} : \sigma_{\{110\}} : \sigma_{\{111\}} = 1 : \sqrt{2} : \sqrt{3}$) which would not be a significant enough increase to produce an average value of the magnitude obtained in this work. Also, there is no reason to believe that the relative areas of these faces would vary regularly with a change in particle size sufficient to produce the curvatures shown in Figures 3 and 4. The presence of steps would provide a more plausible explanation since the energy of atoms in a crystal edge should be higher than those in the

surface (72). However, the results using gold decoration and platinum-carbon shadowing as well as the results of the nitrogen adsorption-desorption investigations ruled out the presence of steps any larger than atomic dimensions and revealed no descernible crystal faces.

The results of the tests where the temperature of the downstream environment was controlled showed that the spherical shape of the particles was imposed by rapid cooling when no temperature control was employed. The implications of rapid cooling lent support to the results reported by Kerker et al. (54)(55) that the particles were not crystalline; i.e., they had a structure corresponding to the supercooled melt. However, examinations by both x-ray and electron diffraction showed the particles to be well crystallized. Recognizing that Kerker and co-workers had used helium rather than nitrogen for their carrier gas and that a significant difference in thermal conductivity exists between these two gases, samples were produced with helium and the generator design similar to the one used by them. Examination of these samples by electron diffraction, showed them to be well crystallized also. It was not possible to determine whether the spherical particles were single crystals or polycrystalline, because this required an electron microscope stage that could be tilted in two directions which was not available.

The next explanation of the anomalous heats of solution that seemed worthy of consideration was the energy contribution of the lattice defects that might have been created by the rapid cooling of molten droplets. It has been established on the basis of both experimental evidence and theoretical calculations that the predominant defects present

in alkali halide crystals are Schottky defects (73). In this type of disorder, ions are envisioned as leaving normal lattice sites and taking up positions on the surface of a solid. This phenomenon is one of thermal equilibrium. An equilibrium sodium chloride crystal at room temperature will have approximately 10^6 defects/cm^3. However, several investigators have found that crystals of sodium chloride prepared from melts can possess from 10^{17} to 10^{18} defects/cm^3 at room temperature (74)(75)(76). The total change in the internal energy of a crystal due to the presence of randomly distributed Schottky defects is just the number of defects times the energy required to remove a pair of oppositely charge ions from the crystal. For sodium chloride this energy is approximately two electron-volts (73). Therefore, a simple calculation shows that the change in internal energy will be only 2 cal/mole and 0.2 cal/mole for 10^{18} and 10^{17} defects/cm^3, respectively. This is quite insufficient to account for the observed difference in the heats of solution between the volatilized sodium chloride and the coarse sodium chloride when obtained by solution crystallization. To account for the observed curvatures shown in Figures 3 and 4, some mechanism would be required whereby the defect concentration would be increased exponentially as the particle size decreased. Such a mechanism would appear to be a most unlikely possibility, since there would not appear to be a significant cooling time difference for the size particles under consideration (i.e., average particle diameters of 0.7 to 0.05 micron). Also, for a constant cooling time, the normal mechanism of annihilation of Schottky defects -- migration to a free surface -- would tend to reduce the defect concentration as the radius decreased rather than increase it.

Finally, consideration was given to the fact that the shape of the alkali halide particles was not an equilibrium shape and, therefore, they probably had not attained the thermodynamic equilibrium upon which the entire experimental analysis was based. The normal crystalline habit of sodium chloride and potassium chloride is a cube with {100} exposed faces. This is a consequence of the dictates of minimum free energy. Therefore, any other shape cannot possess the minimum total free energy, and constraints would be necessary to maintain any non-equilibrium shape. The necessary constraint for these solids under the experimental conditions (i.e., room temperature, atmospheric pressure, and absence of water vapor) could, of course, be supplied entirely by the immobility of the atoms as normally associated with solids. It appears therefore, that as a result of the volatilization process the material was constrained by rapid cooling into a higher energy state.

Extremely rapid solidification of a melt usually produces a polycrystalline solid by the simultaneous formation of randomly oriented crystallites. Although the necessary electron diffraction stage was not available during the performance of this research, there is ample indirect evidence that this was the most probable condition. The very shape of the particles themselves suggests a polycrystalline structure. Since the particles were crystalline and yet exhibited no evidence of crystal faces as a single crystal would be expected to do, the most logical explanation of the final particle shape lies in a polycrystalline structure. Also the amophorous structure observed for similar spheres by Kerker et al. indicates polycrystalline material with very small

(i.e., the order of 10Å) crystallites. Further, the density of Schottky defects for alkali halides produced from melts is sufficient to account for the necessary density of dislocation rings in the normal mosaic or polycrystalline structure of these materials (77)(78). Theoretical estimates of the nucleation frequency in alkali halide droplets three microns in diameter predict that the droplets should solidify to a multitude of crystallites (79).

Despite the strong indications of a polycrystalline structure, the curved surfaces of the particles implies a further constraint imposed upon the particles during the solidification process. This constraint, of course, was the necessity for the solid particles to conform to the spherical chape of the initial droplet. If a rectangular crystalline solid, even a polycrystalline one, is subjected to force couples in the XY plane so as to bend the crystal, the bottom, or concave, side will be stressed in compression, and the top, or convex, side will be stressed everywhere in tension as shown in Figure 17. It is easy to visualize then such a

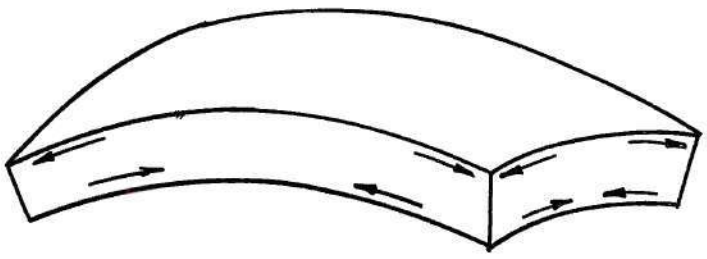

Figure 17. Body Forces in a Bent Crystal

body as an element from the surface of a sphere and to see in the absence of external forces that the material in the interior will be everywhere

in compression with reference to the material in the surface. This uniform stress produced by the constraint of the surface will be exerted uniformly on the body and is analogous to the more familiar concept of hydrostatic stress. This internal stress will produce geometric displacements of points within the solid from positions they would occupy if the stress were somehow removed. Such geometrical displacements are known as strain in the theory of elasticity.

A model, therefore, is proposed to account for the anomalous heats of solution observed for the alkali halides. The principal features of this model are that the spheres are polycrystalline and that the interiors are strained in compression with reference to the external surfaces. These conditions do not correspond, of course, to those used for the analysis presented in CHAPTER II and upon which were based the heat-of-solution measurements for the determination of surface energy. Therefore, an analysis will now be presented, using some of the concepts already developed in CHAPTER II, for a model that is believed to describe the state of the material actually used in these heat-of-solution measurements.

A polycrystalline body contains internal boundaries between crystals of the same phase that are commonly known as grain boundaries. These result from orientation differences. The boundaries may be considered to consist of regions of perfect fit and regions of misfit, resulting in the formation of dislocations at the boundaries. These boundaries which may be either of the tilt type or twist type, are characterized by the angle of misorientation between adjacent planes, i.e., they may be characterized as high-angle boundaries or low-angle boundaries

depending upon the degree of misorientation. These boundaries represent an internal surface with which definite quantities of area and energy of formation may be associated in much the same manner that external surfaces are treated. In fact, the energy of formation of such internal boundaries has been shown to be a function of the energy necessary to form external surface (80). Therefore, the work necessary to form a given amount of internal surface reversibily and isothermally, dw, can be written

$$dw = \sigma_i dA_i \qquad [5.1]$$

where σ_i is the work per unit area or the interfacial Gibbs free energy per unit area, and dA_i is the extent of internal surface.

The work necessary to create a given external surface reversibily and isothermally was discussed in CHAPTER II and can be written

$$dw' = \sigma_e dA_e \qquad [5.2]$$

where σ_e is the work per unit area or the surface Gibbs free energy per unit area, and dA_e is the extent of external surface created.

The work of deformation of any body can be expressed (81) as

$$dw'' = g_{ik} dU_{ik} \qquad [5.3]$$

where g_{ik} is the stress tensor and dU_{ik} is the change in the strain tensor for the solid.

Combining Equation [5.1], [5.2], and [5.3] with the definition of the internal energy, an expression is obtained for the change in energy

of the solid, dE, with changes in the internal and external surface areas and the state of strain

$$dE = dq + \sigma_i dA_i + \sigma_e dA_e + g_{ik} dU_{ik} \qquad [5.4]$$

where dq is the heat necessary to maintain isothermal conditions.

The enthalpy of a deformed body is defined (81) as

$$dH = dE - d\,(g_{ik} U_{ik}) \qquad [5.5]$$

and combining Equations [5.4] and [5.5] the expression

$$dH = TdS + \sigma_i dA_i + \sigma_e dA_e - U_{ik} dg_{ik} \qquad [5.6]$$

is obtained. Therefore, the change in enthalpy for the isothermal and reversible creation of strained, polycrystalline spheres from unstrained cubes with essentially zero internal and external surface is

$$\Delta H = T\Delta S + \sigma_i A_i + \sigma_e A_e - U_{ik} \Delta g_{ik} \qquad [5.7]$$

where ΔS is the change in entropy between the initial and final states, A_i is the amount of internal surface created per mole, A_e is the amount of external surface created per mole, Δg_{ik} represents the change in the state of stress, and ΔH is the enthalpy difference between the initial and final states. This difference in enthalpy per mole represents the quantity measured in the heat-of-solution measurements and is the quantity plotted as the ordinate in Figures 3 and 4.

In order for Equation [5.7] to be really useful, further knowledge concerning the increase in Gibbs free energy due to strain, as

represented by the last term, is necessary. Unfortunately, calculation of the strain energy for real anisotropic crystals is a very complex procedure which has been carried out only in a very few cases where highly simplifying assumptions seemed appropriate. However, the uniform (i.e., hydrostatic) stress of a polycrystalline solid as proposed for the present model simplifies the situation considerably. The polycrystalline model allows the material to be treated as an isotropic medium in which the more random is the polycrystalline array the more exact will be the assumption. In uniform surface, or hydrostatic, compression where shearing stresses are absent, the sum of the non-zero components of the stress tensor are simply equal to the force per unit area directed along the outward normal, or more commonly, the internal pressure. Likewise, for hydrostatic compression, the sum of the diagonal components of the strain tensor are just equal to the relative volume change. Therefore, the strain Gibbs free energy term for hydrostatic compression may be written

$$U_{ik}\Delta g_{ik} = PV_o(\Delta v) \qquad [5.8]$$

where P is the excess internal pressure (internal stress) of the strained state over the unstrained state, V_o is the molal volume and Δv is the change in volume per unit volume.

The excess internal pressure is equal to the difference between the force per unit area exerted on the surface from the interior along an outward normal and the force per unit area exerted on the exterior surface, by the surroundings, along an inward normal. Therefore, it should be recognized that this pressure-volume work is in addition to that included in the definition of σ . This latter pressure-volume

work, as was pointed out in CHAPTER II, is the work of the external pressure acting through whatever volume change occurs for the solid upon the creation of a unit area of equilibrium surface.

The excess internal pressure accompanying small, elastic deformations of a solid under uniform ecompression can be related to the volume change per unit volume (strain) through the use of the bulk modulus of compressibility, K, by

$$-\Delta v = P/K \qquad [5.9]$$

where P is again the excess internal pressure. Therefore, Equation [5.8] becomes

$$U_{ik}\Delta g_{ik} = -\frac{P^2 V_o}{K} \qquad [5.10]$$

Since, however, the internal stress is a result of the constraint imposed on the interior material by the surface, the excess internal pressure can be related to a still more useful quantity, the surface tension.

Gibbs was very careful to point out the difference in surface tension and surface Gibbs free energy when the particular case of solids was considered.* The surface tension, γ, as he defined the term, is the work associated with stretching a surface, while the surface Gibbs free energy is the work expended in forming an equilibrium surface. Unfortunately, since the surface tension and the surface free energy of a one-component liquid are numerically equal and most surface investigations have been conducted with liquids, the two terms

*Gibbs, p. 315

have become to be commonly regarded as equivalent. This, however, is not correct. The only reason the two terms are numerically equivalent for a liquid exhibiting ideal behavior is because of the mobility of the liquid molecules and the lack of any coherency requirements in the liquid structure. This condition will not even hold true for a liquid if the mobility of the liquid at certain conditions of temperature is such that the material (e.g., a wax, pitch, or glass at room temperature) can sustain a surface deformation.

The relationship between the specific surface Gibbs free energy, σ , and the surface tension, γ , has been derived in scalar form by Shuttleworth (82) and shown to be

$$\gamma = \sigma + A \left(\frac{d\sigma}{dA}\right) \qquad [5.11]$$

for an isotropic substance or a crystal face with a three-fold or greater axis of symmetry. In this equation $d\sigma/dA$ is the change in the specific surface Gibbs free energy for an extension in surface area with a constant number of atoms in the surface layer.* The same relationship in the more general, tensor form has been given by Herring (31). For a liquid there is no change in the specific surface Gibbs free energy with surface area and the last term in Equation [5.11] is zero. Unlike liquids, it is possible for a solid to possess a surface tension which is not necessarily equal to the equilibrium specific

---

* The physical significance of the term $d\sigma/dA$ with the provision of a constant number of surface atoms can be readily grasped if it is remembered that the energy of the atoms in a surface are dependent upon the efficienty of packing and, hence, upon bonding to neighbors. This term represents the increase in energy with a reduction in the efficiency of packing due to the stretching of the surface.

surface Gibbs free energy. For example, the process of forming a new surface of a solid by cleavage can be thought of as occurring in two steps. First, the solid is cleaved to expose new surface, keeping the atoms fixed in the same positions that they occupied in the bulk phase, and, second, the atoms in the surface region are allowed to rearrange themselves into their final equilibrium positions. In an ideal liquid these two steps occur as one and the equilibrium surface tension is established within a millisecond or less. For solids the second step may occur only very slowly because of the immobility of the surface region. It is the surface tension that is the driving force for this rearrangement and it is only when the atoms have rearranged to their equilibrium configuration that the value of the surface tension will equal the equilibrium specific surface Gibbs free energy.

The surface tension is the resultant force that exists between surface atoms because they are in a non-symmetrical force field.* The important difference between solids and liquids is, of course, that the spontaneous contraction of a liquid film, which can be prevented only by the application of an external force equal and opposite to the surface tension, has no counterpart in the case of a solid sheet. In a solid the cohesive forces acting inwards on the surface molecules are balanced by elastic reaction set up within the solid itself. It is

---

* Because either tensile or compressive surface stresses can exist in solids as opposed to liquids, the term surface tension is not entirely appropriate for discussing solids. This is particularly true when discussing the surface stresses arising from mechanical deformation, a condition that cannot exist with liquids. Therefore, the more general term surface stress should be used in discussing the quantity γ for solids, with the understanding that positive values represent tension and negative values compression.

unnecessary to apply an external force in order to prevent the contraction of this surface. That surface stresses, both tensile and compressive, can exist in the surfaces of solids has been considered theoretically by several authors (31)(82)(83)(84); a particularly lucid demonstration of the source of such stresses in terms of the attractive and repulsive forces between atoms has been given by Shaler (85). Previous considerations of the surface stress in solids have been concerned principally, however, with the stresses tending to rearrange surface atoms from bulk lattice configurations to the lattice configuration corresponding to an equilibrium surface. Little or no consideration has been given to the situation where the surface tension of a solid may be associated with significant volume strain. This will be considered here.

When a solid surface has zero curvature, the surface stress can be balanced by elastic displacements within the interior such that equal and opposite volume stresses operating parallel to the surface balance the surface stress. If, however, the surface is curved it is also necessary to apply normal forces to each point in the surface. For an isotropic material a relationship between the normal stress produced by this normal force can be developed in terms of the restraining surface stress (tension in this case) and the radius of curvature of the surface. This can be accomplished using the principle of virtual work in a manner similar to that used for determining the excess pressure of a liquid droplet.

Consider first an expression for the work that would be done by the excess internal pressure if the volume of a sphere were allowed to increase reversibly and isothermally by a small increment dV. This work expression may be written

$$dw_1 = -PdV \quad . \qquad [5.12]$$

Next, consider the work that must be done on the surface of the sphere to stretch the surface, A, by an amount dA corresponding to the volume increase dV . Provided this deformation is reversible and isothermal, the work, dw_2, required is equal to the increase in the free energy of the surface.

$$dw_2 = d(\sigma_e A) = \sigma_e \, dA + A \, d\sigma_e \qquad [5.13]$$

where σ_e is the specific surface Gibbs free energy as defined in CHAPTER II and has exactly the same significance attached to it as in the derivation of Equation [5.7]. For an isotropic substance, or a crystal face with a three-fold or greater axis of symmetry where all normal components of the surface stress equal the surface tension, γ, Equation [5.13] can be written

$$dw_2 = \sigma_e \, dA + A d\sigma_e = \gamma \, dA \qquad [5.14]$$

from the definition of surface tension presented in Equation [5.11].

Expressing now the incremental increase in surface area as a function of the incremental increase in the volume without change in shape by

$$dA = \frac{2}{r} \, dV \qquad [5.15]$$

and imposing the condition of virtual work, i.e.,

$$dw_1 + dw_2 = 0 \qquad [5.16]$$

the expression is obtained relating the excess internal pressure to the surface tension

$$P = \frac{2\gamma}{r} \quad . \qquad [5.17]$$

Combining this expression with Equation [5.10] for the increase in the Gibbs free energy due to strain and Equation [5.7] for the change in enthalpy yields

$$\Delta H = T\Delta S + \sigma_i A_i + \sigma_e A_e + \frac{4\gamma^2}{Kr^2} V_o \qquad [5.18]$$

for the increased enthalpy of the strained, polycrystalline spheres over the unstrained cubes with essentially zero specific internal and external surface area such as employed as the reference material in the heat-of-solution measurements.

A qualitative comparison of Equation [5.18] with the heat-of-solution data presented for sodium and potassium chloride in Figures 3 and 4 indicates immediately that the equation can account for the essential features of these curves. For example, as the external specific surface area goes to zero only the first two terms on the right-hand side remain. These express the Gibbs free energy contribution of the internal area and the entropy associated with this disorder. Since, an interfacial energy is always a positive quantity and the entropy change associated with the creation of the interface is also a positive quantity, the contribution of these two terms at zero specific surface area can account for the positive intercept at the ordinate of Figures 3 and 4. As the external specific surface area is increased, the last two terms of Equation [5.17] begin to contribute to the enthalpy as does the entropy

term as the state of disorder is increased. The term $\sigma_i A_i$ representing this Gibbs free energy contribution will decrease because the internal area decreases when the external area increases. The total change in enthalpy from these two terms will be an increase, since, for a constant crystallite size, two square centimeters of external surface area are created for every one square centimeter of interfacial area that disappears through subdivision and since the external surface energy is at least two to three times the value of the interfacial energy (80). That is, a plot of the change in enthalpy with increasing external specific surface area will show a positive change. The last term of Equation [5.18], the term representing the Gibbs free energy of strain will be responsible for the curvature noted in Figures 3 and 4. This term is dependent upon the particle radius squared, whereas the terms containing the specific surface area are actually function of the radius* only. The relative behavior of these Gibbs free energy functions with increasing external specific surface area are shown in Figure 18.

Therefore, enthalpy curves such as shown in Figures 3 and 4 should represent the sum of curves such as those above and a curve representing the entropy variation with change in external specific surface area. Unfortunately, very little detail can be deduced about the shape and contribution of the latter curve except that the entropy contribution associated with each of the previously discussed terms will probably exhibit similar variations with the external specific surface area, and that the total contribution will probably be small.

---

* From purely geometrical considerations it can be shown that specific surface area on a weight basis, S_w, is related to a sphere's diameter or a cube's edge, d, and the density of the material, ρ, by $S_w = 6/\rho d$.

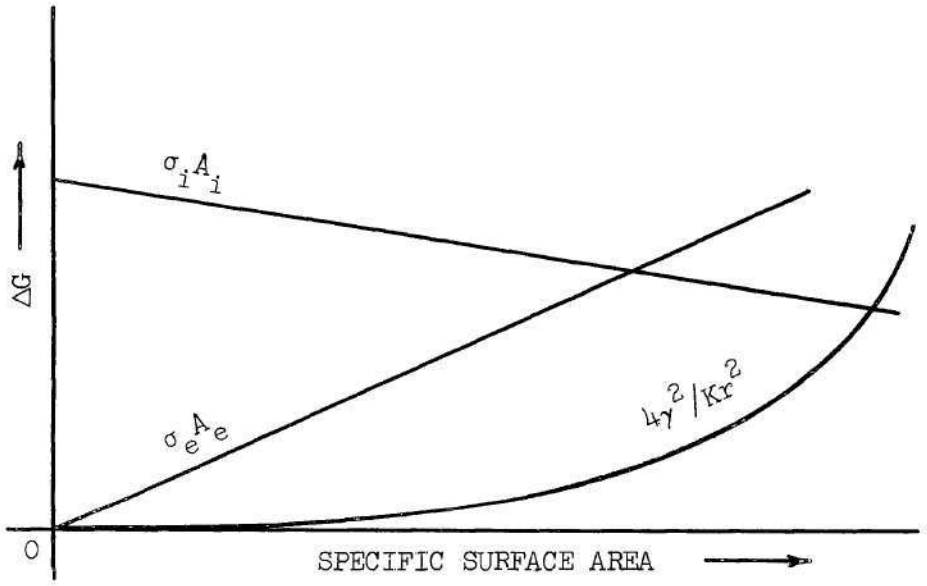

Figure 18. Variation of the Interfacial Gibbs Free Energy, the Surface Gibbs Free Energy, and the Gibbs Free Energy of Strain with the External Specific Surface Area.

It would now seem advisable to ascertain, at least semiquantitatively, whether or not the values necessary to fit Equation [5.18] to some of the experimentally observed quantities are reasonable. Also, it would be of considerable interest to obtain estimates for the surface tensions of sodium and potassium chloride as no values have been obtained prior to this work.

From extrapolated intercepts of Figures 3 and 4 it may be seen that excess energies of approximately 135 and 100 cal/moles, respectively, are found for volatilized sodium and potassium chloride with essentially zero surface area. If the entropy contribution is neglected, an estimate can be obtained of the necessary crystallite size to produce sufficient interfacial or intergranular area to account for this

energy. Taking 188 ergs/cm^2 for sodium chloride and 163 ergs/cm^2 for potassium chloride as being the best theoretical estimates (10) of their specific surface free energies and recognizing that the specific interfacial free energy of crystalline materials can be anywhere from a few per cent to 50 per cent of the specific surface free energy depending on the angle of misorientation between crystallites (80), the necessary crystallite size is found to be between approximately 30 and 150 Å. These do not appear to be unrealistic values.

Since, it has been argued that the curvature in Figure 3 and 4 are the result of the strain energy contribution it is possible to estimate values of the surface tension for sodium and potassium chloride from these plots. From the nature of the curvature and the values of specific surface area at which the plots of Figures 3 and 4 become curved it can be seen that the strain energy term does not become significant until particle diameters are well below a micron. Therefore, at large values of particle radius (i.e., low specific surface area) the principal contributions to the total curve should be the summation of the terms of Equation [5.18], representing the Gibbs free energies associated with the internal and external areas, and the entropy contribution from the presence of interfacial and external area. This is to say, the slope of the total curve at large values of particle radius should be determined principally by the summation of the linear terms, and, because of this linearity, the slope of their summation should be constant. Therefore, a tangent to the differential heat-of-solution plots, as shown in Figure 19, should closely approximate the slope of the summation of the linear terms over the entire range of the data. As can be seen from the

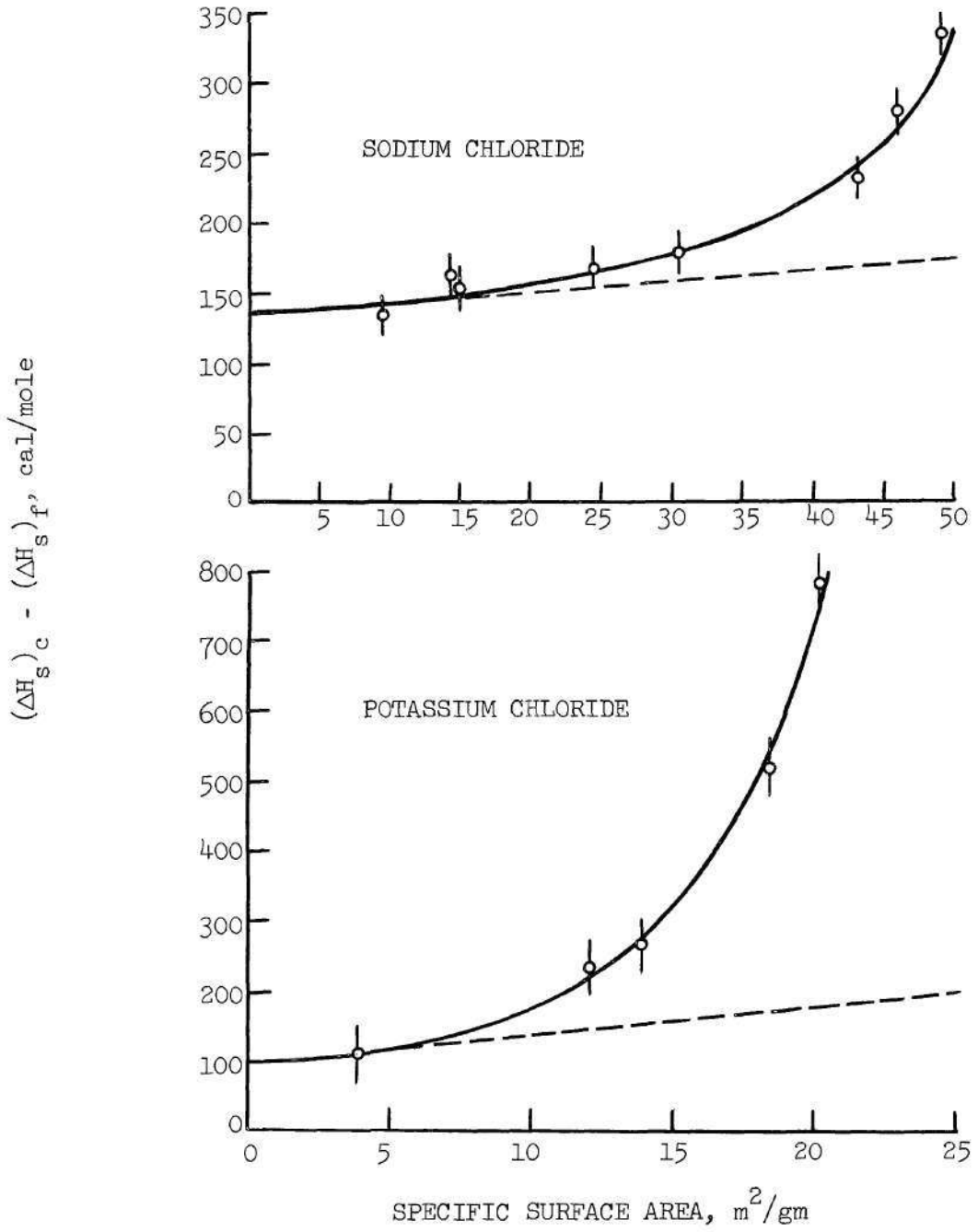

Figure 19. Plots Showing Tangents to the Low Specific Surface Area Portions of the Heat-of-Solution Curves

figure, these slopes are quite small compared to the slopes of the total curves at small values of the particle radii.

It is apparent also then, as one might expect, that the slopes of the total curves where the curvature is quite great are determined almost entirely by the term of Equation [5.18] representing the Gibbs free energy of strain plus whatever small contribution the entropy term associated with the strain might make. Therefore, by utilizing tangents to the total curves where the curvature is large, with the first derivative of strain energy term of Equation [5.18] approximations for the surface tensions of sodium and potassium chloride can be obtained. Using the value 2.5×10^{11} dynes/cm^2 for the bulk modulus of compressibility of sodium chloride (86), tangents to the sodium chloride curve between 40 and 50 m^2/gm yield values of 1×10^5 to 2×10^5 dynes/cm for the surface tension of sodium chloride. The value 1.5×10^5 dynes/cm obtained from the slope of the curve at 45 m^2/gm appears to represent a fair average. Likewise, using the value of 1.9×10^{11} dynes/cm^2 for the bulk modulus of compressibility of potassium chloride (86) a value of approximately 4.5×10^4 dynes/cm is obtained for the surface tension of potassium chloride from a tangent to the potassium chloride plot at a specific surface area of 17.5 m^2/gm.

These values for the work necessary to extend the surface area of a solid, if even reasonably correct, are a very siginificant finding, in that they represent considerably more work than has been previously hypothesized. Values of this magnitude suggest that surface stress may play a significant role in explaining such phenomena as the dependency of the strength of some solid bodies on the age of the surface, the

origin of Griffith flaws in brittle solids, and the extraordinarily high yield strengths of solid bodies with a high surface to volume ratio.

Since there have been no other known estimates of the work necessary to stretch the surface of a solid, the reasonableness of the values cannot be established by direct comparison. Shuttleworth (82) has calculated from purely theoretical considerations of interatomic forces that the energy difference between surface atoms in a configuration corresponding to the bulk lattice and a configuration corresponding to a proposed equilibrium surface configuration is 130 dynes/cm for sodium chloride and 375 dynes/cm for potassium chloride. Shuttleworth calls these values the surface tension, and, in fact, finds the values to be negative, and therefore,a compressive force. However, it is not at all certain that what Shuttleworth has calculated is the same thing as measured here, and by Shuttleworth's own admission the inaccuracies in the model are so great that his values are uncertain even as to sign. Herring has said (31) that the change in free energy with surface area, $d\sigma/dA$, would be expected to be "sizeable" for a solid, but very roughly the same or a little larger than the specific surface free energy. The expectation is expressed also that the surface stress should be of the order of 10^3 dynes/cm for common metals.

An examination of some properties related to the surface tension of the solid may possibly give a feel for the reasonableness of the estimated values. For example, in the analysis of the isotropic sphere it was shown by Equation [5.16] that the internal stress (internal pressure) could be related to the surface tension and the radius. From this relationship it is found that the stress in a particle of sodium chloride

with a radius of 0.03 micron (corresponding to a specific surface area of approximately 46 m^2/gm) is 100 Kg/mm^2. This value compares well with stresses of 60 to 300 Kg/mm^2 estimated from experimental data to have been developed in sodium chloride (87). The internal compressive stresses associated with the estimated surface tensions should result in a decrease, Δa, in the lattice constant, and the relative decrease in the lattice volume per unit volume of the particles as given by Equations [5.9] and [5.16], i.e.,

$$\frac{\Delta a}{a} = \Delta v = -\frac{2\gamma}{Kr} \quad . \qquad [5.19]$$

The relative decrease for a 0.05 micron radius sodium chloride particle is calculated to be about 0.024. This does not appear to compare favorably with the measured decrease of approximately 0.004 found for the lattice constant of a similar size particle by electron diffraction. However, considering the assumptions upon which the calculation is based, not the least of which is the assumption of homogeneous strain, and the fact that the experimental value represents a single, rather imprecise determination of the lattice constant, the agreement may not be too bad. The relative decrease in the lattice constant also represents a measure of the internal strain of the material. For this, Equation [5.19] yields values of 0.040 and 0.140 for particles of sodium and potassium chloride, respectively, of 0.03 micron radius. These are not unreasonable strains.

The results of this investigation are in agreement with those of another investigation involving sodium chloride spheres produced from

molten material, and explain a number of phenomena observed with volatilized alkali halides. Amis and co-workers (67) produced spherical particles of sodium chloride by pouring molten material onto a rapidly spinning wheel. The resulting spherical particles having average diameters of approximately 185 microns were shown by hygroscopicity, calorimetric, halogen sorption, and solubility measurements to possess an abnormally high energy. These investigators mistakenly interpreted their results as indicating an abnormal surface energy. In view of the information presented herein their results were undoubtedly due principally to the interfacial energy of crystallite boundaries and to strain energy. These investigators found an excess free energy for the spheres of approximately 100 to 125 cal/mole, which compares very well with the value of about 135 cal/mole found for the excess enthalpy of similar size particles in this investigation. Very significantly, Amis et al. observed that their spheres actually exploded when added to a saturated solution of sodium chloride. This observation is in agreement with high internal compressive strain suggested for such particles by the present investigation.

The unusually high free energy of the volatilized alkali halides found in this work explains their extreme sensitivity to water vapor. The dependency of an equilibrium specific surface area upon the relative humidity has been observed in every investigation in which volatilized alkali halides have been employed. This was originally believed to be a sintering process due to sites on the particle's surface unusually sensitive to water vapor. It has been shown, however, by Kerker et al., in results published during the course of this investigation, and demonstrated in this investigation, that the process is actually one of

recrystallization of spherical particles to form cubes. The size of the resulting cubes are dependent upon the number of spheres in contact at the time of exposure to water vapor. The driving force for the solution of alkali halide particles exposed to water vapor is, of course, a difference in free energy, and it has been shown previously by this investigator and co-workers (88) that, even with the contribution of the surface free energy, equilibrium particles of sodium and potassium chloride with radii as small as hundreths of a micron should not become solution droplets until the relative humidity is in the neighborhood of 60 per cent. This behavior was confirmed experimentally by Orr et al. (89). Craig and McIntosh (37) found significant sintering of their samples at humidities as low as 5 per cent, and the specific surface area was over 90 per cent destroyed at a relative humidity of only 25 per cent. As a matter of fact, computations based on the results of these investigators, admittedly imprecise, indicate an excess free energy of almost a kilo-calorie per mole for their material.

Once spherical particles have acquired sufficient water vapor to dissolve, the free-energy driving force is toward evaporation and recrystallization (88). The droplets are highly supersaturated and the activity of the sodium chloride in solution is much greater than unity. Therefore, once a spherical particle has dissolved the droplet will nucleate to form an equilibrium cubic particle at any relative humidity below about 60 per cent.

This sensitivity to water vapor appears to be the answer to the discrepancies between this investigation and those of Benson and coworkers. In this work the samples of volatilized material were never

exposed to water vapor as they were always handled in an atmosphere of dry nitrogen or air in which the humidity was effectively zero. That the material was protected from water vapor by the handling techniques employed was confirmed by examination of particle shape by electron microscopy. However, the handling techniques of Benson and co-workers (90) were such that the exclusion of water vapor cannot be stated as certain. In fact, electron microscopic examinations by Balk and Benson (26) of their samples of potassium chloride and by this investigator on samples of sodium chloride supplied by Dr. Benson revealed a mixture of small cubes and large spheres indicating that the material had suffered some exposure to water vapor. Small particles will recrystallize more readily and at a lower relative humidity (88)(89) than will the larger ones; this type of behavior was indicated by the electron micrographs.

It is suggested, therefore, that the samples used for measurements of the surface energies of sodium and potassium chloride by Benson and co-workers had suffered some exposure to water vapor which recrystallized their smaller particles and accounted for the mixture of shapes found in their samples. It is further suggested, in view of the results found in this work with samples composed almost entirely of spherical particles, that the values found by Benson and co-workers for the surface energies of sodium and potassium chloride, which exceeded theoretical values by 40 to 100 per cent, are indeed high due to the presence of non-equilibrium particles. The presence of these non-equilibrium particles would, however, seem to suggest that the intercept of the curves obtained by Benson and co-workers should not have shown a zero enthalpy difference at zero specific surface area in keeping with the behavior shown in this work.

That is until it is noted that in the work of Benson et al. all samples with a specific surface area of less than 15 m^2/gm were obtained by deliberately exposing samples with higher specific surface areas to water vapor. Therefore, the presence of only equilibrium particles was insured for samples of low specific surface area and the enthalpy plots should have exhibited zero intercepts. This investigator believes that they would have obtained intercepts with the ordinate at some positive value of enthalpy difference between zero and the values obtained in this work had they also produced their low specific surface area material by direct volatilization. It is worth emphasizing that the samples of low specific surface area used in this work were obtained directly by volatilization at low gas velocities, and none of them were exposed to water vapor, except the single sample noted that produced a value very close to the heat of solution of the coarse, equilibrium salt.

The anomalous results obtained by Morrison and co-workers (68)(69)(70)(71) for the surface excess heat capacity of, and the chloride ion exchange with, volatilized sodium chloride can be reasonably interpreted with the properties and excess free energy found for such material in this study.

CHAPTER VI

CONCLUSIONS

The following conclusions have been reached from this investigation of the heats of solution of finely divided sodium and potassium chloride prepared by a volatilization technique and an examination of the structure and morphology of the resulting particles.

(1) The mechanism whereby very small particles of the alkali halides are formed by the volatilization process consists of the formation of droplets of molten material from the vapor immediately over the surface of the melt which are swept away by the flowing gas stream and subsequently crystallize to form solid particles.

(2) The size of the particles produced by the vaporization technique is determined by the gas velocity, this influencing the degree of vapor supersaturation and the residence time of the droplets.

(3) The particles cool principally by radiative heat-transfer, and the final particle shape and the particle's approach to thermodynamic equilibrium is controlled by the temperature of the surroundings to which the particles radiate during solidification.

(4) The final particle shape is spherical when the surroundings to which the particles radiate are at normal room temperature; the final shape will be cubic if the surroundings are within approximately 200^{o}C of the material's melting point.

(5) The surfaces of the spherical particles appear to be smooth at least to the order of 12 angstroms and exhibit a total absence of

any structural features.

(6) Spherical particles will become cubic through a process of dissolution and recrystallization in the presence of very low concentrations of water vapor.

(7) Volatilized sodium chloride particles produce electron diffraction patterns typical of a cubic, crystalline system.

(8) Spherical particles possess an excess of energy over the normal cubic particles of a similar size such as might be produced by crystallization from solution.

(9) The excess free energy of spherical particles is responsible for their extreme sensitivity to water vapor.

(10) The excess energy of spherical particles is apparently due to the presence of a polycrystalline structure and to strain.

(11) The surface tension, i.e. the work necessary to increase the surface area by stretching, of sodium and potassium chloride appears to be of the order of 1.5×10^4 and 4.5×10^4 dynes/cm, respectively, and higher than previously thought.

(12) Due to the abnormal energy content associated with spherical, volatilized materials, the volatilization process (as it has been utilized in the past) is totally unsuited for the production of samples for the study of equilibrium surface properties or any other measurements demanding a thermodynamically equilibrium structure.

(13) Previous values of the equilibrium surface energy of sodium and potassium chloride obtained from measurements with volatilized materials are very likely high due to the presence of non-equilibrium spherical particles.

(14) The excess energy associated with the non-equilibrium structure can explain the anomalous results obtained in other investigations that utilized volatilized alkali halides.

CHAPTER VII

RECOMMENDATIONS

The results of this investigation suggest a number of interesting areas for further work. Foremost among these, of course, remains the determination of the equilibrium surface energies of the alkali halides. Although the differential, heat-of-solution technique seems to offer the most promise for obtaining these values, it appears that none of the previous investigations have met all the experimental requirements necessary to give an unambigous value. Before this can be accomplished, however, further research is needed on techniques for producing high specific surface area materials with equilibrium surfaces. This research has shown that the previously accepted technique is unsatisfactory unless careful control of the cooling conditions is incorporated. A technique might also be developed for producing high specific surface area samples with equilibrium surfaces utilizing the atomization of very dilute solutions as mentioned in this research, although major problems with production rate and collection techniques would have to be overcome.

Since it is most probable that a solid surface possessing minimum free energy is rarely, if ever, encountered under normal circumstances, it is equally important that research be undertaken to check values of the surface tension found in this work and then to extend the research to other solid surfaces. An experiment that does not introduce as many

complicating factors such as polycrystalline structures and entropy effects is needed. An experiment based on free energy effects might be the most satisfactory. As an immediate next step, a series of careful determinations of the change in lattice constants using x-ray or electron diffraction and spherical particles similar to those used in this research would be worthwhile. Also, diffraction measurements to confirm the polycrystalline nature of the spherical particles and estimate the crystallite sizes might lend support to some of the hypotheses advanced in the analysis of this research.

Some practical recommendations concerning the design of a better calorimeter for making heat-of-solution measurements may be helpful. First of all, the type K-3 potentiometer is barely adequate for the calorimeter design used in this research. A Six-Dial potentiometer such as is now available from the Leeds and Northrup Company, Philadelphia, Pa., would be more satisfactory. The calibration of the main thermopile should be made against a platinum resistance thermometer for increased precision. The calorimeter vessel should not be constructed of stainless steel, since, this material can establish a significant thermal gradient between various portions of the vessel and makes the establishment of thermal equilibrium difficult. A vessel constructed of copper with a plated interior, possibly gold or rhodium, for corrosion resistance should be more satisfactory. Steps should also be taken to reduce as much as possible the total mass of the vessel in order to obtain the maximum temperature change for the solution of a given mass of material. There is question as to the advisability of using adiabatic shields in view of the attendent difficulties associated with

them. These include the possibility of heat exchange under less than ideal conditions and the inability to cool the shields rapidly enough during endothermic processes. This design aspect of calorimeters for the type of measurements made in this research should be carefully re-examined. If, however, adiabatic shields are used, a better method of control should be developed. For example, power amplifiers that detect the temperature imbalance and provide corrective power input in direct proportion to the imbalance would probably be more satisfactory than the incremental methods used previously. Also, experience has indicated that, if the conical shields are in good thermal contact with the cylindrical shields (as might be obtained by soldering) the difference thermocouples between these portions of the shields might be dispensed with without significant loss of control. This suggested modification assumes, of course, that the heater resistances for the shield elements are maintained in the same ratio as the element masses and that the heater windings are connected in series.

APPENDIX I

CALORIMETER DESCRIPTION

Construction

The calorimeter proper consisted of a stainless steel vessel surrounded by two adiabatic shields, all of which were contained in an evacuated chamber that was, in turn, suspended in a thermostated water bath. A schematic diagram of the chamber and its contents is presented in Figure 20. The calorimeter vessel was cylindrical in shape, 18 cm long and 4 cm in diameter, with an approximate volume of 200 cc. It was constructed from a single bar of corrosion-resistant stainless steel to eliminate welds which would present points for corrosion. It contained a wire track for holding a glass bulb in which was placed the material to be studied and a guillotine-like knife to break the bulb at the start of a heat-of-solution measurement. The track and knife were constructed of the same type, corrosion-resistant, stainless steel as the vessel and the track was press-fitted into the vessel cap, again to avoid welds. The calorimeter vessel with the track and knife assembly is shown in Figure 21. The vessel top was closed with six 1/2-inch machine screws and sealed by means of a polytetrafluoroethylene gasket set into the rim of the vessel so that it mated with a ridge inside of the vessel cap.

A heater of manganin wire was wound noninductively around the vessel, and both the vessel and heater were covered with aluminum foil to

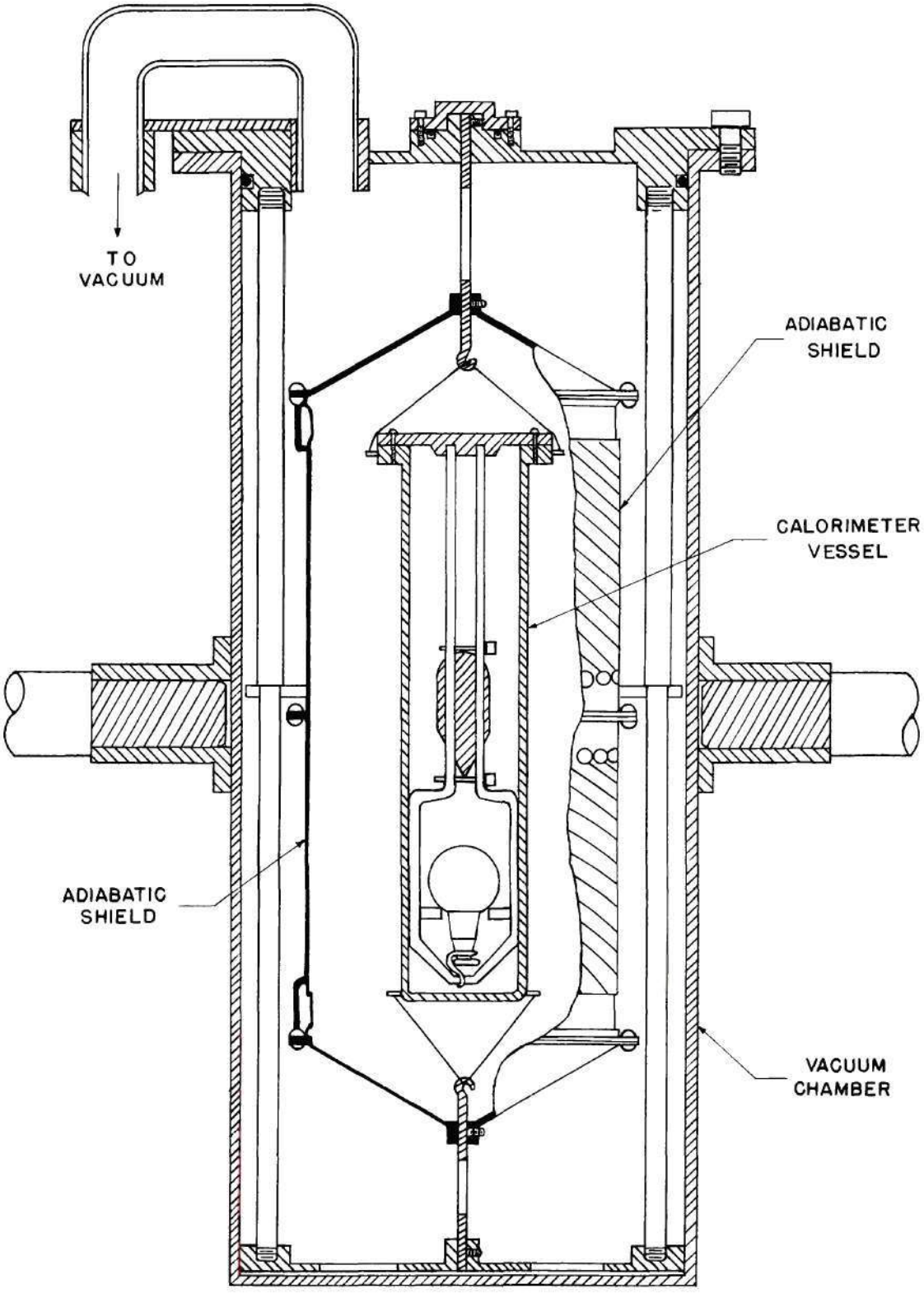

Figure 20. Schematic Diagram of Calorimeter

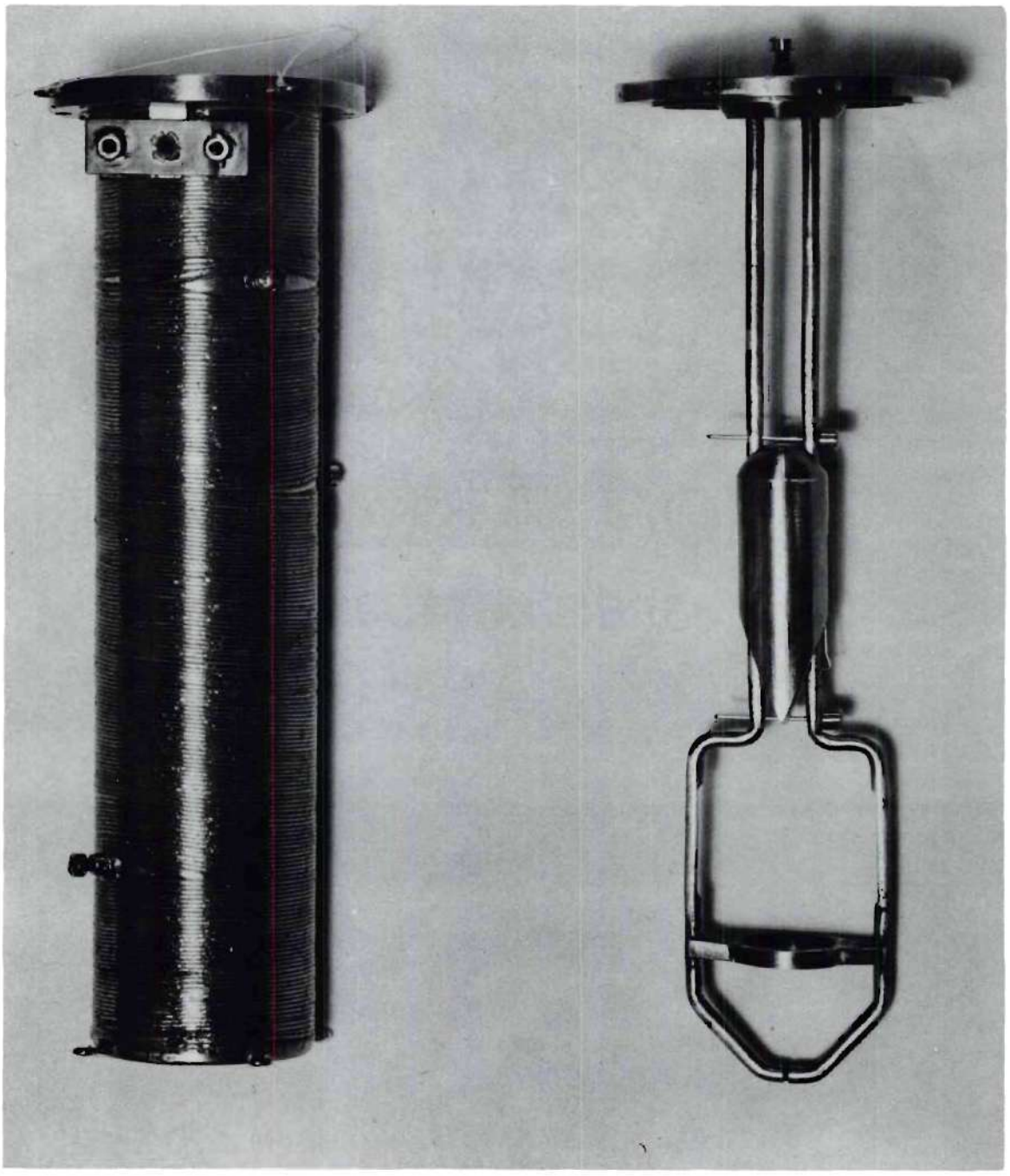

Figure 21. Calorimeter Vessel With Aluminum Foil Removed.

reduce radiation losses. There were eight points for attaching nylon thread to the vessel. These loops suspended the vessel inside the adiabatic shields (see Figure 20) by means of hooks which passed through the ends of the heater shields and fastened to the vacuum chamber framework. The hooks were of monel metal, and between them and their attachment points there was a 3-inch section of nickel silver tube having a wall thickness of 0.004 inch. This served to reduce to a minimum the heat transfer from the interior of the shield to the vacuum chamber.

The adiabatic heater shields, consisting of two cylinders and two cones which completely enclosed the calorimeter vessel, are shown in Figure 20. The shields were constructed of 0.032 inch thick copper, and were gold plated and highly polished on the inside. The shields were held in place by setscrews which contacted the hooks supporting the calorimeter vessel, and by screws that held the open ends of the cylinders together. The cylindrical sections had 0.017 inch wide by 0.017 inch deep spiral grooves cut into their exterior surfaces. These grooves made one and a half turns about the axis of the cylinder, terminating at small Micarta insulators through which there were holes leading to the inside of the cylinders. Thermocouple and heater wires to the calorimeter vessel were wound in these grooves before entering the shields through the Micarta insulators. Then heater wire having a resistance of approximately 500 ohms was wound over the cylindrical portion of each shield and covered with aluminum foil. This arrangement tended to bring all wires leading to or from the calorimeter vessel to the interior temperature and helped to maintain thermal equilibrium. The conical sections of the shields were also wound with heater

wire having a total electric resistance of approximately 150 ohms and were covered with aluminum foil. Details of the heater shields are shown in Figure 22.

The adiabatic shields and calorimeter vessel were supported in the vacuum chamber by means of a telescoping framework. This framework could be removed from the vacuum chamber and extended, enabling the heater shields to be drawn back from around the calorimeter vessel and thus allowing the calorimeter vessel to be removed. Figure 23 pictures the framework with the shields drawn back from around the calorimeter vessel. Figure 24 shows the assembly closed and ready for lowering into the vacuum chamber.

The vacuum chamber was a cylindrical vessel 15 inches long and 6 inches in inside diameter. It was sealed by means of an O-ring in the cap which formed the top of the inside framework. The cap had an opening to which was fitted a heavy duty vacuum hose for evacuating the chamber. The vacuum chamber was supported at its middle by means of shafts extending outward on the chamber's axis which rode in bearings in either side of a 40 gallon, thermostated water tank. One shaft extended through the side of the tank and externally was fitted with a rack and pinion gear arrangement so that the vacuum chamber and its contents could be rotated through 90 degrees. The water tank with the vacuum chamber rack raised for removal of the calorimeter vessel is shown along with the calorimeter instrument panel in Figure 25.

The temperature of the water bath was controlled by a Model S Thermonitor, manufactured by the E. H. Sargent Company, Chicago, Illinois, connected to a 250- and a 300-watt heater. This

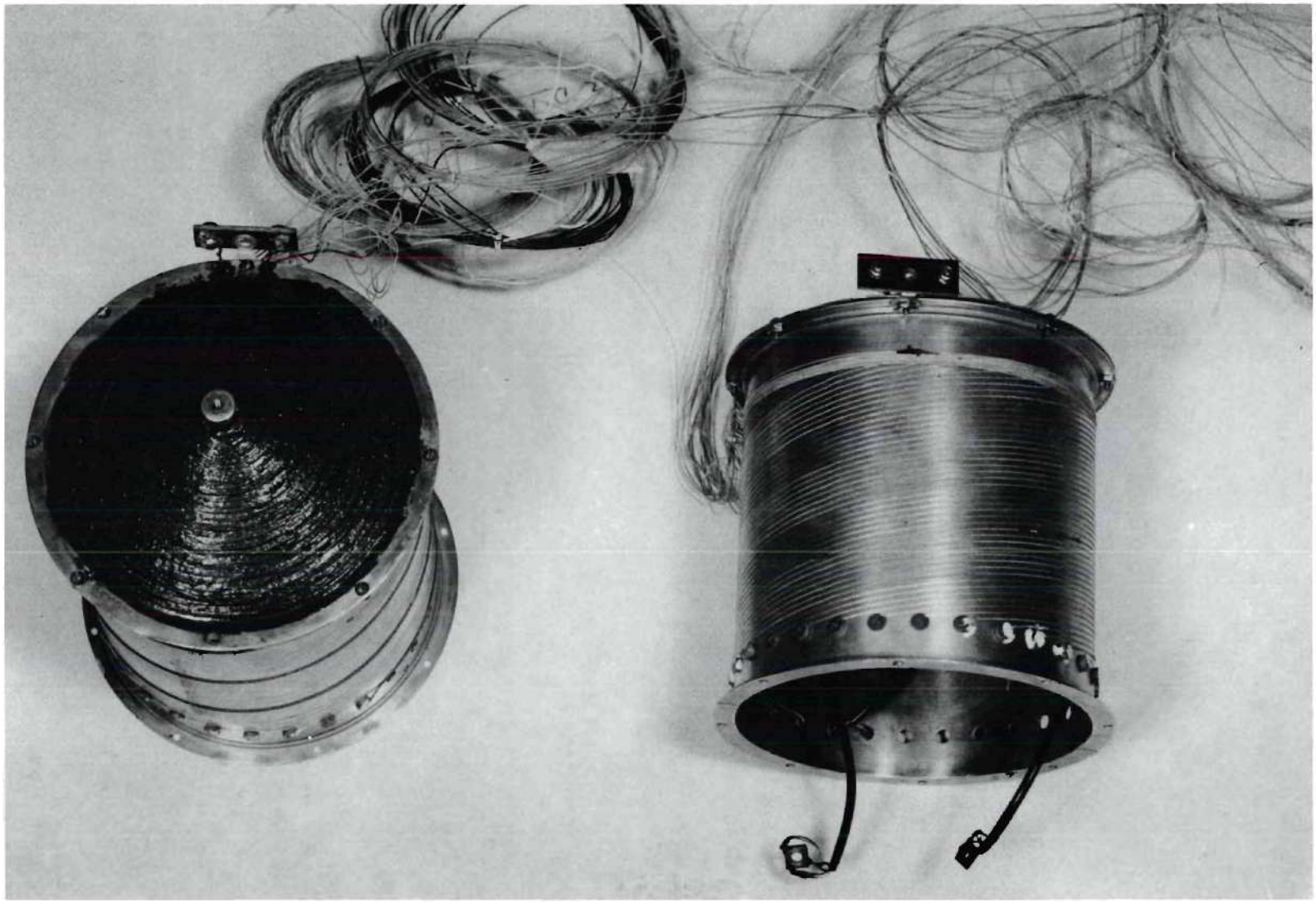

Figure 22. Adiabatic Shields With 500 ohm Heaters and Aluminum Foil Removed.

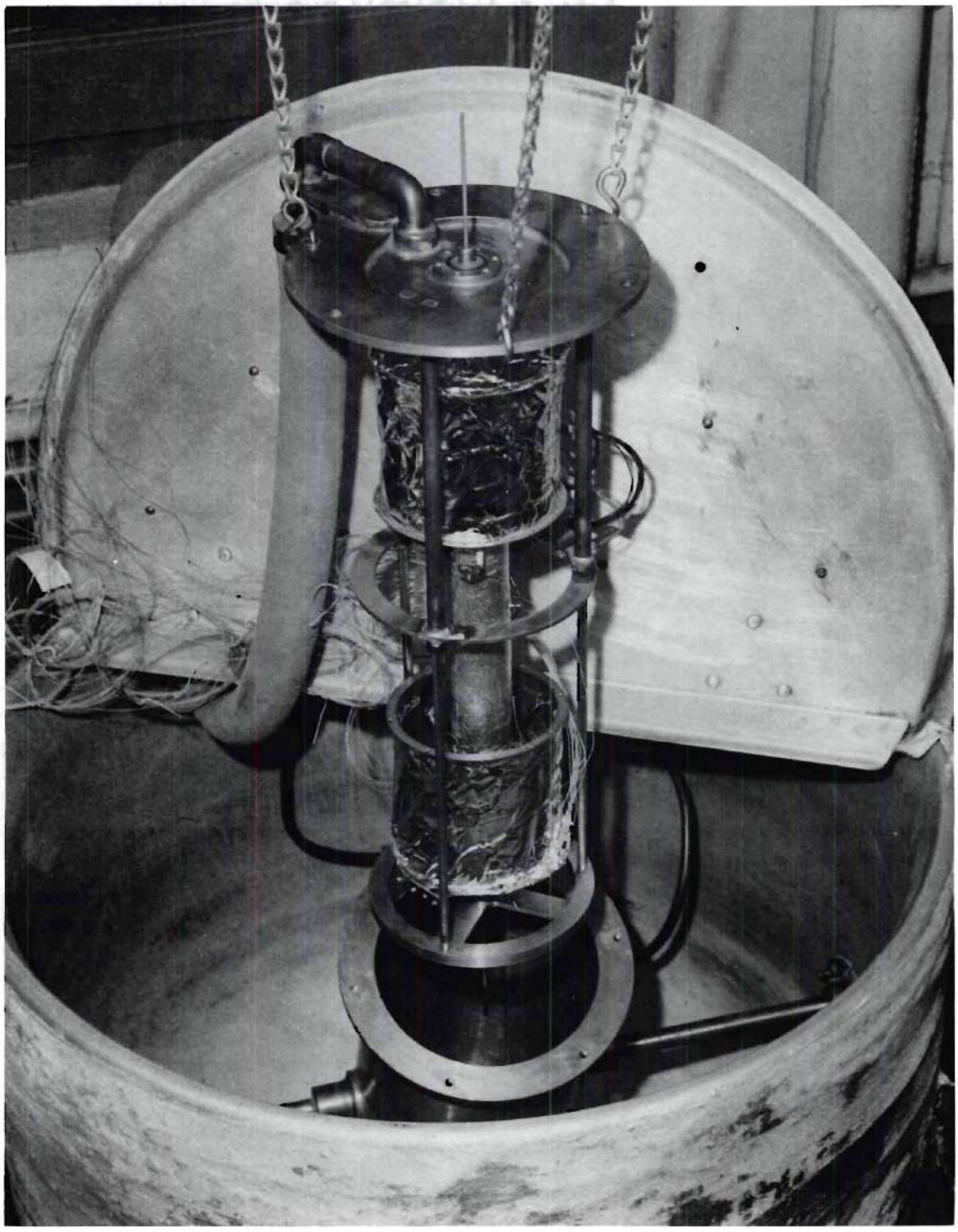

Figure 23. Calorimeter Assembly With Vacuum Chamber Frame Expanded and Adiabatic Shields Opened.

Figure 24. Calorimeter Assembly With Vacuum Chamber Frame Telescoped and Adiabatic Shields Closed.

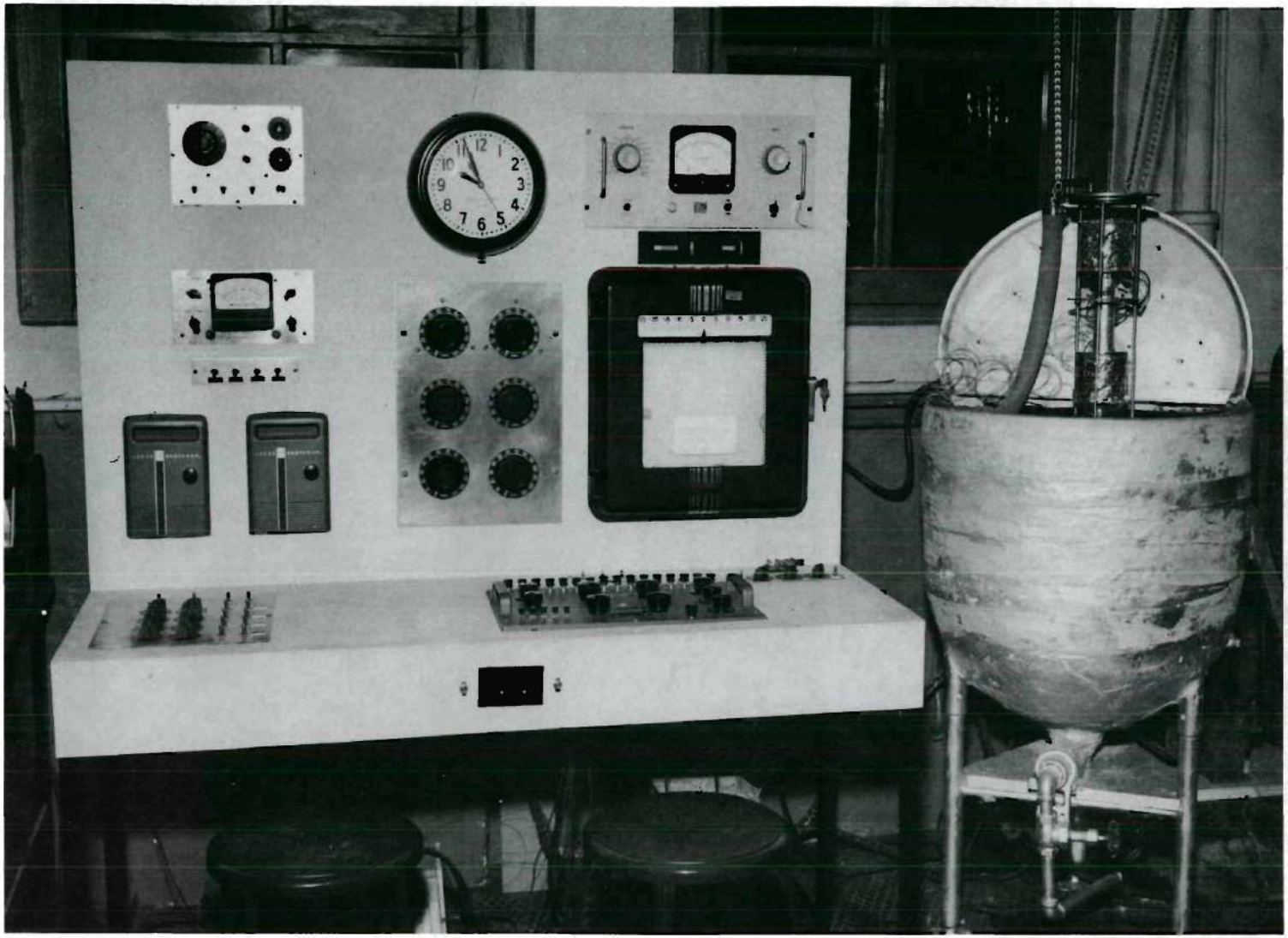

Figure 25. Adiabatic Heat-Of-Solution Calorimeter Showing Instrument Panel.

thermoregulator utilized a thermistor detector as one leg of a bridge network and also employed a saturable core reactor to eliminate undesirable overshooting of temperature during a heating period. This instrument was capable of regulating a well-stirred bath within $\pm$ 0.01°C. The water-bath arrangement employed one vertically mounted stirrer fitted with a 3-inch marine-type impeller.

The motor which rotated the vacuum chamber from 45° above the horizontal to 45° below the horizontal (hereafter called tipping the calorimeter) was controlled from the instrument panel. Switch-and-cam mechanisms were also provided on the motor assembly enabling the operator to interrupt the current to the tipping mechanism as convenient yet have the vacuum chamber come to rest in a predetermined position every time. This was accomplished by having the motor continue to run until current to it was finally interrupted by a cam-opening micro-switch that was wired in parallel with the panel switch. Two separate switch and cam mechanisms were provided. One stopped the chamber in its upright position (45° above the horizontal), and the other stopped the chamber in the inverted position (45° below the horizontal). Whether or not the chamber was stopped in an upright or inverted position was determined by when the switch on the instrument panel was opened. For example, if the chamber was to be stopped in its inverted position, the panel switch was opened any time after one cam had passed the microswitch that stopped the chamber in the upright position, but before (or as) the other cam reached the microswitch that stopped the chamber in its inverted position. The latter microswitch also actuated a pilot light on the instrument panel to indicate when the chamber was in, or

was passing, its inverted position. One cam also actuated a counter manufactured by Veeder-Root, Inc., Hartford, Conn., mounted on the instrument panel, once every time the chamber made a complete tip (i.e., from 45° above the horizontal to 45° below the horizontal and back).

The vacuum chamber was evacuated by means of a mechanical and an oil-diffusion pump operated in series and connected to the chamber by heavy-duty vacuum hose. The pressure inside this chamber was measured by a Phillips gauge, type PHG-1, manufactured by the Consolidated Vacuum Corporation, Rochester, New York. All thermocouple and heater wires to the calorimeter vessel and heater shields were brought in through the vacuum hose, the wires being introduced through a grooved plastic plug which was sealed into a joint near the diffusion pump. After entering the vacuum chamber the wires passed through the adiabatic shields as previously described.

The heater shields were fitted with four sets of four-junction, copper-constantan, difference thermopiles. Each shield had a difference thermopile between its cylindrical and conical sections and a difference thermopile between its cylindrical section and the calorimeter vessel. The calorimeter vessel was fitted with a 12-junction copper-constantan thermopile consisting of four small copper blocks containing three junctions each. These copper blocks were attached to the calorimeter vessel with screws which tightened into small studs (see Figure 21). The vessel top had a large mass compared to the rest of the vessel so a 4-junction, copper-constantan, difference thermopile was attached between the top and the side of the vessel. This difference thermopile indicated when the entire calorimeter vessel was

in thermal equilibrium. The electromotive force of this difference thermopile and the main thermopile was measured with a Leeds and Northrup Company, Philadelphia, Pa., type K-3 potentiometer and a Leeds and Northrup stabilized, indicating dc-amplifier attached to a Leeds and Northrup Speedomax type G, recorder. The sensitivity of this galvanometer system was 0.25 microvolt per millimeter of deflection. The electromotive force of the main thermopile was measured relative to an ice bath at $0^{o}C$ and the primary voltage standard was an Eppley Laboratory Inc., Newport, R. I., cadmium cell of the unsaturated type. This cell was kept in a thermally insulated box.

The reference ice bath consisted of a one gallon Dewar vacuum flask contained in an insulated chamber. The 12-thermocouple reference junctions were contained in individual glass tubes, filled with mineral oil, which passed through the plexiglass Dewar cover. These tubes were arranged concentrically around a 2-inch diameter copper tube, also attached to the plexiglass cover, that extended the entire depth of the Dewar. This tube effectively eliminated any temperature gradient between the bottom and top of the ice bath. The bath was filled with crushed ice and distilled water, and it could maintain a constant reference temperature for at least 8 hours without replenishment.

The difference thermopiles for the adiabatic heater shields were connected to two Leeds and Northrup, model 2430, enclosed lamp and scale galvanometers, which had, in conjunction with the associated thermopiles, a sensitivity of $0.005^{o}C$ per millimeter of deflection. These galvanometers were mounted in the instrument board directly above the controls to the electric heaters of the adiabatic shields. This

arrangement enabled the operator to determine when parts of the shield or the shield and the calorimeter vessel were not in thermal equilibrium and to correct this by adjusting the energy input to the shield heaters. Switching of the thermopiles was used to overcome the necessity of four galvanometers to monitor the four difference thermopiles, i.e. the two thermopiles between the cylindrical shields and the vessel, and the two between the conical shields and the cylindrical shields. By means of switching, a single galvanometer could be used to monitor the thermopile between a cylindrical shield and its associated conical shield. Energy to each of the adiabatic shields was taken from a 110-volt ac source fed into a voltage stabilizer, two 110-volt variable transformers, two potentiometers wired in series, and rectified to dc before going to the shields. It was found necessary to rectify the voltage to the shield heaters despite their noninductive widing. Without rectification a spurious emf could sometimes be detected in the main thermopile output that was apparently induced by switching transients in the heater control circuit. Each heater circuit was fitted with on-off switches as well as momentary switches with which periodic boosts in the current could be made. A schematic circuit diagram of the shield heater controls is presented as Figure 26.

Automatic controllers were wired in parallel with the momentary switches and the on-off switches of the heater control circuit in order to maintain the calorimeter vessel at a constant temperature over a long period of time without needing attention. The calorimeter could therefore be left overnight, or during calculation of heat capacity measurements without having to re-establish equilibrium upon returning.

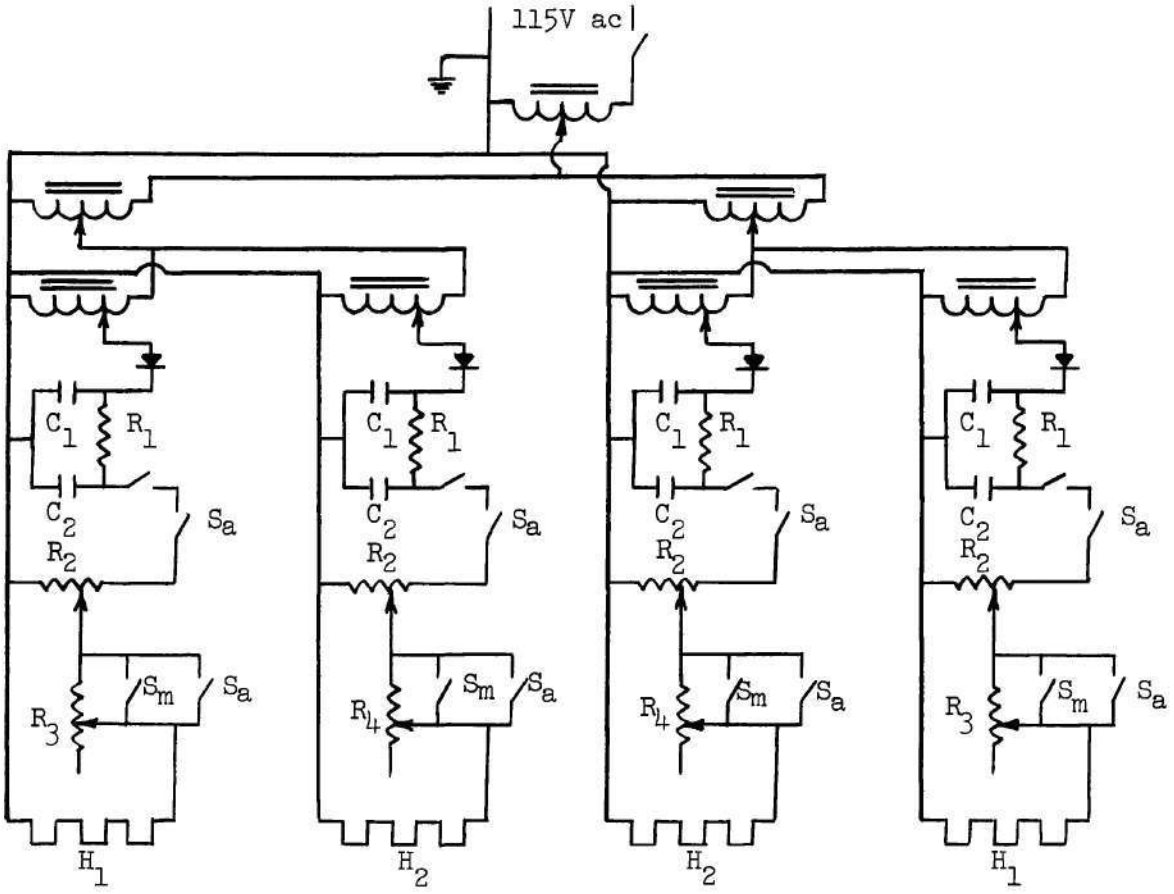

Notes: All variable transformers are 5 amp, 110V ac.
All diodes are 750 milliamp, 400 piv.
Resistors R_1 are 300 ohm, 25 watt.
Resistors R_2 are 500 ohm, 25 watt.
Resistors R_3 are 250 ohm, 25 watt.
Resistors R_4 are 1500 ohm, 25 watt.
Capacitors C_1 are 30 μfd, 150 wvdc.
Capacitors C_2 are 50 μfd, 150 wvdc.
Switches S_a are microswitches in automatic control system.
Switches S_m are momentary switches.
Heaters H_1 are for conical shields and are 150 ohms.
Heaters H_2 are for cylindrical shields and are 500 ohms.

Figure 26. Schematic of Control Circuit for Adiabatic Shields.

These automatic controllers consisted of four photocells, two each placed in front of the lamp-and-scale galvanometers approximately one centimeter on either side of the null position, connected to four Compactrol controllers of the Victory Engineering Corporation, Union, N.J., that responded to the change in resistance of the photocells with exposure to light, and opened or closed microswitches. The basis for the internal operation of the Compactrols was the firing of a thyratron tube when the photocell resistance dropped below a certain value, and the movement of a solenoid, triggered by the thyratron, to operate the microswitch. When the galvanometer lamp moved across the face of the photocell in the direction of cooling, for example, the triggered microswitch would take out some of the resistance in the heater control circuit and increase the power input to the shield, exactly as an operator would have done with the manual momentary switch. Likewise, if the lamp moved in the direction of the shield becoming too hot the activated microswitch would interrupt the current until the shield cooled. Overshooting during automatic control was avoided by balancing manually the resistance put into the circuit by the last potentiometer with the response time of the shield before leaving the control to entirely automatic operation. The thermopiles between the cylindrical sections and the vessel were used for automatic control although the switching affected both the cylindrical and conical shield on a particular side. This less-than-ideal situation was accepted, because to have controlled both cylindrical sections and both conical sections separately would have required four galvanometers, eight photocells, and eight Compactrols. In spite of this, however, control to within a tenth of a

degree or so could be maintained for periods of 12 to 18 hours.

Current for the calorimeter-vessel heater was provided by two, 12-volt, lead storage batteries connected in parallel. The current was measured to determine the energy input to the calorimeter vessel and contents by use of the type K-3 potentiometer and a certified, 10 ohm, standard resistor wired in series with the calorimeter-vessel heater. The lead storage batteries were connected into a circuit with a dummy load of very nearly the same resistance as the calorimeter vessel heater when not in actual use. This served to maintain a stable output to prevent voltage fluctuations upon supplying current to the heater. The switch that transferred the voltage supply from the dummy load to the heater also actuated an electric stop-timer, enabling the time of the current passage to be measured to $\pm$ 0.01 second.

All switches used for switching thermocouple leads were of the rhodium-plated wiping-type. The leads were soldered to the switches with Leeds and Northrup thermal-free solder. The switches were completely enclosed with plastic covers to prevent chemical contamination of the switch contacts. Their cases were lagged to reduce thermal fluctuations.

Calibration

The electrical resistance of the calorimeter-vessel heater was determined by connecting the heater in series with a resistance of approximately the same value (the dummy load) and a 10-ohm standard resistor. The addition of the additional resistance to the circuit was necessary to reduce the voltage drop across the heater to a value that fell into the high range of the type K-3 potentiometer. A 2-volt, lead,

storage battery was then attached to this circuit. The calorimeter-vessel was placed in the vacuum can and the water bath was controlled at approximately 25°C. Current was allowed to flow in the circuit until the heater and vessel established a constant temperature. Measurements were next made of the vessel temperature, the voltage drop across the heater, and the voltage drop across the standard resistor. From the voltage drop across the standard resistor, the current in the circuit was calculated. The resistance of the heater was then determined from this value and the voltage drop across the heater. Fifteen measurements of this type were made at temperatures ranging from 20°C to 30°C. No detectable change in resistance with temperature could be noted, in keeping with the characteristics of manganin wire. The average of these measurements was found to be 390.66 ohms with a standard deviation of ± 0.08 ohms. The accuracy assigned to this measurement, as estimated from the limits placed on the standard resistor and the type K-3 potentiometer by their manufacturers, was ± 0.12 ohms.

An independent measurement of the heater resistance was then made with a Wheatstone bridge of the Honeywell Company, Philadelphia, Penna., at approximately 25°C. The value found for the heater was 390.54 ohms. The two measured values of the resistance agreed to within the limits of accuracy on the former measurements, so the value used was 390.66 ohms.

The various four-junction, copper-constantan, difference thermopiles were checked for zero emf output when at the same temperature. The junctions were placed in intimate contact with a copper block immersed in a thermostated oil bath at approximately 25°C. Only thermopiles that were found to generate less than ± 0.5 microvolts difference

were used. This corresponded to a temperature difference of $\pm$ 0.003°C or less in the shield control circuit.

The main, 12-junction, copper-constantan thermopile was calibrated against a mercury-in-glass thermometer certified by the National Bureau of Standards. The thermometer was placed in a well inside a large copper block, the thermopile hot-junctions were placed in intimate contact with the block, and the block was immersed in an oil bath thermostated to within $\pm$ 0.01°C. Fifty measurements of emf versus temperature were obtained between approximately 20°C and 35°C. These data were then fitted to first, second, third, and fourth order polynomials by the method of least squares with the aid of a digital computer. The data were described significantly better by a second order polynomial than a first order polynomial but not significantly better than a third or fourth order polynomial. Therefore, the second order polynomial

$$T = 0.18008 + 2265.17140(\text{emf}) - 4.69196(\text{emf})^2$$

was chosen to represent the temperature - emf relationship of the thermopile. This second order polynomial produced an average deviation of 0.022°C between calculated and measured temperatures over the range from 20 to 35°C and an average deivation of 0.014°C over the range 23 to 28°C, which included entirely the temperatures over which the calorimeter was used. The magnitudes of these deviations are in agreement with the precision to which the temperature would be estimated with the mercury-in-glass thermometer $\pm$ 0.01°C.

The calibration of the main, 12-junction thermopile was by far the greatest source of error in the calorimeter measurements of the heats of

solution, although the lack of precision was certainly not as great as indicated by the average deviation obtained for the fit of the emf temperature data. This figure applies more to the measurement of the temperature at which a heat of solution was determined, and, therefore, limited the accuracy of the corrections applied to the measured heats of solution. In this correction, of course, the uncertainty in the temperature was no greater than any number of other uncertainties involved. The temperature difference used for the actual heat measurements were taken over a very small interval -- on the order of tenths of a degree -- and the electrical calibrations for heat capacity were always made back across this same temperature interval or very close to it. Therefore, the uncertainties in these interval measurements were undoubtedly less than $\pm$ 0.014^{o}C although they were still large enough to make this the greatest uncertainty in the heat-of-solution measurements.

The adiabatic shields if they operated ideally sould allow no drift in the temperature of the calorimeter vessel under constant conditions. However, a slight heat leak was detectable with the calorimeter contents at thermal equilibrium and the shields under manual control. This leak, which varied with calorimeter contents, was of the order of 0.002^{o}C per hour per degree centigrade of thermal head between the vessel and thermostated bath for the calorimeter vessel when containing 100 grams of water. The normal thermal head between the vessel and the bath was approximately 2^{o}C, so a leak of this magnitude would have corresponded to a drift of 0.004^{o}C per hour. This deficiency was compensated by adjusting the galvonometer zeros of the vessel-shield galvonometers before each run until the drift was undetectable over a

period of an hour or two.

Sixteen measurements of the heat capacity of the vessel containing 49.890 grams of water were made over the range 23°C to 27°C. These heat capacities were corrected for the heat required to vaporize the water in going from the initial to the final temperature (see APPENDIX II), and examined for any indication of variation of heat capacity with temperature. No dependency of the heat capacity on temperature was detected over the range of temperature investigated. The average of the sixteen values, corrected to 25°C for the variation in heat capacity of the water with temperature, was 96.88 cal/°C. The average deviation of these results was 0.54 cal/°C. The temperature interval over which the vessel and contents were raised during one of these determinations was approximately the same (i.e. a few tenths of a degree centigrade) as used in the heat capacity determinations for the heat-of-solution measurements.

Operation

To operate, the calorimeter was positioned with a glass bulb containing the sample attached to the guillotine track with a small wire and the knife locked by small pins passing through the track above and below the knife (see Figure 21). These pins were positioned so that in the normal direction of tipping the pins would not fall from the track. The calorimeter vessel and contents were brought to thermal equilibrium with infrequent tipping to stir the contents. This condition was checked, in addition to a zero-drift graph of the temperature, by monitoring the difference thermopile between the side and top of the

vessel until no emf difference could be detected. The vacuum chamber was then disconnected from the automatic tipping mechanism and rotated manually through 225° opposite to the normal direction of tipping. This allowed the pins holding the knife in place to drop out and the knife to slide to the end of the track opposite the glass sample bulb. The vacuum chamber was then rotated smartly to its original position and reconnected to the automatic tipping mechanism. As this was done the knife slid down the track and broke the sample bulb. In so doing the knife passed a small umbrella type latch that sprung from one side of the track immediately behind the upper end of the knife and prevented motion of the knife during subsequent tipping.

During the solution period that followed, the calorimeter was tipped infrequently to stir the contents for a total of 10 tips. The temperature change of the calorimeter vessel was often so rapid during the solution process that the adiabatic shields could not be cooled rapidly enough, by interrupting the power to them to maintain them at the temperature of the vessel. This difficulty was overcome, since the solution process was endothermic, by small additions of heat through the vessel heater to prevent the temperature of the vessel from dropping too rapidly. This enabled the shields to be kept in balance with the vessel, and the quantity of heat added was taken into account when the heat effect due to solution was calculated. The period required for establishment of thermal equilibrium, as determined by the attainment of a constant temperature and by a zero output from the difference thermopile between the vessel side and top, was usually of the order of 30 minutes.

After the vessel and contents had attained thermal equilibrium and the final temperature was recorded, the heat capacity of the vessel and contents were determined by electrical calibration. During this electrical calibration the temperature was raised across approximately the same temperature interval covered in the solution process. During the calibration the calorimeter assembly was tipped infrequently for a total of 10 tips. The emf across the standard resistor was determined with the type K-3 potentiometer to $\pm$ 0.00001 volt and the battery output was usually stable to this voltage during a heating period. The time of current passage was usually of the order of 15 minutes and was determined with an electrical stop-timer to within $\pm$ 0.01 second. The period for equilibrium was the same order of that for the solution process, and the conditions of final thermal equilibrium were the same, i.e., constant temperature and zero output of the difference thermopile. The electrical calibration was determined at least twice and the agreement was usually within 0.5 per cent.

It was impossible, of course, even with careful manual control to maintain the temperature difference between the shields and the vessel at zero. However, the deviations for each vessel-shield thermopile was noted at alternate minutes (the cylindrical shield-conical shield thermopiles were monitored on alternate half-minutes) and the algebraic sums of the deviations were kept to a minumum; always to within plus or minus a centimeter of galvanometer deflection which corresponded to about $\pm$ 0.05°C.

The vacuum in the calorimeter during operation was always less than 5×10^{-4} torr.

APPENDIX II

SAMPLE CALCULATION

The enthalpy change for the solution process, ΔH_{T_i}, was computed according to the relationship

$$\Delta H_{T_i} = q_g + q_t - C\,(T_f - T_i) \qquad [1]$$

where q_h was the heat added with the vessel heater during the process to aid in maintaining the balance between the vessel and the adiabatic shields, q_t was the heat effect associated with the breaking of the sample bulb as outlined in CHAPTER III, C was the heat capacity of the vessel and its contents after the solution process, and the initial and final temperatures of the vessel are represented by T_i and T_f, respectively. As outlined in CHAPTER III, the total effect associated with the breaking of the sample bulb, q_t, is the sum of an evaporation term, q_e, and a term of the desorption type

$$q_t = q_e - \frac{0.10\,(V_f - V_i)}{1 + (30\,V_f/m_w)} \qquad [2]$$

where V_i and V_f are the initial and final free volumes in the calorimeter vessel in cubic centimeters, m_w is the weight of water in grams, and q_t and q_e are in calories. The evaporation term, which accounted for the evaporation of water into the free space provided by the breaking of the sample bulb and for the condensation of water vapor

on the temperature's lowering due to the solution process, was obtained from the relationship

$$q_e = - \left[\frac{p_f V_f}{T_f} - \frac{p_i V_i}{T_i} \right] \frac{\Delta H_{vap}}{R} \qquad [3]$$

where p_i is the vapor pressure of H_2O at the initial temperature T_i, p_f the vapor pressure of the 0.5m salt solution at the final temperature T_f, ΔH_{vap} is the heat of vaporization of water, and R is the gas constant equal to 6.237×10^4 cm^3-mm/mole-^oK.

The energy added to the vessel with the vessel heater to prevent the former's temperature from dropping too rapidly was calculated from the relationship

$$q_h = 0.23918 \left(\frac{E}{R_s} \right)^2 t R_h \qquad [4]$$

where E is the emf in volts across the standard resistor R_s whose value was 10.0000 ohms, t is the time of current passage in seconds, R_h is the resistance of vessel heater in ohms, and q_h is the energy input to the vessel in calories. This same relationship, of course, was used for determining the energy input to the vessel and contents for a heat capacity determination. The heat capacity was corrected for the evaporation of water in a manner similar to that outlined in connection with Equation [3].

Since the use of the heat capacity of the vessel and solution leads to a calculated enthalpy change referred to the initial temperature (50) and since the initial temperature was never exactly 25^oC, supplementary

heat capacity data were used to correct the enthalpy change to 25°C by means of the relationship

$$\Delta H_{25} = \Delta H_{T_i} + [m_w(c_w - c_a) + m_s(c_s - c_a)] (T_i - 25) \qquad [5]$$

where ΔH_{25} is the enthalpy change at 25°C, m_w the weight of water, c_w the specific heat of water, c_a the specific heat of the 0.5m salt solution, m_s the weight of sodium chloride (or potassium chloride), and c_s the specific heat of sodium chloride (or potassium chloride).

The heat of solution per mole of salt dissolved in 2000 gms of water at 25°C, ΔH_s, was calculated by

$$\Delta H_s = \frac{\Delta H_{25} M}{m_s} \qquad [6]$$

where M is the molecular weight of the salt and m_s is the weight of the salt.

The heat capacity determinations of the vessel and its contents were corrected for the heat of vaporization of water with the relationship

$$q = - \left[\frac{p_f}{T_f} - \frac{p_i}{T_i} \right] \frac{V_f \Delta H_{vap}}{R} \qquad [7]$$

where q is the heat required for vaporization, p_i and p_f are the vapor pressures of the 0.5m salt solution at the initial and final temperatures T_i and T_f, V_f is the final free volume in the calorimeter, ΔH_{vap} is the molal heat of vaporization of water, and R is the gas constant equal to 6.237×10^4 cm^3-mm/mole-°K.

The sources of the necessary supplementary data were: the International Critical Tables (91) for the vapor pressure of sodium and potassium chloride solutions, the Handbook of Chemistry and Physics (92) for the specific heats of sodium and potassium chloride solutions.

The following experimental data and calculations are typical:

specific surface area of sample: 14.9 m^2/gm
sample weight: 1.23567 gms
bulb volume: 10 cm^3
weight of water: 42.204 gms
time of current passage: 293.03 secs
emf across standard resistor: 0.27932 volts
tips: 10
initial temperature: 25.62652°C
final temperature: 24.66629°C

The average of three determinations of the heat capacity of the vessel and contents, corrected for the heat of vaporization of water by means of Equation [7], was found to be 89.333 cal/°C.

$$q_h = 0.23918 \ \frac{(0.27932)^2}{100.00} \ (293.03)(390.66) \text{ cal}$$

$$\underline{q_h = 21.36199 \text{ cal}}$$

$$q_e = -\left[\frac{22.895}{297.83}(148.2) - \frac{23.240}{297.79}(137.2)\right] \frac{10504}{6.237 \times 10^4} \text{ cal}$$

$$\underline{q_e = -0.11540 \text{ cal}}$$

$$q_t = q_e - \frac{0.10(10)}{1 + \frac{30(149)}{42.204}} \text{ cal}$$

$$q_t = -(0.11540 - 0.00937) \text{ cal}$$

$$\underline{q_t = -0.10603 \text{ cal}}$$

$$\Delta H_{T_i} = [21.36199 - 0.10603 - 89.333\ (24.66629-24.62652)]\ \text{cal}$$

$$\Delta H_{T_i} = (21.36199 - 0.10603 - 3.55277)\ \text{cal}$$

$$\underline{\Delta H_{T_i} = 17.62947\ \text{cal}}$$

$$\Delta H_{25} = 17.62947 + [42.204(0.0349) - 1.23567(0.7563)]\ (-0.37348)\ \text{cal}$$

$$\Delta H_{25} = (17.62947 - 0.20107)\ \text{cal}$$

$$\underline{\Delta H_{25} = 17.42840\ \text{cal}}$$

$$\Delta H_s = \frac{17.42840\ (58.448)}{1.23567}\ \text{cal/mole}$$

$$\underline{\Delta H_s = 824.4\ \text{cal/mole}}$$

LITERATURE CITED*

1. E. Madelung, "Das elektrische Feld in Systemen von regelmassig angeordneten Punktladungen," Physikcal. Z. 19, 524-33 (1918); "Die atomistische Konstitution einer Kristalloberflache," Physikcal. Z. 20, 494-6 (1919).

2. M. Born and O. Stern, "Surface Energy of Crystals and its Influence on Crystal Form," Sitzber preuss. Akad. Wiss. 48, 901-13 (1919).

3. M. Born, "Atomtheorie des festen Zustundes," Encyk. d. math. Wiss. 5, pt. 3, 529-774, esp. 733-52 (1923).

4. J. E. Lennard-Jones and P. A. Taylor "Some Theoretical Calculations of the Physical Properties of Certain Crystals," Proc. Roy. Soc. 109A, 476-508 (1925).

5. J. E. Lennard-Jones and B. A. Dent, "Cohesion at a Crystal Surface," Trans. Faraday Soc. 24, 92-108 (1928).

6. B. M. Dent, "The Effect of Boundary Distortion on the Surface Energy of a Crystal," Phil. Mag. 8, 530-39 (1929).

7. J. Biemuller, "Uber die Oberflachenenergie der Alkalinhalogenide," Zeit. Physik. 38, 759-71 (1926).

8. R. Fricke, "Eigenscheften und Auswirkungen aktiver fester Stoffe und Oberflachenchemie," Naturwiss 31, 469-82 (1943).

9. R. Shuttleworth, "The Surface Energies of Inert-Gas and Ionic Crystals," Proc. Phys. Soc. (London) 62A, 167-79 (1949).

10. F. van Zeggeren and G. C. Benson, "Calculation of the Surface energies of Alkali Halide Crystals," J. Chem. Phys. 26, 1077-82 (1957).

11. F. van Zeggeren and G. C. Benson, "The Quantum Mechanical Calculation of the Surface Energy of Sodium Chloride - A First Approximation," Can. J. Phys. 34. 985-92 (1956).

12. J. W. Obreimov, "The Splitting Strength of Mica," Proc. Roy. Soc. 127A, 290-7 (1930).

13. V. D. Kuznetsov, Surface Energy of Solids, translation from the Russian, Department of Scientific and Industrial Research, Her Majesty's Stationary Office, London, 1957.

14. J. J. Gilman, "Direct Measurements of the Surface Energies of Crystals," J. Appl. Phys. 31, 2208-18 (1960).

15. M. L. Dundon and E. Mack, Jr., "The Solubility and Surface Energy of Calcium Sulfate," J. Am. Chem. Soc. 45, 2479-85 (1923).

16. M. L. Dundon, "Surface Energy of Several Salts," J. Am. Chem. Soc. 45, 2658-66 (1923).

17. F. van Zeggeren and G. C. Benson, "A Determination of the Surface Free Energy of Sodium Chloride," Can. J. Chem. 35, 1150-56 (1957).

18. B. V. Enustun and J. Turkevitch, "Solubility of Fine Particles of Strontium Sulfate," J. Am. Chem. Soc. 82, 4502-10 (1960).

19. S. G. Lipsett, F. M. G. Johnson and O. Maass, "The Surface Energy and the Heat of Solution of Solid Sodium Chloride I, II, III," J. Am. Chem. Soc. 49, 925-43, 1940-9, (1927); 50, 2701-3 (1928)

20. G. Jura and C. W. Garland, "The Experimental Determination of the Surface Tension of Magnesium Oxide," J. Am. Chem. Soc. 74, 6033-4 (1952).

21. G. C. Benson and G. W. Benson, "Surface Energies of the Alkali Halides," Can. J. Chem. 33, 232-9 (1955)

22. G. C. Benson H. P. Schreiber, and F. van Zeggeren, "An Experimental Determination of the Surface Enthalpy of Sodium Chloride," Can. J. Chem. 34, 1553-6 (1956).

23. S. Brunauer, D. L. Kantro, and C. H. Weise, "The Surface Energies of Calcium Oxide and Calcium Hydroxide," Can. J. Chem. 34, 729-42 (1956).

24. S. Brunauer, D. L. Kantro, and C. H. Weise, "The Surface Energies of Amorphous Silica and Hydrous Amorphous Silica," Can. J. Chem. 34, 1483-96 (1956).

25. S. Brunauer, D. L. Kantro, and C. H. Weise, "The Surface Energy of Tobermorite," Can. J. Chem. 37, 714-23 (1959).

26. P. Balk and G. C. Benson, "Calorimetric Determination of the Surface Enthalpy of Potassium Chloride," J. Phys. Chem. 63, 1009-12 (1959).

27. G. E. Boyd and W. D. Harkins, "The Energy of Immersion of Crystalline Powders in Water and Organic Liquids I.", J. Am. Chem. Soc., 64, 1190-94 (1942).

28. J. E. Wertz, Private Communication reported in reference 35.

29. E. Hutchinson and K. E. Manchester, "Semi-Micro Calorimeter," Rev. Sci. Inst., 26, 364-67 (1955).

30. J. W. Gibbs, "On the Equilibrium of Heterogeneous Substances," Collected Works 1, 55-353, Longmans, Green and Co., New York, 1928; Scientific Papers 1, 55-353, Dover Publications, Inc., New York, 1961.

31. C. Herring, "Surface Tension as Motivation for Sintering," The Physics of Powder Metallurgy, 151-4, W. E. Kingston, ed., McGraw-Hill Book Co., Inc., New York, 1951.

32. C. Herring, "The Use of Classical Macroscopic Concepts in Surface-Energy Problems," Structure and Properties of Solid Surfaces, 5-72 esp. 13-18, R. Gomer and C. S. Smith, eds., Chicago University Press, Chicago, 1953.

33. W. F. Giauque, "An Example of the Difficulty in Obtaining Equilibrium Corresponding to a Macrocrystalline Non-Volatile Phase," J. Amer. Chem. Soc. 71, 3192-4 (1949).

34. G. C. Benson and G. W. Benson, "Adiabatic Calorimeter for Measuring Heats of Solution at Room Temperature," Rev. Sci. Instr., 26, 477-81 (1955).

35. G. C. Benson, E. D. Goddard and C. A. J. Hoeve, "Adiabatic Solution Calorimeter," Rev. Sci. Instr., 27, 725-27 (1956).

36. S. Brunauer, P. H. Emmett, and E. Teller, "The Adsorption of Gases in Multimolecular Layers," J. Am. Chem. Soc. 60, 309-19 (1938).

37. A. Craig and R. McIntosh, "The Preparation of Sodium Chloride of Large Specific Surface," Can. J. Chem. 30, 448-53 (1952).

38. D. M. Young and J. A. Morrison, "An Apparatus for Preparing Sodium Chloride Crystals Having Large Specific Surface," J. Sci. Inst. 31, 90-2 (1954).

39. F. van Zeggeren, H. P. Schreiber, and G. C. Benson, "The Purity of Small Sodium Chloride Particles Prepared by Electrostatic Precipitation," Can. J. Chem. 34, 1501-5 (1956).

40. A. Craig and R. McIntosh, "The Preparation of Sodium Chloride of Large Specific Surface," Can. J. Chem. 30, 448-53 (1952).

41. C. Orr, Jr., and J. M. DallaValle, Fine Particle Measurement, p. 176, Macmillan Company, New York, 1959.

42. D. S. MacIver and P. H. Emmett, "Adsorption of Nitrogen on Pure Sodium Chloride," J. Phys. Chem. 60, 824-5 (1956).

43. A. S. Joy, "The Determination of Specific Surface by Gas Adsorption," Vacuum 3, 254-78 (1953).

44. T. F. Young and O. G. Vogel, "The Relative Heat Contents of the Constituents of Aqueous Sodium Chloride Solutions," J. Am. Chem. Soc. 54, 3030-40 (1932).

45. A. C. Zettlemoyer, G. J. Young, J. J. Chessick, and F. H. Healy, "A Thermistor Calorimeter for Heats of Wetting," J. Phys. Chem. 57, 649-52 (1953).

46. F. E. Bartell and R. M. Suggitt, "Heat of Wetting of Copper, Graphite and Silica Gel," J. Phys. Chem. 58, 36-40 (1954).

47. C. M. Slansky, "The Heats of Solution of Alkali Halides and of Hydrogen Chloride in Water and Methyl Alcohol Solutions at 25°C," J. Am. Chem. Soc. 62, 2430-4 (1940).

48. F. LaPorte, "Etude Experimentale et Theorique de L'Immersion dun Solide Pulverulent dans un Liquide pur. Construction dun Micro-calorimetre," Ann. phys. 5, 5-79 (1950).

49. E. F. Westrum, Jr. and L. Eyring, "The Heat of Solution of Neptunium Metal and the Heats of Formation of Some Neptunium Chlorides," J. Am. Chem. Soc. 74, 2045-7 (1952).

50. T. W. Richard, "Note Concerning the Calculation of Thermochemical Results," J. Am. Chem. Soc. 25, 209-14 (1903).

51. Selected Values of Chemical Thermodynamic Properties, Circular of the National Bureau of Standards 500, U. S. Government Printing Office, Washington, D. C., p. 487, 1952.

52. A. G. Keenan and J. M. Holmes, "The Adsorption of Nitrogen, Argon and Oxygen on Potassium Chloride at 78 - 90° K," J. Phys. Colloid Chem. 53, 1309-20 (1949).

53. J. P. Lodge and B. J. Tufts, "An Electron Microscope Study of Sodium Chloride Particles as Used in Aerosol Generation," J. Colloid Sci. 10, 256-62 (1955).

54. E. Matijevic, W. F. Espenscheid and M. Kerker, priviledged communication; later appearing as "Aerosols Consisting of Spherical Particles of Sodium Chloride," J. Colloid Sci. 18, 91-4 (1963)

55. M. Kerker, Private Communication, May 1963.

56. D. E. Bradley, "High-Resolution Shadow Casting Technique for the Electron Microscope Using the Simultaneous Evaporation of Platinum and Carbon," Brit. J. Appl. Phys. 10, 198-203 (1959).

57. G. A. Bassett, "A New Technique for Decoration of Cleavage and Slip Steps on Ionic Crystal Surfaces," Phil Mag. 3, 1042-5 (1958).

58. G. A. Bassett, "Nucleation of Evaporated Metal Layers on Single Crystal Substrates," International Congress for Electron Microscopy, Berlin, 1958, p. 512-5, Springer Verlag, Berlin, 1960.

59. S. Brunauer, The Adsorption of Gases and Vapors, Vol. 1, p. 346-8, Princeton University Press, Princeton, N. J., 1943.

60. S. Brunauer, L. S. Deming, W. E. Deming, and E. Teller, "On a Theory of the van der Waals Adsorption of Gases," J. Am. Chem. Soc. 62, 1723-32 (1940).

61. C. Pierce and R. N. Smith, "Adsorption in Capillaries," J. Phys. Chem. 57, 64-8 (1953).

62. W. J. C. Orr, "The Adsorption of Non-polar Gases on Alkali Halide Crystals," Proc. Roy. Soc. 173A, 349-67 (1939).

63. T. J. Gray, The Defect Solid State, p. 96, Interscience Publishers, Inc., New York, 1957.

64. E. B. Maxted, K. L. Moon and E. Overgage, "The Relationship Between Sensitivity to Poisoning and Catalytic Surface," Disc. Faraday Soc. 8, 135-40 (1950).

65. G. C. Benson, Private Communication, 1963.

66. A. K. Schellinger, "Solid Surface Energy and Calorimeter Determinations of Surface Energy Relationships for Some Common Minerals," Mining Eng. 4, 369-74 (1952).

67. E. D. Jones, D. S. Burgess and E. S. Amis "The Abnormal Surface Energy of Atomized Sodium Chloride," Z. Physik. Chem. 4, 220-32 (1955).

68. D. Patterson, J. A. Morrison, and F. W. Thompson, "A Low Temperature Particle Size Effect on the Heat Capacity of Sodium Chloride," Can. J. Chem. 33, 240-44 (1955).

69. L. G. Harrison, J. A. Morrison, and G. S. Rose, "An Investigation of Chloride Ion Diffussion in Subsurface Layers of Sodium Chloride by an Isotopic Exchange Technique," J. Phys. Chem. 61, 1314-18 (1957).

70. L. G. Harrison, and J. A. Morrison, "The Surface Structure of Sodium Chloride," J. Phys. Chem. 62, 372-73 (1958).

71. L. G. Harrison, I. M. Hoodless, and J. A. Morrison, "Exchange Reactions Involving Surface Regions in Sodium Chloride Crystals," Disc. Faraday Soc., No. 28, 103-12 (1959).

72. W. D. Harkins, The Physical Chemistry of Surface Films, 291-93, Reinhold Publishing Corp., New York, 1952.

73. L. V. Azaroff, Introduction to Solids, 99-102, McGraw-Hill Book Co., Inc., New York, 1960.

74. R. G. Brickenridge, "Dispersion in Ionic Crystals," J. Chem. Phys. 16, 959-67 (1948).

75. H. W. Etzell and R. J. Maurer, "Vacancies in Sodium Chloride," J. Chem. Phys. 18, 1003-7 (1950).

76. D. E. Straumanis, "Density Determination by a Modified Suspension Method; X-ray Molecular Weight and Soundness of Sodium Chloride," Amer. Min. 38, 662-70 (1953).

77. F. Seitz, "On the Formation of Dislocations from Vacancies," Phys. Rev. 79, 890-1 (1950).

78. F. Seitz, "Properties of the Silver Halide Crystals," Rev. Mod. Phys. 23, 328-52 (1951).

79. E. R. Buckle and A. B. Ubbelohde, "Studies on the Freezing of Pure Liquids III. Homogenous Nucleation in Molten Alkali Halides," Proc. Roy. Soc. A261, 197-206 (1961).

80. R. A. Swalin, Thermodynamics of Solids, 203-5, John Wiley and Sons, Inc., New York, 1962.

81. L. D. Landau and E. M. Lifshitz, Theory of Elasticity, 1-12, Pergamon Press, London, 1959.

82. R. Shuttleworth, "The Surface Tension of Solids," Proc. Phys. Soc. 63, 444-57 (1950).

83. C. Gurney, "Surface Forces in Liquids and Solids," Proc. Phys. Soc. 62, 539-48 (1949).

84. M. M. Nicolson, "Surface Tension in Ionic Crystals," 228A, 490-510 (1955).

85. A. J. Shaler, "The Mechanical Properties of Crystalline Metal Surfaces," Structure and Properties of Solid Surfaces, 120-46, R. Gomer and C. S. Smith, eds., Chicago University Press, Chicago, 1953.

86. C. V. Raman and D. Krishnamurti, "Evaluation of the Four Elastic Constants of Some Cubic Crystals," Proc. Indian Acad. Sci. 42A, 111-30 (1955).

87. E. Schmid and W. Boas, Plasticity of Crystals, 253-4, 262-3, F. A. Huges and Co., Lts., London, 1950.

88. C. Orr, Jr., F. K. Hurd and W. J. Corbett, "Aerosol Size and Relative Humidity," J. Colloid Sci. 13, 472-82 (1958).

89. C. Orr, Jr., F. K. Hurd, W. P. Hendrix and C. Junge, "The Behavior of Condensation Nuclei Under Changing Humidities," J. Meteorology 15, 240-2 (1958).

90. G. C. Benson, Private Communication, April 1963.

91. International Critical Tables 3, 297-8, McGraw-Hill Book Co., Inc. New York, 1933.

92. Handbook of Chemistry and Physics, 42 ed., 2272-3, Chemical Rubber Publishing Co., Cleveland, 1960.

93. C. B. Hess and B. E. Gramkee, "The Specific Heats of Some Aqueous Sodium and Potassium Chloride Solutions at Several Temperatures, I," J. Phys. Chem. 44, 483-94 (1940).

OTHER REFERENCES

1. Adamson, A. W., Physical Chemistry of Surfaces, Interscience Publishers, Inc., New York, 1960.

2. Geguzin, Ya. E., and Ovcharenko, N. N., "Surface Energy and Surface Processes in Solids," Usp. Fiz. Nauk. 76, 283-328 (1962); english translation, Soviet Physics Uspekhi 5, 129-57 (1962).

3. Gregg, S. J., The Surface Chemistry of Solids, 2 ed., Reinhold Publishing Corp., New York, 1961.

4. Rice, J., "The Thermodynamics of Strained Elastic Solids" and "The Influence of Surfaces of Discontinuity Upon the Equilibrium of Heterogeneous Masses. Theory of Capillarity" 395-505, 505-678, A Commentary on the Scientific Writings of J. Willard Gibbs I, F. G. Donnan and A. Haas eds., Yale University Press, New Haven, Conn., 1936.

5. Semenchenko, V. K., Surface Phenomena in Metals and Alloys (english translation) Pergamon Press Ltd., London, 1962.

* Abbreviations for journals correspond to those given in the "List of Periodicals" published by Chemical Abstracts (1961).

VITA

William James Corbett was born in Gadsden, Alabama, on January 23, 1934. He attended the public schools in Gadsden and graduated from Gadsden High School in 1951. He entered the Georgia Institute of Technology in the same year and was graduated in June, 1956, receiving the degree of Bachelor of Chemical Engineering. In September of 1955 he entered the Graduate Division of the Georgia Institute of Technology on a part-time basis.

In June of 1955, Mr. Corbett joined the staff of the Engineering Experiment Station of the Georgia Institute of Technology as a Research Assistant. He was promoted to the position of Assistant Research Engineer in 1958 and to Research Engineer in 1962. In addition to his full time engagement in sponsored research he has instructed in the Engineering Evening School for nine years. He is the author or co-author of a dozen technical papers and publications, as well as a contributor to a major encyclopedia, and a member of Sigma Xi.

Mr. Corbett was married in 1957 to the former Mary Lewis Brown of Atlanta, Georgia. They have two sons.